



Project acronym: **LASH FIRE**
Project full title: **Legislative Assessment for Safety Hazard of Fire and Innovations in Ro-ro ship Environment**
Grant Agreement No: **814975**
Coordinator: **RISE Research Institutes of Sweden**



Deliverable D09.3
Evaluations and recommendations for visual fire confirmation and localisation
September 2023

Dissemination level: **[Public]**

Abstract

When a fire alarm is triggered, it is critical to obtain detailed information on the situation at the location of the detector to be able to make an informed decision. Currently, the operator on the bridge first evaluates the warning of the detector and its location, then requests a member of the crew to run to the appropriate site, and this runner evaluates the situation as best as possible and subsequently reports back to the bridge via radio. However, this process can take a substantial amount of time (often in the order of many minutes), and it may be very inefficient, especially if access to the site is limited due to the presence of smoke, flames, or narrow spaces along the way. Accordingly, to improve the fire confirmation and localisation method, the present study evaluates visual fire detection systems through operational evaluations and laboratory experiments, considering appropriate operating conditions under different scenarios. It is found that the video fire analytics and thermal imaging are both highly useful in this area, with each method offering certain advantages. It is expected that these detection methods have the potential to improve the safety and efficiency of fire confirmation and localisation, such that the required time is often not longer than a few minutes.



This project has received funding from the European Union's Horizon 2020 research and innovation programme under grant agreement No 814975

The information contained in this deliverable reflects only the view(s) of the author(s). The Agency (CINEA) is not responsible for any use that may be made of the information it contains.

The information contained in this report is subject to change without notice and should not be construed as a commitment by any members of the LASH FIRE consortium. In the event of any software or algorithms being described in this report, the LASH FIRE consortium assumes no responsibility for the use or inability to use any of its software or algorithms. The information is provided without any warranty of any kind and the LASH FIRE consortium expressly disclaims all implied warranties, including but not limited to the implied warranties of merchantability and fitness for a particular use.

© COPYRIGHT 2019 The LASH FIRE Consortium

This document may not be copied, reproduced, or modified in whole or in part for any purpose without written permission from the LASH FIRE consortium. In addition, to such written permission to copy, acknowledgement of the authors of the document and all applicable portions of the copyright notice must be clearly referenced. All rights reserved.

Document data

Document Title:	D09.3 – Evaluations and recommendations for fire confirmation and localisation		
Work Package:	WP9 – Detection		
Related Task(s):	T09.11, T09.12		
Dissemination level:	Public		
Deliverable type:	R, Report		
Lead beneficiary:	3 – FRN		
Responsible author:	Davood Zeinali		
Co-authors:	Reidar Stølen, Lei Jiang, Ellen Synnøve Skilbred		
Date of delivery:	2023-09-18		
References:	D04.1, D05.6, D05.7, D05.8, D05.9, D09.1, and D09.2		
Approved by	Ola Willstrand on 2023-09-12	Rick Jeffress on 2023-09-14	Maria Hjøhlman on 2023-09-18

Involved partners

No.	Short name	Full name of Partner	Name and contact info of persons involved
3	FRN	RISE Fire Research AS	Davood Zeinali, davood.zeinali@risefr.no Reidar Stølen, reidar.stolen@risefr.no Lei Jiang, lei.jiang@risefr.no Ellen Synnøve Skilbred, ellen.synnove.skilbred@risefr.no
1	RISE	RISE Research Institutes of Sweden AB	David Schmidt
20	FKE	Fike	Rick Jeffress, rick.jeffress@fike.com
6	UNF	Unifire AB	Roger Barrett James, roger@unifire.com Mattias Eggert, mattias@unifire.com
24	DFDS	DFDS AS	Lena Brandt, lebra@dfds.com Sif Lundsvig, silun@dfds.com

Document history

Version	Date	Prepared by	Description
01	2021-09-07	Reidar Stølen	Draft of structure
02	2023-09-11	Davood Zeinali	Draft of final report circulated to reviewers
03	2023-09-18	Davood Zeinali	Final report

Content

1	Executive summary	5
1.1	Problem definition.....	5
1.2	Method.....	5
1.3	Results and achievements.....	5
1.4	Contribution to LASH FIRE objectives.....	5
1.5	Exploitation.....	5
2	List of symbols and abbreviations	7
3	Introduction.....	8
4	Operational aspects.....	9
4.1	Key questions	9
4.1.1	Where is the fire?	9
4.1.2	Where is the smoke?.....	9
4.1.3	What is burning?	9
4.1.4	Who is in the area?.....	10
4.1.5	Which mitigation actions should be initiated?.....	10
4.2	Organisation of responsibilities and timeline.....	11
5	Sources of information and challenges	12
5.1	Manual confirmation.....	12
5.2	CCTV monitoring.....	12
5.3	Fire detectors	13
5.3.1	Flame wavelength detectors	13
5.3.2	Thermal imaging fire detection	14
5.3.3	Video fire detection.....	14
5.4	Drones and robots.....	15
6	Integration and presentation	16
6.1	Integration with fire detection system interface	16
6.2	Activation and guidance of automatic fire suppression systems.....	17
7	Evaluation criteria	20
7.1	Performance.....	20
7.2	Operational aspects and cost assessment	20
7.2.1	Thermal imaging fire detection for a generic ship	20
7.2.2	Video fire detection for a generic ship	23
7.3	Conclusions.....	24
8	Laboratory evaluations.....	26

8.1	Fire detection experiments with four ISO 8ft containers.....	26
8.1.1	Experimental setup.....	26
8.1.2	Fire sources.....	31
8.1.3	Results and discussion.....	33
8.2	Propane burner calibrations for wind tests and onboard evaluations	44
8.3	Wind experiments	46
8.3.1	Experimental set-up	46
8.3.2	Results	47
8.4	Large-scale fire detection combined with fire suppression	48
8.4.1	Experimental set-up	49
8.4.2	Results	51
8.5	Main findings from laboratory tests.....	55
9	Onboard evaluations	58
9.1	Objective and selection of detectors	58
9.2	Installations and initial testing	58
9.3	Alarms during normal operations on board.....	62
9.4	Other operational observations	64
9.5	Fire experiments in open ro-ro space with side walls simulating trucks	66
9.5.1	Setup.....	66
9.5.2	Results	66
9.6	Fire experiments on the weather deck	67
9.6.1	Setup.....	67
9.6.2	Results	69
9.7	Video fire detection experiments in closed ro-ro space	70
9.7.1	Setup.....	70
9.7.2	Results	71
9.8	Main findings from onboard evaluations.....	72
10	Recommendations.....	74
10.1	Video fire detection.....	74
10.2	Thermal imaging fire detection.....	75
11	Conclusion	78
12	References.....	79
13	Indexes	81
13.1	Index of tables	81
13.2	Index of figures.....	81

1 Executive summary

1.1 Problem definition

After a fire alarm is triggered, it is critical for the bridge to visually confirm the fire and its location as early as possible to respond swiftly, e.g., to activate the fire suppression system in the affected area. The current practice is that the officer on the watch asks a runner, an able seaman or AB (often bridge watch or fire patrol), to run to the site of the alarm and manually confirm the fire [1]. The runners examine the area and report an overview of the situation back to the bridge via radio. However, manual fire confirmation by runners is not always possible safely and efficiently. A strategic alternative is the use of visual fire detection systems, i.e., systems that enable assessing the area causing a fire alarm remotely using live video (regular or thermal footage). This is the focus of the present document to improve the fire confirmation and localisation method, thereby enabling good assessments and decision-making for the mitigation of fire incidents and their respective consequences on board ro-ro ships.

1.2 Method

A combination of available information and the development of new systems like fire detection combined with cameras is used to approach the problem of fire localisation and confirmation. The assessments in the present document include laboratory experiments considering appropriate operating conditions under different scenarios as well as operational evaluations on board a ro-ro ship for over a year.

1.3 Results and achievements

The performed evaluations suggest that many of the assessments made by the runners cannot be easily replaced by automatic sensors and software. The most advanced and flexible source of information, in most cases, will still be provided by the runners, especially for ruling out nuisance alarms. Nevertheless, despite the many advantages of manual observations, there are some limitations to what a human can do, and that is where visual systems can be of assistance. For instance, thermal cameras can see through thin smoke more easily, and this allows for locating the fire source when regular cameras or manual observations are not possible.

Automatic fire detection, in combination with cameras, can give live images of an incident without any delay, providing the location of the affected area and thereby improving situation awareness regarding the incident. Nevertheless, the visibility of the event may be obscured by smoke both for ordinary video cameras and for manual observations. In this case, other types of sensors, such as infrared cameras, can give insight into how the event is developing. On the other hand, frequent fire alarms may be raised by a nuisance source, and it would be important to find the root cause of such false alarms to prevent them from happening regularly. A quick clarification that the alarm was not caused by a fire will reduce the workload for the crewmembers, and this improves their motivation to respond to the system quickly and efficiently in a real fire alarm scenario.

1.4 Contribution to LASH FIRE objectives

This report and the studies discussed herein contribute to LASH FIRE Action 9-C focusing on the investigation and development of new and advancing technologies for visual fire confirmation and localisation.

1.5 Exploitation

The findings are primarily useful for implementation and exploitation by end users, i.e., ship operators, because it helps them spend less time for confirmation of alarms manually. Moreover, the report provides insights for optimising the fire detection algorithms and their method of data presentation.

In the case of real fires, better information can be obtained this way, and firefighting can be started earlier, possibly saving the first responders from dangerous situations and allowing the investigations of fires via recordings.

The information is likewise useful for shipyards (e.g., for reduction of losses), suppliers of ship equipment and components (e.g., for optimisation of products), providers of engineering and technical services (e.g., for optimisation of services), research centres and university departments (e.g., for collection and analysis of information from fires and false alarms), insurance companies (e.g., for reduction of paybacks), classification societies as well as regulatory and standardisation bodies (e.g., for regulatory improvements).

2 List of symbols and abbreviations

AB	Able seaman
AFV	Alternative fuel vehicle
CCR	Cargo Control Room - a location on board RORO ships used during cargo operations
CCTV	Closed-Circuit Television
CNG	Compressed natural gas
DNV	Det Norske Veritas (international registrar and classification society based in Norway)
EV	Electric Vehicle
FRMC	Fire Resource Management Centre
FSA	Formal safety assessment
IACS	International Association of Classification Societies
IAMCS	Integrated Alarm Monitoring Control System – equipment
IMDG	International Maritime Dangerous Goods - regulation; dangerous cargo
IMO	International Maritime Organization
IR	Infrared
IR3	Triple-IR, i.e., 3 infrared sensors monitoring 3 radiation ranges for flame distinction
NMC	Nickel manganese cobalt oxides (Lithium battery cathode chemistry)
OOW	Officer on watch
RCM	Risk control measure
RCO	Risk control option
Ro-Ro	Vessel type with cargo type roll-on roll-off
Ro-Pax	Vessel type with both roll-on roll-off cargo and passengers
SOLAS	International Convention for the Safety Of Life At Sea
UV	Ultraviolet
VFD	Video Flame Detection
VSD	Video Smoke Detection
WP	Work package (in the LASH FIRE project)

3 Introduction

Main author of the chapter: Reidar Stølen, FRN

When a fire alarm is triggered, the operators on the bridge need to get further information on the situation to decide which actions to take, and this process may take many minutes when the primary reliance is on the runners. Remote visual confirmation and exact localisation of the fire are two of the essential pieces of information that are required to speed up the decision-making process.

It is noteworthy that runners from the crew may not be the first to reach the site, but they can still sense and evaluate more extensively than an automatic sensor system. However, the visibility may be reduced by smoke from a fire, making it difficult to see the source of the fire via manual observations or ordinary video cameras. In these cases, other sensor technologies may be used to provide information on the source of the smoke. For instance, (point) heat detectors or smoke detectors can trigger alarm on detecting heat or smoke, which can operate in harsh environments and provide relevant information such as the temperature distribution or gas concentration across the deckhead. Another example is infrared thermal imaging cameras, which can see through the smoke and give thermal information in a whole area. For exact localisation of the fire, visual detection systems give more comprehensive and intuitive information than heat or smoke detections and are the focus of this report.

The regulations for visual fire confirmation do not include detailed requirements, but there are useful recommendations, such as SSE 7/6/4 from the Chinese delegation recommending CCTV cameras with video analytics for fire detection. Such video camera coverage of the ro-ro spaces can give a useful and quick visual overview of the situation. Moreover, automatic fire detection based on or integrated with video cameras can give live video of an incident without any delay, providing the location of the affected area, thereby improving situation awareness regarding the incident. The visibility of the event may be obscured by smoke both for ordinary video cameras and for manual observations. However, other types of sensors, such as infrared cameras, can, in such cases, give insight into how the event is developing.

Further information on the risk of fire or smoke spreading and possibilities to suppress the fire with automatic or manual firefighting is also important if the fire is confirmed. On the other hand, fire detection could be caused by a nuisance source, and it would be important to find the root cause of the false alarm to prevent it from happening regularly. Reducing such alarms will reduce the workload for the crewmembers and improves their motivation to respond to the system in a real fire alarm scenario.

In the current report, first, the operational aspects are discussed, including key questions, organisation of responsibilities and timeline. Next, the different sources of information are presented, including results from experiments performed with several fire detection systems, namely, video analytics, flame detectors, smoke detectors and thermal imaging cameras. Subsequently, the integration of these automatic means into the regular alarm response procedure is described, followed by the evaluation. Finally, the conclusions are provided.

4 Operational aspects

Main author of the chapter: Lei Jiang, FRN

4.1 Key questions

4.1.1 Where is the fire?

According to SOLAS II-2/3 [2], ro-ro spaces are defined as ‘spaces not normally subdivided in any way and normally extending to either a substantial length or the entire length of the ship in which motor vehicles with fuel in their tanks for their own propulsion and/or goods (packaged or in bulk, in or on rail or road cars, vehicles (including road or rail tankers), trailers, containers, pallets, demountable tanks or in or on similar stowage units or other receptacles) can be loaded and unloaded normally in a horizontal direction’. Depending on the operational and design characteristics, the ro-ro ships have various types, including ro-ro passenger ships, ro-ro cargo ships and vehicle carriers [3].

According to Wikman et al. [4], 90% of the fires in ro-ro spaces originated from the cargo (vehicles, trailers, etc.). In this report, the focus is on the vehicle and cargo fires in the ro-ro space, while fires originating from the ship itself, such as ship engine room fires or kitchen fires, will not be discussed.

A discussion of the main cargo fire hazards and the related conditions in the ro-ro spaces has been provided in LASH FIRE deliverable D09.2 [5].

4.1.2 Where is the smoke?

The smoke from the exhaust of vehicles and that from fires are similar unwanted by-products of combustion containing a mixture of gases, particles, and chemicals which can occupy a considerable amount of volume in a short period of time. In the event of a fire on a ro-ro ship, smoke can be present in a variety of locations depending on the source and severity of the fire. Smoke can spread quickly and may be carried throughout the ship by air flows and ventilation systems. Typically, the location of the fire and the type of material involved will determine where the smoke is most concentrated. In a ro-ro space, the ventilation system is expected to be shut off and the smoke is likely to be contained inside the ro-ro space.

Smoke from a fire tends to rise and thus it accumulates near the ceiling of the space where the fire is located. Smoke can cause damage to sensitive equipment and suffocate engines when accumulates in enclosed spaces. Moreover, smoke can have serious health consequences for people who are exposed to it. By limiting visibility, smoke also makes it more difficult to localise fires. In this case, visual systems based on thermal imaging may be useful for seeing through the smoke and helping to localise the fire.

4.1.3 What is burning?

As discussed in LASH FIRE deliverables D09.2 [5] and D04.1 [6], vehicles constitute a major source of fire in ro-ro spaces [7], [8]. The ignition is typically caused by electrical failure [4], which may occur in the vehicle’s engine compartment, chassis or cab. Apart from electrical faults, fire can also be caused by mechanical overheating, leakage of easily flammable substances or chemical reactions. The involved vehicles can be divided based on their type into used and new vehicles; special vehicles and machines; alternatively powered vehicles; as well as heavy goods vehicles and buses [6]. The alternatively powered vehicles can be further classified into vehicles powered by liquids and gases kept under high pressure (e.g., hydrogen, CNG) and electric vehicles (EVs). It should be noted that while EVs are becoming much more common, there is currently insufficient data to determine whether used EVs on ro-ro ships are more prone to fire incidents than conventional vehicles. Nevertheless, major EV fires on ro-ro ships are expected to be difficult to extinguish [9].

Refrigerator trucks, commonly referred to as reefer units or reefers, are occasionally subject to electrical faults and constitute a significant fire hazard in ro-ro spaces [7]. Refrigeration units that are connected to a power supply are more likely to catch fire than other sources of ignition. The fire in reefer units can be caused by an electrical fault in the cable, in connections, and in the unit itself [6]. Electrical fire in new vehicles can be caused by energised electrical circuits since new vehicles are usually shipped with their batteries connected and keys in their ignition. Electrical fire in used vehicles can be caused by internal electrical connections deterioration as a result of salt air corrosion, the breakdown of insulation of electrical cables due to being lying idle for a long time, as well as personal use. Disconnecting the battery and removing the key fully may assist in isolating the circuit and preventing any sparks that may ignite residual flammable material remaining in the vehicle.

In a report released by the North of England P&I Association [8], 38 fire accidents are analysed, the classification of which is presented in Table 1. It is found that ‘electrical fire on reefer’ and ‘electrical fire on vehicle’ are the two most common fire causes.

Table 1. Classification/location of fires on vehicle decks, from the North of England P&I Association [8].

Classification of fire	Number of reports
Electrical fire on reefer	12
Electrical fire on vehicle	9
Fire in vehicle cab	6
Vehicle engine fire	5
Other cause	4
Fire on reefer (other cause)	2

4.1.4 Who is in the area?

During voyage, no passengers are expected to be present in the ro-ro space with only fire patrols regularly inspecting all the areas in the ship. During the loading and unloading process, however, passengers and crew members may be present and close to the fire zone in the ro-ro space, as fire incidents can happen if vehicles are damaged or inadequately secured. Once a fire is detected, a runner is sent for confirmation. After the fire is confirmed, first responders may enter the fire zone for fire suppression. If the fire cannot be easily controlled, evacuation of crew members and passengers is needed, even if the people are not directly in the ro-ro space.

4.1.5 Which mitigation actions should be initiated?

In the case of a fire situation, there are no specific action requirements from the IMO regulations to activate or shut down the mechanical ventilation of ro-ro spaces nor to open or close openings. Those actions should be understood as operational and up to onboard procedures or to Master’s and/or crew’s appraisal, depending on the fire situation. To fight the fire, the ability to contain/confine a fire and close down the ventilation system of vessel’s vehicle deck is an important initial step [8]. The containment of fire and smoke spread is studied and discussed in Firesafe II [10]. The fire spread can be prevented by various actions or a combination of them, such as the activation of the drencher, the activation of the drencher in adjacent sections to prevent the spread to other cars, as well as the closing of air vents and boundary cooling. Boundary cooling is not only effective in controlling the spread of a fire to adjoining spaces, but it also forms a vital part of the overall effort to ensure that there is no re-ignition after initial firefighting efforts [8]. Due to the limited distance between vehicles and the lack of subdivision in large open areas, the fire can grow rapidly and the effectiveness of a water drenching system can be reduced if not operated effectively at an early stage. For water

drenching systems, heads and pipes may become blocked if seawater has not been rinsed out with fresh water after testing. In the case of carbon dioxide (CO₂) extinguishment systems, the amount of CO₂ required for fire suppression is relatively high, and such systems have limited effectiveness for boundary cooling [8]. The smoke spread can be contained by shutting off the ventilation on decks or in accommodation sections, or both. Some other actions include closures of fire doors, dampers (manual closure) and air vents. In the case of the fire on Pearl of Scandinavia, altering the ship's course and speed was also used to prevent the smoke from spreading over and along the ferry. In the case of the accident of Amorella, overpressure was implemented in the accommodation sections and under-pressure in the car decks to avoid smoke propagation in the passenger compartments. This was achieved by stopping the ventilation of the car deck and opening the suction channels while maintaining the ventilation of the cargo spaces in operation. In this regard, it is noteworthy that not all of the crew are aware of how to fully lock the ventilation housing louvres into a 'closed' position, and certain training is required [8].

4.2 Organisation of responsibilities and timeline

European Maritime Safety Agency [3] provides operational guidance in case of AFVs (alternative fuel vehicles) fire accidents. The guidance is also considered to be effective for conventional vehicles. In the guidance, the fire incidents are divided into several stages, including alarm level, confirmation, elementary first response, fire suppression and manual activity during suppression by a fixed system.

According to SOLAS [2], fire patrols are trained to be familiar with the arrangements of the ship as well as the location and operation of any equipment he may be called upon to use. Efficient fire patrols can discover potential fire hazards, such as leakages from the vehicles, conditions of electrical connections and ship's power supply cables to vehicles and common cargo fire hazards.

When a fire signal is detected, confirmation is mandatory. The officer on the watch asks an able seaman (AB) (often bridge watch or fire patrol) to run to the site of the fire to manually confirm and identify the fire. The confirmation can also be done through video monitoring systems. Once the fire is confirmed, the officer activates the suppression system or sends first responders to the fire site. The ventilation/fire dampers should be put in suitable fire mode. If necessary, the officer organizes the evacuation of passengers and crew members to an area clear of smoke. If significant signs of deterioration and uncontrolled fire growth are observed with the whole ship endangered, the officer makes the decision if it is necessary to prepare lifeboats and abandon the ship. The evacuation should consider the smoke/fire conditions.

The overall timeline of actions when a fire is detected is shown in Figure 1. Throughout this timeline, the CCTV camera can give real-time fire development information, and this must be monitored closely during the suppression process. If the fire is deemed uncontrollable and the areas outside the ro-ro space are endangered, an evacuation directive for passengers and crew members is given.

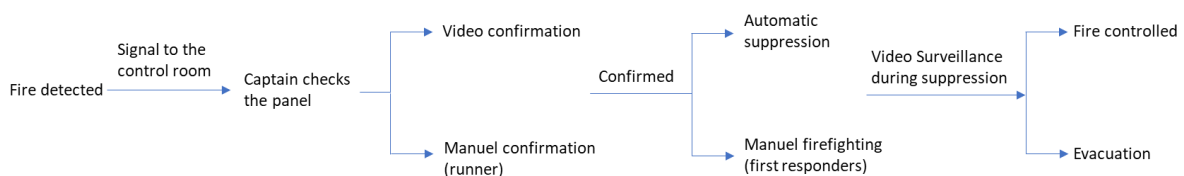


Figure 1. Timeline of actions when a fire is detected.

5 Sources of information and challenges

Main author of the chapter: Davood Zeinali, FRN

5.1 Manual confirmation

The main source of information for confirmation, localisation and assessment of a fire is the manual observations made by the crew dispatched to the site. Many of the observations and assessments that the crewmember makes on the way to and at the site of the event cannot easily be replaced by electronic sensors and software systems. The most complete, advanced, and flexible source of information on the situation will still be that provided by the crewmembers, especially for ruling out false alarms. Nevertheless, despite the many advantages of manual observations, there are some limitations to what a human can do, and that is where electronic systems may be of assistance. The limitations that can be supplemented by automatic systems include several aspects:

Time: The operator will not be able to make observations until a runner is on site, and this may come with a delay. Automatic systems will always be on site and can provide information on what has happened even before the event is initiated.

Capacity of sensors: The human senses can detect many parameters and recognise various types of smoke (wood, plastic, etc.). Electronic sensors can, on the other hand, measure exact concentrations of gases, including odourless and colourless species like carbon monoxide that humans cannot smell or see. Infrared thermal cameras can detect high-temperature regions at much longer distances compared to human senses, and video analytics can display an outline around smoke, oil mist, or flame. Electronic sensors may also be at many different locations, providing more extensive information.

Health hazards: Without firefighting equipment, the operators cannot safely enter an area where environmental conditions like gas concentrations in the air or temperatures are unsafe. Electronic systems may operate in most types of gases and in a wider range of temperatures.

Human insights: The manual inspector may combine the situation with practical experience on the spot, and relay information that sensors cannot, e.g., whether there is room for a firefighting team to manoeuvre from a certain angle or not, whether there are elements of the surrounding cargo that should be considered (such as material, size, and fire resistance); whether there is a problem with cargo not being lashed sufficiently in extreme weather situations. The provision of such insights is difficult to integrate into electronic sensors because the corresponding strategies and situations vary from one case/ship to another.

5.2 CCTV monitoring

If video is available for the relevant position, the operators on the bridge can access and get an overview of the situation without delay needed for a crew member to be contacted to run to the position. For this purpose, the indexing of the CCTV cameras needs to be logically arranged in relation to the fire detectors to be able to find the camera that has an overview of the relevant area. Securing a free line of sight for the camera can be challenging as the field of view can be blocked by high vehicles close to the camera. Some cameras can pan, tilt, and zoom, but they have a fixed position that cannot be changed to get a better view of the situation. Accordingly, having several cameras covering the same area will increase the possibility of getting a good overview that is not blocked by cargo items, such that ruling out false alarms is also easier. However, smoke or any similar obscuration medium can still block the view from standard CCTV cameras.

Video fire detection is reliant on the video streams from CCTV cameras as an input and uses algorithms to detect smoke or flames in the video. This system can immediately trigger an alarm, display live

images of the area of the triggered alarm, and include the outline of smoke or oil mist as well as any flame boundaries. Video image detection is widely utilised in machinery space applications to identify and track atmospheric oil mist vapour or spray, and it is included in the ship classification rules of Det Norske Veritas (DNV, international registrar and classification society based in Norway).

5.3 Fire detectors

The present document focuses on *visual* fire confirmation and localisation, and thus this section discusses only *visual* fire detectors, i.e., optical detectors that enable assessing the area causing a fire alarm remotely using live video (regular or thermal footage). Correspondingly, point detectors of smoke/heat installed on the deckhead of ro-ro spaces are not discussed here, as they currently do not provide visual outputs to be used for fire confirmation and localisation.

5.3.1 Flame wavelength detectors

The term “*flame detector*” [11] is classically used exclusively for detectors that have sensors for detecting infrared (IR) or ultraviolet (UV) light expected of flame radiation wavelengths commonly associated with combustion products such as carbon dioxide. Such detectors are not to be confused with other flame detection sensors that employ different technology such as video flame detection relying solely on visible light. Accordingly, to avoid confusions hereafter, the present document refers to classic flame detectors as “*flame wavelength detectors*,” and especially uses it to focus on multi-spectrum IR flame detectors which have long-range detection capability suitable for ro-ro spaces and weather decks, as opposed to UV/IR detectors which have short-range detection capability.

Triple-IR (IR3) flame wavelength detectors can identify flames and their reflections by monitoring the ratios of infrared energy for three wavelength ranges which are specific to flames, particularly in the vicinity of 4.4 μm in the electromagnetic spectrum. IR3 flame detectors can be accompanied by a built-in camera. This provides live visual images for fire confirmation. If the detector does not come with a built-in camera, it cannot be used for real-time visual fire confirmation.

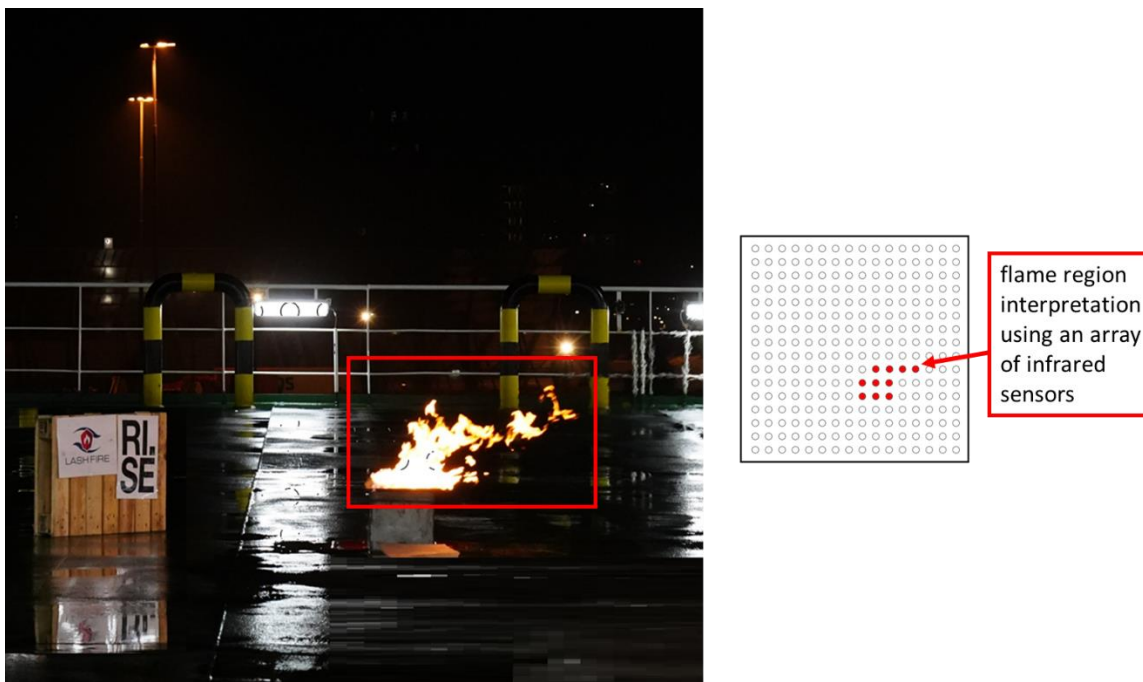


Figure 2: Concept of flame localisation with an IR array flame wavelength detector using a 16x16 array of infrared sensors.

IR array flame wavelength detectors have an array of infrared sensors, and may use video analytics, that can locate and highlight one or multiple flames within the field of view (see Figure 2). Like ordinary IR3 flame wavelength detectors, IR array detectors perform multi-spectrum (IR3) wavelength monitoring to identify flames. Moreover, IR array detectors can be accompanied by a built-in camera to provide live visual images which can be used both for fire confirmation and for fire localisation (usually built into the detector software and video). If the detector does not come with a built-in camera, it cannot be used for real-time visual fire confirmation and localisation.

5.3.2 Thermal imaging fire detection

With thermal imaging detection systems, i.e., systems employing thermal (infrared) cameras, the detection is based on the thermal radiation from high-temperature surfaces or media (gases, particles, etc.). Using such systems, the location of the fire is determined and highlighted in the live image available to the operators. Therefore, the infrared image detection system can provide the location of the fire as an input to autonomous fire suppression systems, just as IR array flame wavelength detectors can. Infrared cameras can also see relatively well through thin smoke and thus may be able to monitor the situation much longer than other visual methods. However, thick smoke can block radiation emitted from targets behind the smoke, such that it becomes difficult to use an infrared camera for monitoring the temperatures and fire area behind such smoke.

An advantage of thermal imaging over flame wavelength detectors is that thermal imaging can detect developing heat before a fire breaks out, contributing to earlier fire detection without the need for a line of sight to flames. However, thermal imaging systems still need to see the area affected by heat to be able to raise an alarm based on high temperatures or the rate of rise of temperatures. Moreover, thermal imaging cameras are more prone to nuisance alarms, for example due to the hot exhaust pipes of regular vehicles which are easily at the same temperature as hazardous hot spots meant to be detected by the fire detection system. The analytics software may avoid nuisance alarms by methods such as monitoring the hot spot for growth or increase in temperature and movement, e.g., to distinguish a moving vehicle from a fire hazard.

Another advantage of thermal cameras is their sensing resolution which gives a more detailed overview of the area as compared to flame wavelength detectors. This higher resolution of thermal cameras enables the use of more advanced detection criteria and allows differentiating between different parts of the field of view. Accordingly, the parts of the view that cover known hot surfaces or areas of nuisance alarms (e.g., the sea surface or the sky) can be masked by the detection software to prevent false alarms from those regions.

Like flame wavelength detectors, thermal cameras need to be protected against bad weather conditions in open environments, as the lens of the camera may be affected by elements such as frost, saltwater, and dirt, thereby affecting the ability of the detector to trigger a fire alarm. The cameras require a free line of sight to the fire or hot surfaces to be able to trigger an alarm.

5.3.3 Video fire detection

Video flame detection (VFD) and video smoke detection (VSD) are two types of video fire detection methods which use video analytics on regular camera footage to detect flames and smoke, respectively. The camera footage can be from an already existing surveillance camera system (CCTV) which is analysed using video analytics software on a computer connected to the CCTV system. Alternatively, dedicated detectors are available with a video camera and the analytics software which can perform video fire detection without the need for a separate computer.

Video fire detection software can identify flame and smoke in video images through their visual characteristics. Flames often display bright and reddish colours, with frequent movements and pulsations that can be used to distinguish flames from background objects in video footage. Similarly, smoke often displays greyish colours and upward motion which can be used for smoke identification. Accordingly, the video analytics algorithms look for these characteristics by considering a combination of texture, shape, size, flicker pattern, motion, energy, transparency, and colours in the video footage to identify flames and smoke. As such, the video analytics software requires a free line of sight to the fire or its reflection to be able to identify the said visual characteristics for the detection of flame and smoke.

The main advantage of video fire detectors over conventional point smoke/heat detectors is that one video fire detector can cover a large area and detect fires from a distance typically as long as 30 to 45 meters as a minimum design standard and up to 80 meters depending on the sensitivity settings. This is while point smoke/heat detectors require the smoke/heat to reach the position of the detector itself for detection.

Video fire detection is usually sensitive to shifting light conditions, such that it is difficult to avoid nuisance fire alarms in video analytics of outdoor environments. Accordingly, adequate fire detection using video analytics is expected to be primarily possible for closed ro-ro spaces, whereas detection in open environments may only be possible if the video analytics software is tested for such environments appropriately.

5.4 Drones and robots

Mobile platforms can provide visual data and other sensor measurements from many positions of interest. Flying drones or rolling vehicles can be automatically dispatched or manually addressed to go to a specific position or be completely manually controlled. Compared to human runners, the mobile platforms can be on standby and prepared in seconds, manoeuvre in small spaces above, below or in between vehicles, and go through toxic smoke and gases. Reliable communication to transfer images and data from the robot to the bridge is essential. Most of the other relevant types of sensors, like video or infrared cameras, temperature, gas concentration or smoke sensors, can be installed on a drone and be manoeuvred to the desired location. During the event, the drone can also be relocated in case the view is blocked by smoke or if the situation changes in any other way.

To have a drone system stand by and ready for dispatch in short notice at any time, a system is needed to ensure that the batteries are charged, and all components are ready to go. The drones also need to be able to navigate from their base to all relevant positions. In this regard, obstructions like doors, steps and cargo items, cables, and lashings must be considered. Harsh weather conditions are also another challenge for the use of drones and robots, both in terms of the functioning of the devices themselves and in terms of any built-in technologies for fire detection.

6 Integration and presentation

Main author of the chapter: Lei Jiang, FRN

When a fire alarm is activated, a series of events is started to decide which actions to initiate. These events are managed on board in the Firefighting Resource Management Centre, or FRMC. The officer on watch, or OOW, needs to evaluate whether the alarm is caused by a real fire, a harmless nuisance source, or a fault in the detection system. This can be a stressful operation, and it is crucial that the required information is easily available to help the responsible person make the right decisions as quickly as possible.

6.1 Integration with fire detection system interface

The location of any detector that triggers a fire alarm is indicated in a fire detection panel as shown in Figure 3. A red lamp lights up on a map of the ship where the detector is located, and a screen shows more detailed information about the detectors in the area. In addition to this, a panel with video streams from CCTV cameras is available on many ships, like the one shown in Figure 4 from Pearl Seaways. For visual confirmation, efforts are needed for the responsible person to first localise the cameras corresponding to the detector and then localize the fire from the screen.



Figure 3: Fire detection panel on Pearl Seaways.

To aid visual confirmation, the fire detectors can be coupled together with the CCTV system and the fire location can be highlighted once a detection is made. Such an example can be found in Figure 4. In this scenario, the video, as well as the fire location, can be highlighted for quick confirmation. Additional information on the situation that is relevant for the management of the fire situation could also be presented in or near these systems on the bridge. Such live video streams from CCTV cameras or infrared thermal cameras located near the detected fire can provide a great overview of the situation.



Figure 4: CCTV panel from Pearl Seaways (left) and imagined presentation of the alarm information via highlighting the CCTV from fire area. The flame and smoke boundaries may also be highlighted by the detection system as shown in Figure 31.

6.2 Activation and guidance of automatic fire suppression systems

If it is confirmed that the alarm is triggered by a real fire, one of the relevant actions is to initiate fire suppression using systems such as drencher and fire monitors. The functions of these systems may be

automatic or manual, i.e., the operator may choose where the water or foam must be released. For drencher systems, the choice is split into sections where the suppression can take place. In the case of fire monitors, each monitor may be activated and manoeuvred to direct the stream of water or foam toward the fire area.

A description of the remote-controlled and autonomous fire-extinguishing systems developed for weather decks during the LASH FIRE project is discussed through deliverable D10.3 [12], with onboard demonstration of the solutions discussed in deliverable D10.2 [13]. Regarding the developed alternative fixed fire-fighting systems and their large-scale validations, the reader is referred to deliverables D10.1 [14] and D10.4 [15], respectively.

In the case of autonomous suppression systems which must activate automatically, the detection system must provide the respective trigger signal based on the corresponding detected location of the fire. In the case of systems like fire monitors that have the possibility to direct the stream of water or foam at any desired direction, the detection system must provide X and Y coordinates, i.e., the horizontal and vertical distances with respect to a reference point defined for the suppression system. However, arriving at the correct X and Y coordinates for each fire monitor requires a three-dimensional analysis of the fire location in the space using the third coordinate Z regarding depth. For that reason, the X and Y coordinates must be available from two different locations. The relevant detection systems considered suitable for this purpose during the LASH FIRE project are primarily IR array flame detectors, but also video fire detection and thermal imaging detection systems. The LASH FIRE experiments with autonomous fire monitors (suppression system suitable for weather decks) are discussed in detail in deliverable D10.3 [12]. Figure 5 shows an illustration of the setup used for the experiments, which included fire detection testing, precision testing using one autonomous fire monitor, precision testing using two autonomous fire monitors, testing the influence of wind (generated using a snow cannon), and testing the influence of rain and fog (generated using a snow cannon and a fire hose).

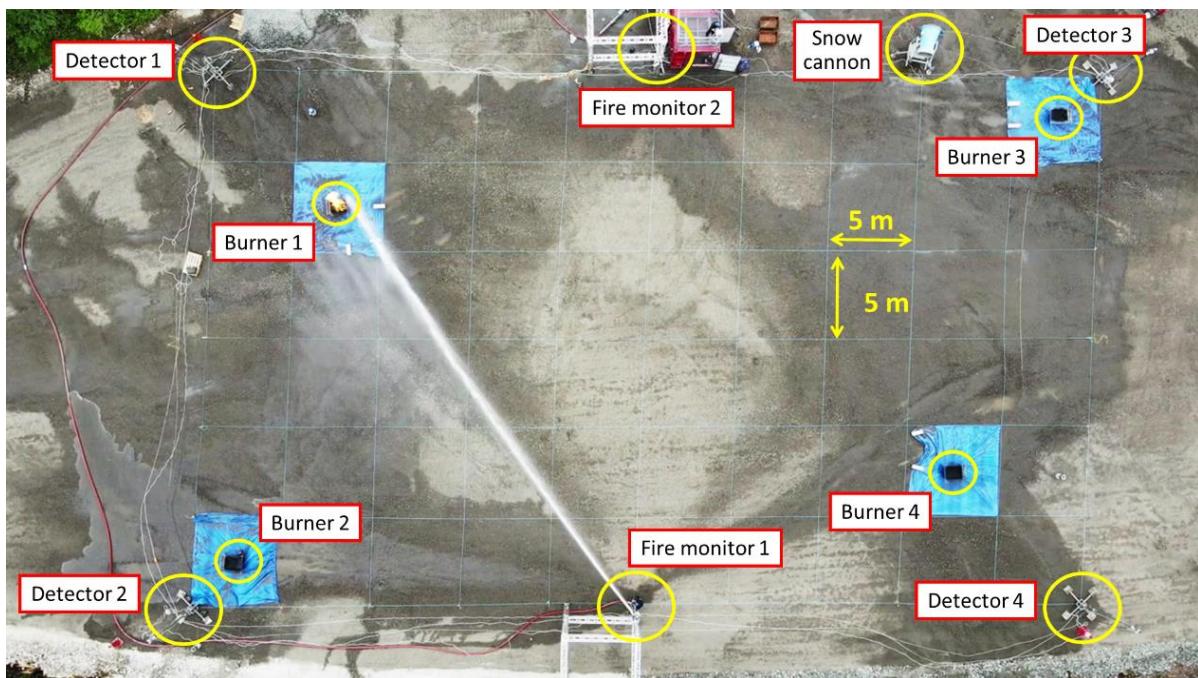


Figure 5: Setup of LASH FIRE experiments with autonomous fire monitors (suppression system for weather decks) [12]. The photo shows an experiment where one fire monitor is projecting water towards a fire identified using two IR array flame wavelength detectors. The test area is 50 m by 30 m and has been marked on the ground with squares measuring 5 m by 5 m.

Each tested autonomous system was comprised of two IR array flame wavelength detectors, a fire monitor, as well as associated software and hardware enabling the system to detect and track the presence, three-dimensional size, and location of a fire in real time automatically and autonomously. Upon the identification of a fire, the software dynamically guided the fire monitor to direct the water stream toward the fire location without any human intervention, although the autonomous function could be overridden by an operator at any time if desired. For a detailed description of the system specifications and the analysis of the test results, the reader is referred to chapter 8 of deliverable D10.3 [12].

Video fire detection and thermal imaging detection methods both utilize camera footage, albeit the first method uses regular images while the second method uses thermal images. Correspondingly, obtaining X and Y coordinates for the fire location using both these methods is possible by finding the location of the fire pixels in the image. Figure 6 shows an example identification of flame coordinates using a video fire detection system provided by Fike.

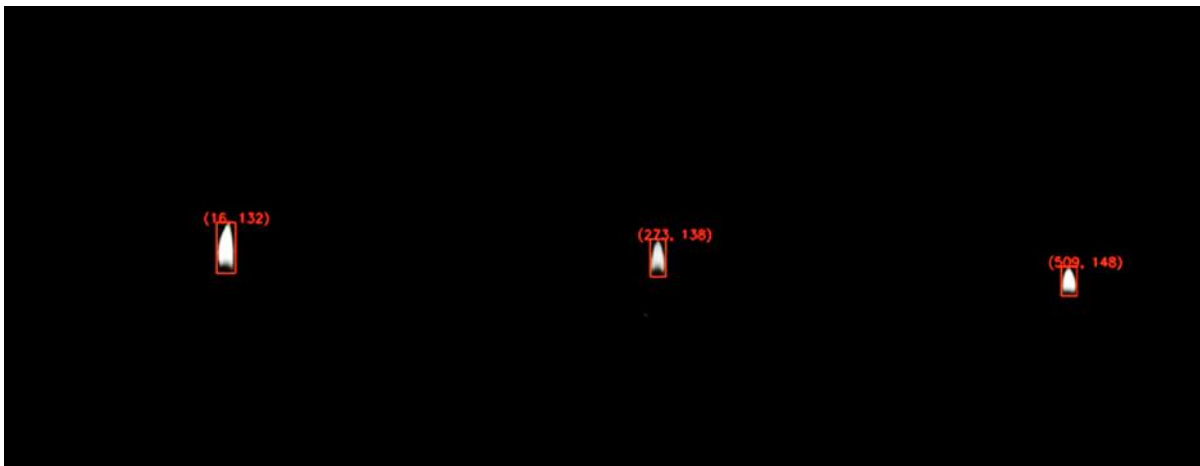


Figure 6: Coordinates identified for three flames using Fike video fire analytics. The numbers written beside each flame are X and Y coordinates based on the number of horizontal and vertical pixels from the top left side of the image, respectively.

7 Evaluation criteria

Main author of the chapter: Davood Zeinali, FRN

The performance criteria of systems for visual fire confirmation and localisation were assessed through experiments in a corresponding laboratory environment and then on board an operational ship. Moreover, the compatibility and cost-effectiveness criteria were studied in cooperation with work package 5 of LASH FIRE which deals with ship integration (see deliverables D05.6 [16], D05.7 [17], D05.8 [18], and D05.9 [19]).

7.1 Performance

Visual systems applicable to fire confirmation and localisation have an inherent overlap with fire detection systems which have various applications and standards (e.g., see [11] and [20]). Correspondingly, the focus of the present document is not to assess the working mechanism of the systems or their compliance with standards. Rather, the goal is to assess the suitability of the underlying technology for fire confirmation and localisation in ro-ro ship environments given the challenges discussed in chapter 5. Among other elements, the following main factors are considered critical to assess:

- **Light sources:** both artificial and natural sources of light can challenge visual fire detection systems.
- **Cargo:** the normal operations related to cargo loading/unloading as well as the emission of (direct/reflected) light from the cargo surfaces can cause nuisance alarms and reduce the use of automatic systems for fire localisation. The obstruction of field of view could also be a problem.
- **Wind:** the dispersion of smoke and the tilting of the fire plume due to wind can make the visual localisation of fires difficult.
- **Other environmental factors:** weather conditions (rain, snow, frost, condensation, sunlight, vibrations, wind, etc.) can affect the performance of the systems to be used for fire confirmation and localisation.

7.2 Operational aspects and cost assessment

LASH FIRE deliverable D05.6 [16] discusses the ship integration requirements for the detection systems relevant for fire confirmation and localisation in ro-ro spaces, while deliverables D05.7 [21] and D05.8 [18] discuss the corresponding integration evaluations and cost assessment based on the input provided by the lead author of the present document. Therefore, the information is not repeated here in detail. Instead, two examples including thermal imaging and video fire detection systems are presented in this document to demonstrate the main concepts and to discuss the related insights.

It is noteworthy that for the thermal imaging detection systems, most of the cost items would be the same for existing ships and newbuilds. For the video fire detection systems, the retrofitting may be possible by using the existing cameras installed on board, while the rest of the cost items will be like those for newbuilds. In the present document, the cost assessment examples are provided only for existing ships, namely for the LASH FIRE generic ship Magnolia Seaways (ro-ro cargo ship), assuming that the a new CCTV system will be installed as part of the proposed video fire detection solution.

7.2.1 Thermal imaging fire detection for a generic ship

The detection system based on thermal imaging is made up of a few infrared cameras (example shown in Figure 7), as well as some cables connecting the cameras back to the ship's fire control panel and

computer with the software required to receive and process the alarm signals and thermal images provided by the infrared cameras.

Infrared cameras are sensitive to hot surfaces, so they can detect areas that are hotter than other surfaces nearby. This can be used to detect potential ignition sources before any flame or smoke is released, but this may cause false alarms if the hot surface is not a real fire hazard. As a result, pre-registering areas with known hot objects at specific temperatures in the detection system can be an option for eliminating false alarms generated by those sources of heat. Correspondingly, the proper commissioning of the thermal imaging fire detection system must consider the hot areas that are expected in normal operations. Moreover, the effectiveness of the thermal imaging cameras may be affected when their lens is covered by dirt, saltwater, or ice, so they require some general maintenance. The cameras also require free line of sight to the fire zone to trigger an alarm.



Figure 7: Example thermal imaging (infrared) camera installed on board Hollandia Seaways for LASH FIRE evaluations.

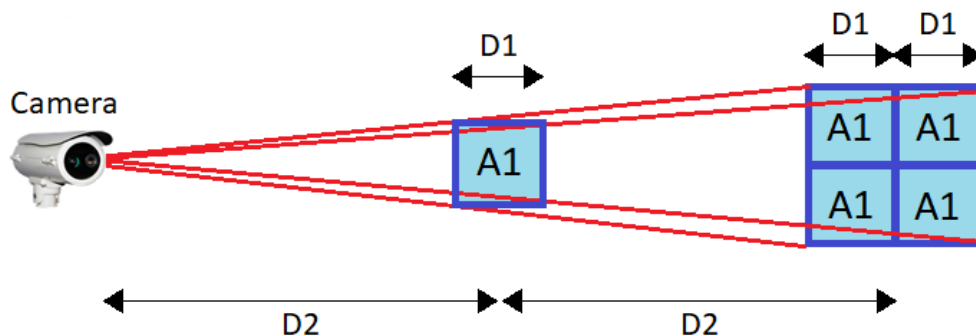


Figure 8: Square law between distance and area of detection (applicable when $D2 \gg D1$): if an object that has an area of $A1$ is detectable at the distance of $D2$, detection at a distance of $2 \times D2$ requires nearly an area of $4 \times A1$.

The detection range of infrared cameras may be as long as 250 m for objects as big as a human, but the detection depends also on the sensitivity settings of the camera, where low sensitivity settings may be used for close-range detection, while high sensitivity settings may be used for long-range detection. As infrared cameras are optical devices, their detection range also follows the square law between distance and area of detection illustrated in Figure 8, such that detection at twice the distance requires nearly four times the area (or fire size). In this regard, cameras installed on weather decks have the advantage of a wide view over the area, whereas the cameras installed below the deckhead in ro-ro

spaces have only a limited view to the narrow space above the cargo (see Figure 9). The location of the cameras and their sensitivity settings may be fixed according to the application, desired detection time, and acceptable frequency of nuisance alarms. Often several cameras are used to ensure adequate coverage of the desired area based on the working range and acceptable sensitivity of the cameras. In addition to triggering fire alarms, thermal imaging detection systems can provide the location of fire in terms of X and Y coordinates to autonomous fire suppression systems (refer to section 6.2).



Figure 9: Typical free space above cargo items (height shown with yellow arrows) which limit the field of view of cameras installed on the deckhead of ro-ro spaces. The tallest items in the field of view will define the extent of free height available.

Figures 10 and 11 show a thermal imaging detection system for the closed ro-ro spaces of Magnolia Seaways consisting of 4 infrared cameras on the main deck and 2 infrared cameras in the tank top. In this example, different cameras and sensitivity settings are used with effective detection ranges as follows: 45 m at 53° horizontal angle and 40° vertical angle (1 camera on main deck), as well as 100 m at 25° horizontal angle and 20° vertical angle (3 cameras on main deck and 2 cameras on tank top). A total of 400 m of power and signal cables is estimated for the proposed design. Table 2 shows the cost estimate for this system. Examples for other generic ships can be found in deliverable D05.8 [18].

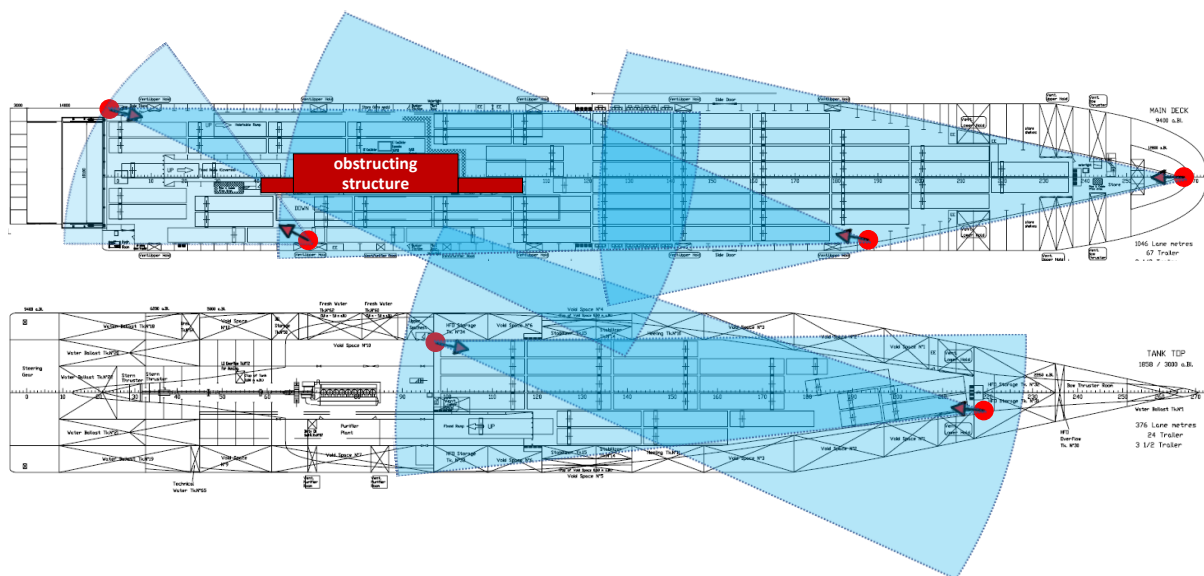


Figure 10: Integrated example of a thermal imaging fire detection system for the closed ro-ro spaces on Magnolia Seaways consisting of 4 cameras for the main deck (top figure) and 2 cameras for the tank top (bottom figure).

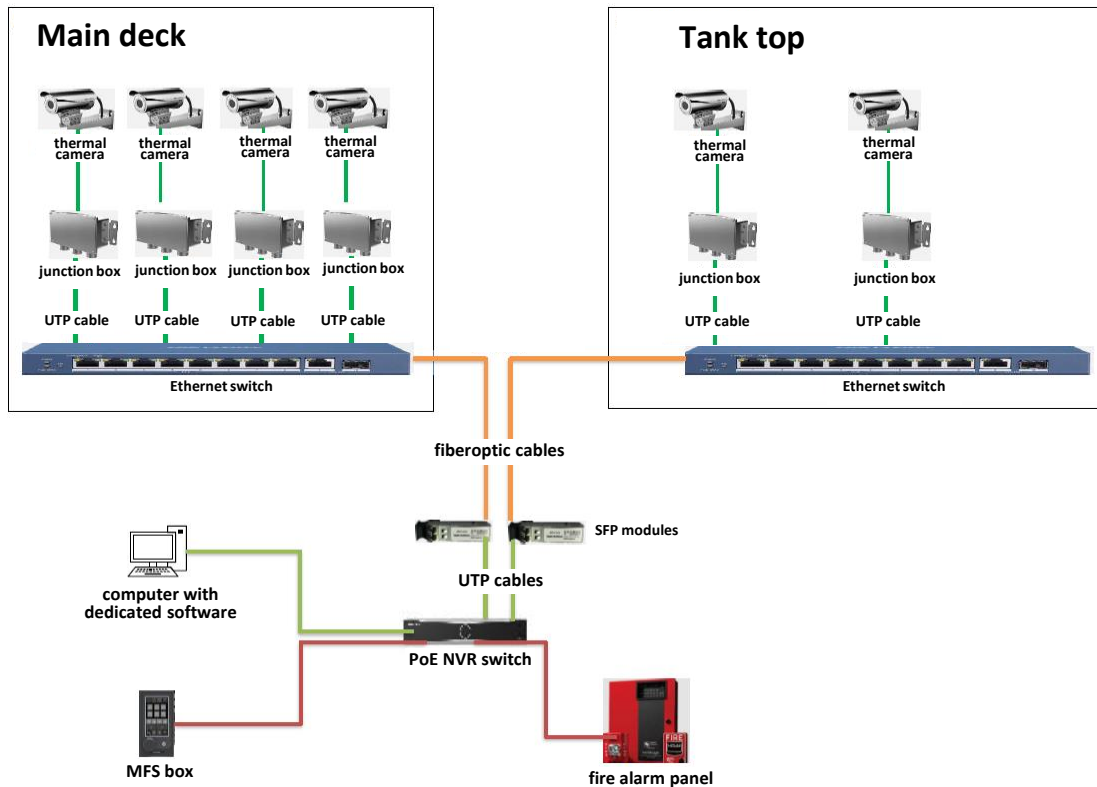


Figure 11: Concept of a detection system based on thermal imaging (infrared) cameras for closed ro-ro spaces on Magnolia Seaways, i.e., on the main deck and the tank top as shown in Figure 10.

Table 2. Estimated costs for the proposed thermal imaging detection system shown in Figure 11 for Magnolia Seaways.

Investment item	Cost in EUR
Purchase of system	73 850
Integration design and validation	8 000
Assembly/installation	31 350
Commissioning	1 000
Administration	12 000
Operator training	500
Total maintenance cost (assuming lifetime for existing ship is 22.9 years)	80 835
Total	207 535

7.2.2 Video fire detection for a generic ship

Just as other optical detectors, regular cameras used for video detection rely on a free line of sight to the flame or smoke. Moreover, the detection range for the cameras follows the square law between distance and the area of detection as long as the distance is high compared to the characteristic length of the object to be detected, such that detection at twice the distance requires nearly four times the area, as illustrated in Figure 8. Moreover, the area is proportional to the fire size in terms of radiant heat output (RHO). Therefore, if a flame detector is able to detect a fire with RHO = 40 kW at 30 m, detection at 60 m is expected to require a fire with RHO = 160 kW.

Using a video fire detection system, each camera can cover a large area for fire detection. However, the use of cameras below the deckhead of ro-ro spaces limits their field of view, especially if a tall vehicle is loaded directly in front of the camera (see Figure 9).

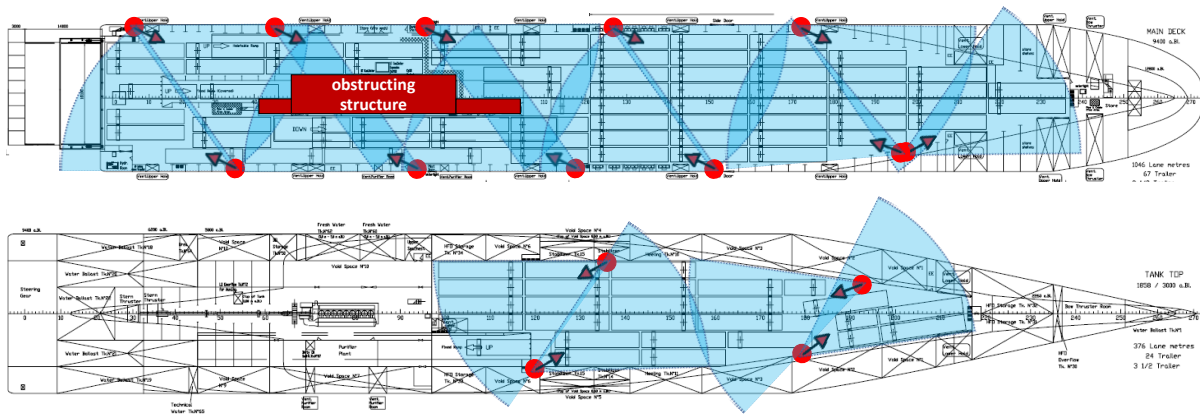


Figure 12: Integrated example of a video fire detection system for the closed ro-ro spaces on Magnolia Seaways consisting of 11 cameras for the main deck (top figure) and 4 cameras for the tank top (bottom figure).

Figure 12 illustrates an example video fire detection system integrated into the closed ro-ro spaces on Magnolia Seaways (ro-ro cargo ship), consisting of 11 cameras for the main deck and 4 cameras for the tank top. The cameras in this example have medium sensitivity settings allowing effective detection range of nearly 40 m at 54° horizontal angle and 40° vertical angle. The cost estimate for this system is presented in Table 3. Examples for other generic ship types can be found in deliverable D05.8 [18].

Table 3. Estimated costs for the proposed video detection system shown in Figure 12 for closed ro-ro spaces on Magnolia Seaways, consisting of 11 cameras for the main deck (top figure) and 4 cameras for the tank top (bottom figure).

Investment item	Cost in EUR
Purchase of system	114 840
Integration design and validation	8 000
Assembly/installation	33 900
Commissioning	1 000
Administration	8 000
Operator training	500
Total maintenance cost (assuming lifetime for existing ship is 22.9 years)	48 500
Total*	214 740
* This cost estimate is highly conservative. Increasing the detection sensitivity settings may allow the use of fewer cameras, thereby reducing the costs significantly. However, the level of sensitivity must not be too high such that it leads to frequent nuisance alarms.	

7.3 Conclusions

Video fire detection systems offer a good potential for ro-ro cargo decks which commonly incorporate CCTVs. However, for existing ships, integrating a video analytics algorithm with the existing CCTV may require supplementary hardware such as a computer that serves as a server for the in-situ analytics.

The cost estimations suggest that the installation of a thermal imaging system on ro-ro ships can cost lower than or comparable to that of a video fire detection system when fewer thermal cameras are needed than regular video cameras to cover a large area (see also examples discussed in D09.2 [5] and D05.8 [18]). For smaller ships, the overall cost of a thermal imaging system may be higher because of the higher camera costs. Nevertheless, thermal imaging systems provide the advantage of being more usable for both open and closed decks, whereas video fire detection systems are primarily recommended for closed decks where light conditions are stable. Moreover, thermal imaging can highlight hot spots that video analytics cannot. All in all, the most significant system costs are those

related to the purchase of the components and the installation work, while lower costs are associated with inspection, testing, and maintenance. It is also noteworthy that the cost estimations presented herein incorporated conservative assumptions and are expected to be moderately dependent on the ship's design. Specifically, obstruction arrangements such as engine casing, staircases as well as deck area size and shape, have an impact on the number of detection units to be installed, which represent most of the installation and maintenance cost.

8 Laboratory evaluations

Main author of the chapter: Davood Zeinali, FRN

This chapter discusses the laboratory experiments performed as part of the detection work package (WP9) of LASH FIRE. Firstly, indoor laboratory experiments are discussed regarding fire detection using several thermal imaging systems and a video fire detection system under conditions relevant to ro-ro spaces. Subsequently, several outdoor large-scale fire suppression tests are discussed regarding the usefulness of thermal and regular cameras during fire suppression activities in weather deck environments. These large-scale experiments were performed along with fire suppression studies done by the extinguishment work package (WP10) as described in deliverable D10.3 [12], which also discusses the validation experiments of an autonomous fire suppression system guided by two IR array flame wavelength detectors for weather deck environments (see explanations for Figure 5 in the present document). Lastly, this chapter discusses several fire experiments conducted as part of WP9 to evaluate the wind effects on flame perception using thermal imaging and regular video cameras.

8.1 Fire detection experiments with four ISO 8ft containers

A variety of fire scenarios with four ISO 8ft containers were studied through two separate test series, namely, a test series in November 2020 and another test series in June 2021. Table 4 presents the nomenclature of the detectors used for visual fire localisation and confirmation. The first test series included one flame wavelength detector and two thermal imaging cameras, while the second test series included two flame wavelength detectors, three thermal imaging cameras, and a video fire detection algorithm which included both flame and smoke detection. The systems were tested with their default sensitivity settings for detection.

Table 4: List of the tested detectors in the two series of laboratory experiments for open and closed ro-ro spaces.

Detector ID	Detector type	Test series
FD1	IR array flame wavelength detector (16x16 IR sensors)	1 and 2
FD2	Triple-IR flame wavelength detector	2
FD3	Triple-IR flame wavelength detector	2
IR1	IR thermal imaging camera 1	1 and 2
IR2 a/b*	IR thermal imaging camera 2 with settings 'a' and 'b'	1 and 2
IR3***	IR thermal imaging camera 3	2
VSD	Video smoke detection analytics using a regular camera**	2
VFD	Video flame detection analytics using a regular camera**	2
* IR2a used settings that allowed vehicle nuisance source discrimination. IR2b used default settings without this feature. ** The camera was HIKVISION DS-2CD2342WD-I, 2.8mm Lens, 4 MP. *** IR3 here means the third IR camera, and it is not to be confused with triple-IR technology used by FD1 and FD2.		

8.1.1 Experimental setup

Two series of tests were conducted in the large fire test hall at RISE Fire Research in Trondheim, Norway. The hall has an adjustable ceiling height as shown in Figure 13. The test area was made with 4 steel ISO 8ft containers measuring 2.43 m x 2.2 m x 2.26 m (Length x Width x Height) which were spaced 0.5 m apart, placed 0.2 m above the floor on supporting blocks at their corners as shown in Figure 14. As the fire location in different tests was at different positions relative to the containers, the fire was not directly visible to the detectors in some scenarios. The positions of ignition sources and detectors are shown through Figures 15, 16, and 17. Positions P6 and P5 were openly visible from the detectors, while the others were shielded. Position P4 from test series 1 is the same position as F3 in series 2, but the door in the container was open in the first series and closed in the second series.

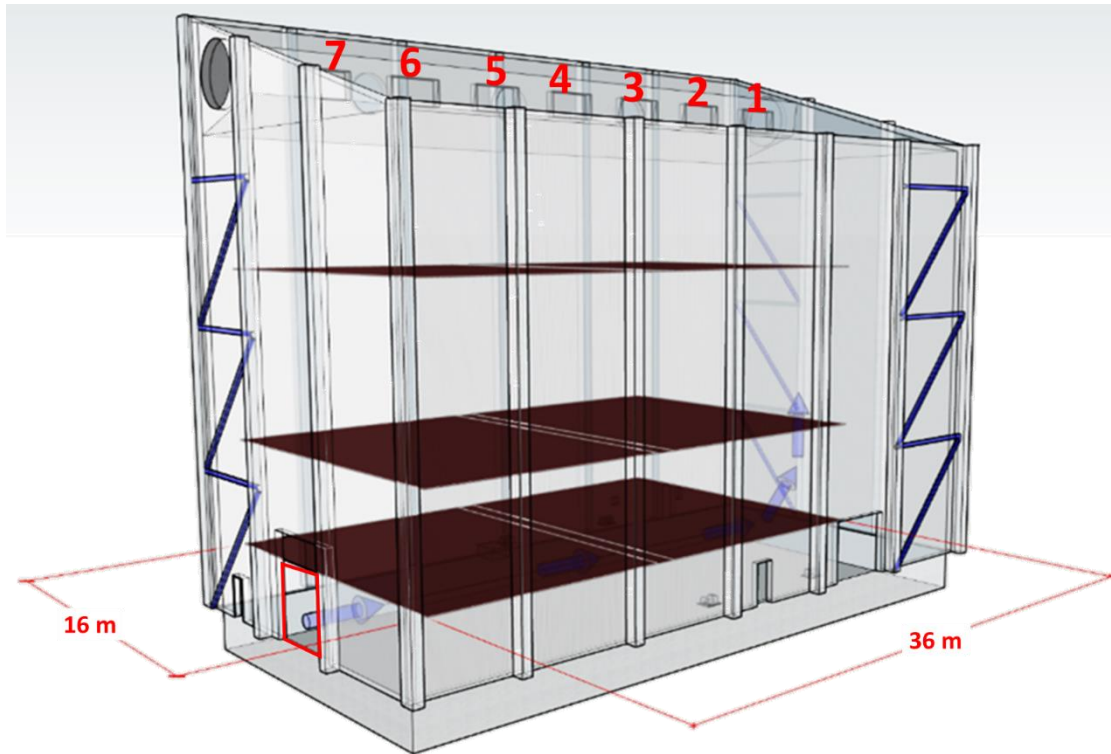


Figure 13: The large fire test hall at RISE Fire Research in Trondheim, Norway. The purple arrows indicate the wind direction across the test hall when using an open western gate measuring 4.5 m wide and 4.3 m high (marked with a red rectangle) and ventilation fans at the top of the hall (numbered 1 to 7 with red digits). The adjustable ceiling measuring 25 m long and 16 m wide was fixed at heights of 3 m and 5 m for ro-ro space tests, and at 16 m for weather deck tests as illustrated.

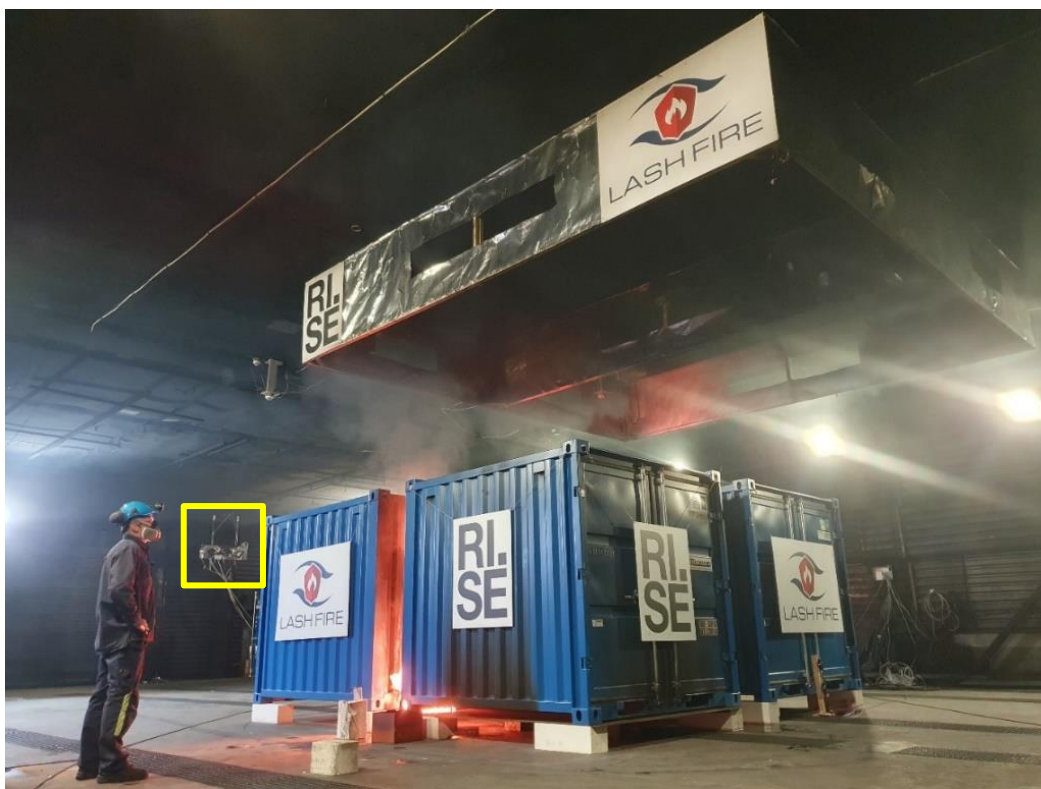


Figure 14. The experimental setup with 5 m ceiling height. The detectors relevant for visual fire confirmation and localisation can be seen to the left, marked with a yellow rectangle (location specified more accurately in Figure 17).

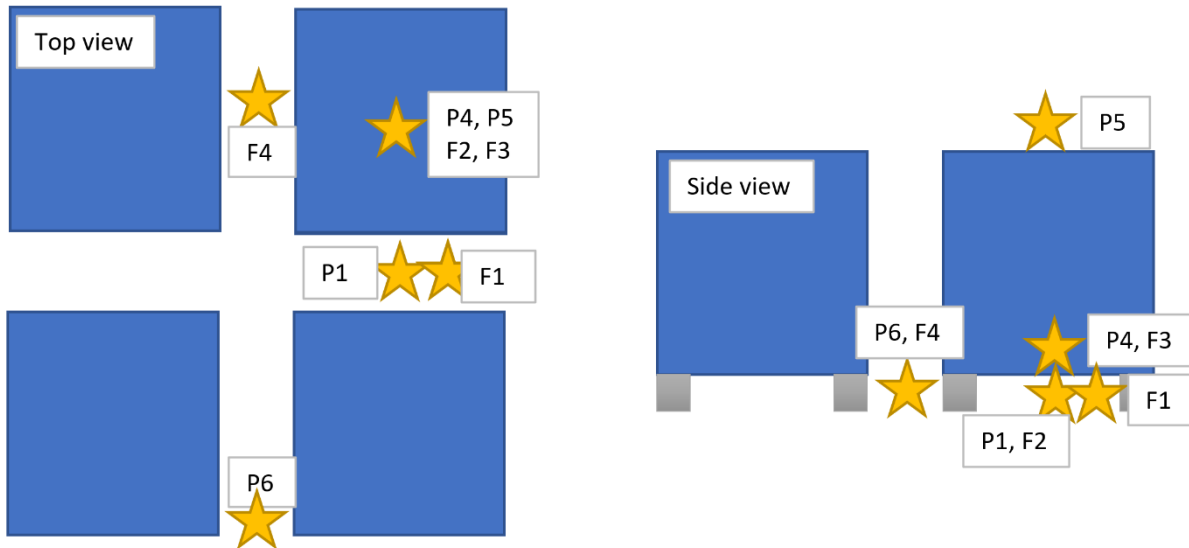


Figure 15: Positions of the ignition sources relative to the steel containers. Positions used in test series 1 are marked with P1, P4, P5 and P6, and positions used in test series 2 are marked with F1 to F4.

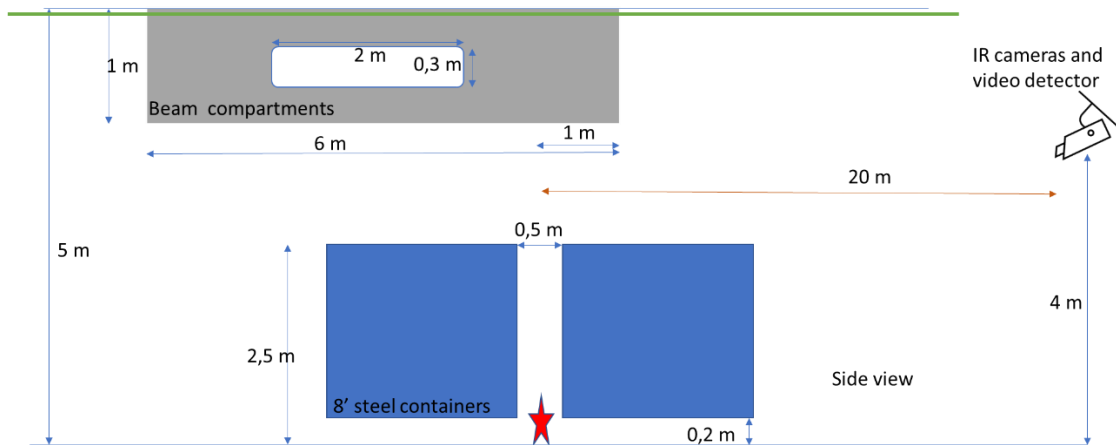


Figure 16: Side view sketch of the experiment configuration in the second test series with a ceiling height of 5 m. The camera height was different for other ceiling heights tested (see explanations for Figure 17).

During the tests without wind, the fans were inactive, and the gates of the test hall were closed, such that the only air circulation in the room was that created by the fires. In the tests with wind (conducted only during the first test series), windy conditions were generated by extracting air using ventilation fans and by opening the test hall's western gate (measuring 4.5 m wide and 4.3 m high as shown in Figure 13), creating wind blowing from west to east across the test hall. The maximum wind velocity achieved was with both ventilation fans active and a ceiling height of 3 m, which was approximately 5 m/s at 3 m west of the 8ft containers and 1.5 m height near the centre of the hall (see central wind sensor location shown in Figure 17), where the total airflow through the gate was 106 m³/s. The wind velocities reported in the next section through Table 5 are for this central location. In addition, the velocities were characterised along the transversal wind measurement plane shown in Figure 17 across the height and in the transversal direction, the results of which are presented in Figure 18.

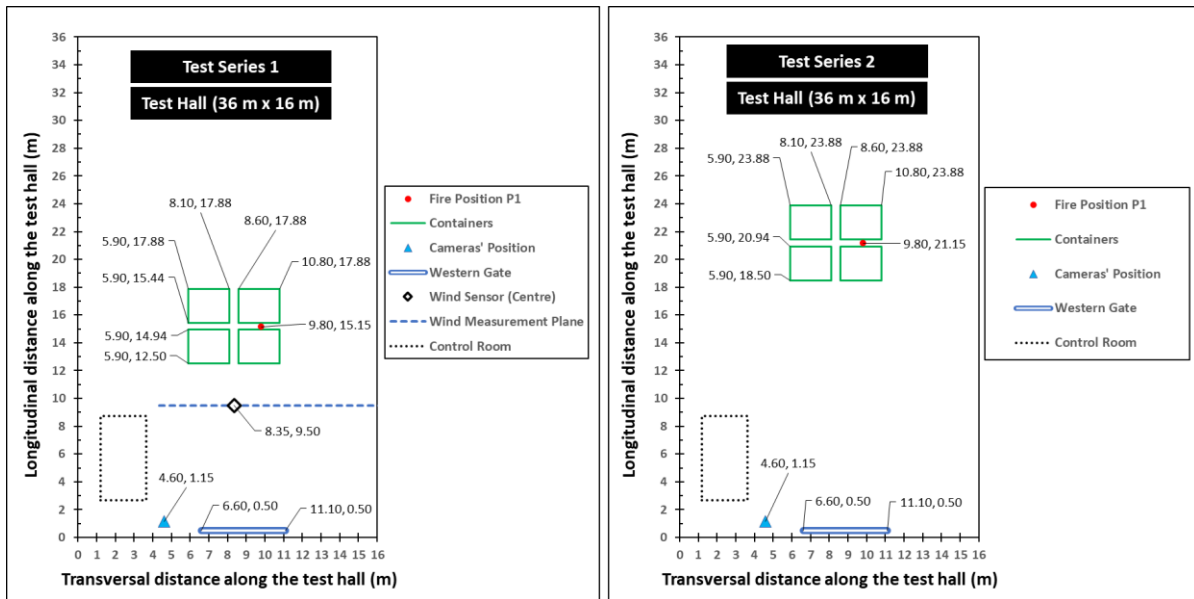


Figure 17: Top view of setup used in the two series of LASH FIRE tests. The numbers indicate the X and Y positions of items in the test hall. The four green squares indicate the outlines of the ISO 8ft containers. During the first test series, the detector cameras were mounted at the height of 2 m for ro-ro space tests with a ceiling height of 3 m, while they were mounted at the height of 5.5 m during weather deck tests with a ceiling height of 16 m. During the second test series, the detector cameras were mounted at the height of 4 m for ro-ro space tests with a ceiling height of 5 m and weather deck tests with a ceiling height of 16 m. The wind sensor was used only during the first test series and its central location was at the height of 1.5 m. Other wind measurements were made across the transversal plane which is marked with a dotted line in the diagram (wind data shown in Figure 18).

As shown in Figures 14 and 17, the detector cameras were installed on the wall beside the western gate at different heights depending on the chosen ceiling height. During the first test series, the ro-ro space tests had a ceiling height of 3 m and the detector cameras were mounted at the height of 2 m, while the weather deck tests had a ceiling height of 16 m and the cameras were mounted at the height of 5.5 m. During the second test series, the ro-ro space tests had a ceiling height of 5 m and the detector cameras were mounted at the height of 4 m, while the weather deck tests had a ceiling height of 16 m and the cameras were mounted at the height of 4 m.

The first test series was conducted with a flat ceiling, while the second test series was conducted with vertical barriers mounted on the ceiling to simulate the beam constructions that are common in ro-ro decks. The vertical barriers were wooden beams covered by welding cloth and divided the ceiling into two rectangular compartments measuring 3 x 6 x 1 m. Experiments with ceiling barriers were conducted both with these barriers sealed and with openings measuring 10% of the total area of each of the barrier walls. These dimensions are found to be typical for many ro-ro ships and correspond well with those of deck 3 on Stena Flavia as shown in Figure 19. The star in Figure 19 indicates the primary beam compartment to be filled with smoke, while the yellow rectangles will be filled next, and the green compartments that contain smoke detectors will be filled lastly.

In the second series of tests, several experiments were also dedicated to evaluating whether the reflections of a flame can trigger the thermal imaging and video fire detection systems. In these tests, the fire was not directly visible in the field of view of the cameras. The corrugated steel wall of a container was placed as a mirror to reflect the light from the fire to the cameras as shown in Figure 20. The distance between the reflection surface of the container and the detectors was varied from 5 m to 14.5 m.

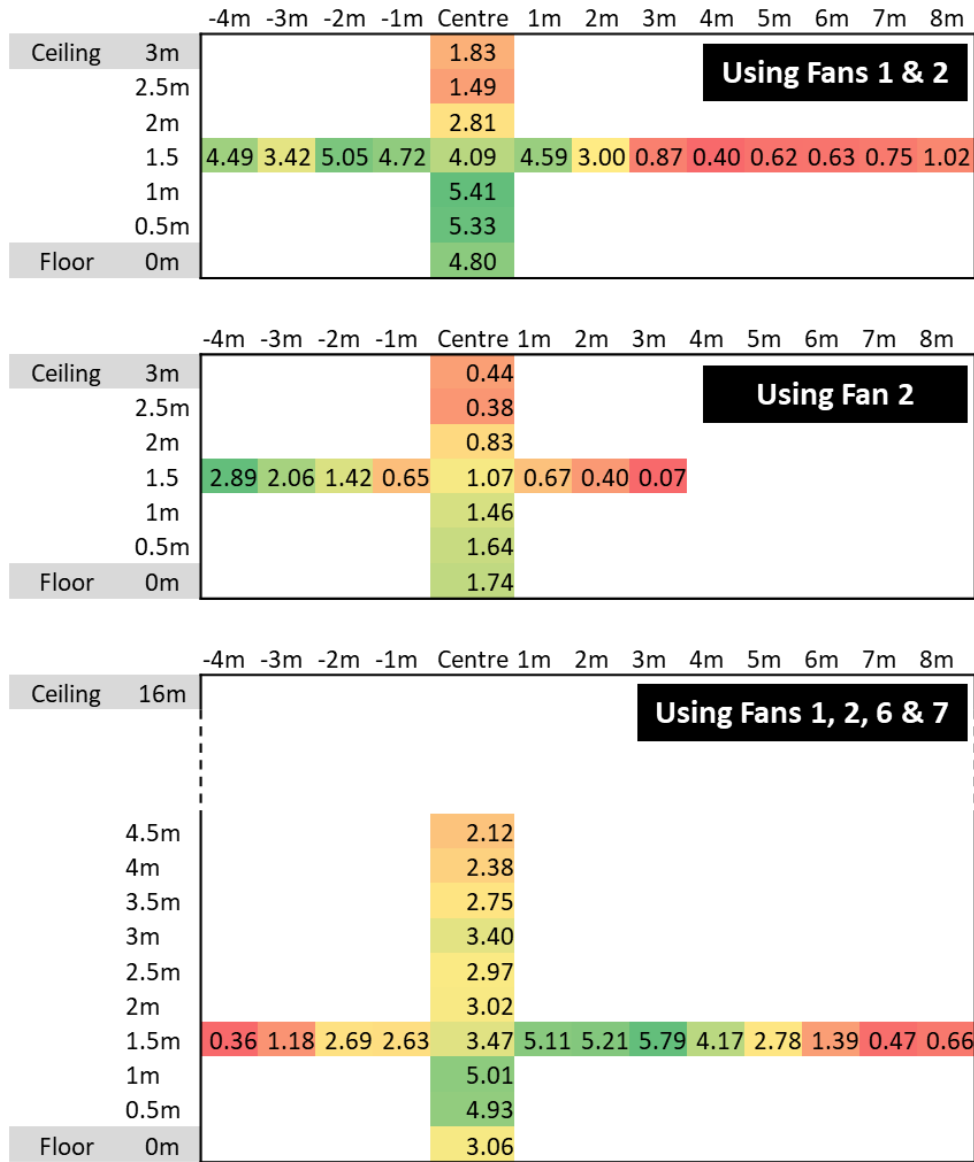


Figure 18: Wind velocities (m/s) along the wind measurement plane shown in Figure 17 with active fans shown in Figure 13: (top) ro-ro space test with fans 1 & 2; (middle) ro-ro space test with fan 2; (bottom) weather deck test with fans 1, 2, 6 & 7.

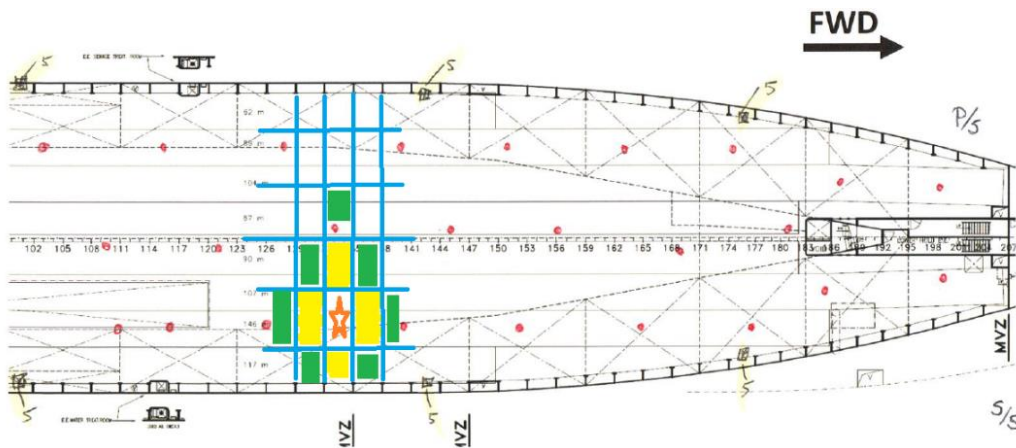


Figure 19: Sketch of deck 3 in Stena Flavia with ceiling beams drawn with blue lines and smoke detectors marked with red dots. The star indicates a worst-case fire position where smoke needs to pass the most beams to reach smoke detectors.

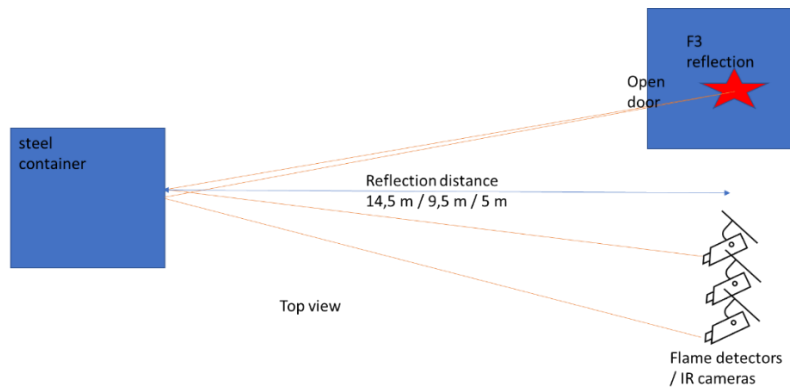


Figure 20: Top view sketch of the test configuration used in the reflection tests in the second test series. The fire was placed in a container with open doors outside the field of view of the detectors and a steel container was used as a reflective surface with distances of 5 m, 9.5 m, and 14.5 m from the detectors.

8.1.2 Fire sources

The laboratory experiments were conducted with three types of fire sources: beechwood sticks on a hot plate, liquid pools of heptane and ethanol, and lithium-ion batteries.

The beechwood sticks on a hot plate ignition source is based on the test setup described in EN 54-29 annex I of a smouldering wood fire [22]. The beechwood sticks are sized 20 mm x 25 mm x 75 mm and are heated on a hot plate to release a light grey smoke without ignition, as shown in Figure 21. The heat ramp of the heater was such that it reached 350°C in 4 minutes.



Figure 21: Beechwood sticks on a hot plate generating light grey smoke without flames.

Liquid pool fires with ethanol and n-heptane were tested according to the guidelines of EN 54-10 [11]. The fuel was added to a water base in trays of different dimensions. In the first test series, a square tray measuring 30 x 30 cm², a circular tray with a diameter of 10 cm, and a circular tray measuring 15 cm in diameter were used. In the second test series, heptane was the only fuel source used, with rectangular pools of three sizes, namely 30 x 30 cm, 50 x 50 cm, and 60 x 60 cm. The corresponding average heat release rate of each fire was estimated at 65, 302 and 364 kW, respectively (calculated based on the fuel amount, burn time, as well as assumptions of a heat of combustion of 33 MJ/litre, a constant mass loss rate over the burn time, and complete combustion). The maximum flame height is

shown in Figure 22. The flames from the smallest pool fire did not reach the top of the containers, while the flames of the medium sized pool extended beyond the top intermittently, and the largest pool fire extended beyond the top of the containers for most of the time. Hence, only the two larger fires were visible from the location of the wall-mounted optical detectors. Both the heptane fires and ethanol fires produced visible smoke and luminous flames, but the smoke was more visible for the heptane fires and its flame was more luminous.



Figure 22: Maximum extension of the flame lengths for the three heptane pan fires of 30 x 30 cm (left), 50 x 50 cm (middle) and 60 x 60 cm (right).



Figure 23: Overheating three lithium-ion battery cells in a steel enclosure with electric heating elements. The steel box was open in the front. Insulation was placed on top of the box during tests to get a more uniform heating of all three cells.

The lithium-ion battery experiments in the first test series involved initially two experiments with a battery module containing 24 cells (each being a 3.63-Volt, 60-Amp hour, 218-Watt hour LGY LGCHEM li-ion pouch cell, measuring 35.3 cm x 10.0 cm x 1.6 cm), connected to a short-circuit device employing several hundred amperes of current through a coil around a pipe with internal water cooling, but this scenario did not produce much overheating or smoke because the short-circuit of the battery broke within a second. Therefore, a third experiment was conducted, including heating a single cell (235-Watt-hour LG JP3 NMC pouch cell), namely by placing it over the heater shown in Figure 21. During the second test series, two experiments were conducted using a steel box containing three battery cells (each being a 235-Watt-hour LG JP3 NMC pouch cell as in the first test series), heated with two 500-W electric heating elements until the end of the experiment as shown in Figure 23. The battery

cells were placed inside the test container, 60 cm above the floor, and with the container door fully open. This corresponds to position P4 in Figure 15.

8.1.3 Results and discussion

The detection times for the tested detectors in the two test series are shown in Tables 5, 6, 7, and 8, while an analysis of the results for each detector is presented below in the next subsections. Some of the tests and detectors could not be analysed, as they were not comparable due to differences in fire visibility or data output from the detection systems.

Table 5: Detection time of detectors (in seconds) during ro-ro space experiments in the first test series (ceiling height = 3 m, detectors' height = 2 m), sorted based on the ignition position. 'ND' means 'No Detection'. Empty fields mean that the detector was not active during the test. The wind velocities were measured at the central wind sensor position shown in Figure 17.

Test no	Fuel	Fuel amount (l)	Pool size	Ignition position	Wind (m/s)	Flame wavelength detector	Thermal imaging cameras		
						FD1	IR1	IR2a	IR2b
8	Beech, hot plate	6 Sticks		P1	0	ND	ND	ND	ND
19	Ethanol	1	30 x 30 cm	P1	0	ND	ND	ND	ND
30	Ethanol	1	30 x 30 cm	P1	1	ND	ND	ND	ND
13	Heptane	1	30 x 30 cm	P1	0	ND	ND	ND	ND
42	Heptane	1	30 x 30 cm	P1	0	ND	ND	ND	ND
10	Heptane	0.1	∅ 10 cm	P1	0	ND	ND	ND	ND
22	Heptane	1	30 x 30 cm	P1	1	ND	97	ND	ND
39	Heptane	1	30 x 30 cm	P1	5	ND	125	ND	ND
6	Beech, hot plate	6 Sticks		P4	0	ND	ND	ND	ND
21	Beech, hot plate	6 Sticks		P4	1	ND	ND	ND	ND
38	Beech, hot plate	6 Sticks		P4	5	ND	ND	ND	ND
31	Ethanol	1	30 x 30 cm	P4	1	ND	ND	ND	ND
1	Heptane	0.3	∅ 15 cm	P4	0	ND	ND	ND	ND
2	Heptane	1	30 x 30 cm	P4	0	ND	75	ND	ND
5	Heptane	1	30 x 30 cm	P4	0	ND	74	ND	ND
4	Heptane	0.3	∅ 15 cm	P4	0	ND	ND	ND	ND
7	Heptane	0.2	∅ 15 cm	P4	0	ND		ND	ND
20	Heptane	1	30 x 30 cm	P4	1	ND	185	ND	ND
37	Heptane	1	30 x 30 cm	P4	5	ND	ND	ND	ND
33	Li-ion module	24 cells		P4	0	ND	ND	ND	ND
34	Li-ion module	24 cells		P4	0	ND	ND	ND	ND
35	Li-ion cell	1 pouch		P4	0	ND	ND	ND	ND
18	Ethanol	0.01	∅ 10 cm	P5	0	ND	9	ND	23
29	Ethanol	0.01	∅ 10 cm	P5	1	ND	117	ND	ND
9	Heptane	0.01	∅ 10 cm	P5	0	ND	10	ND	ND
27	Heptane	0.01	∅ 10 cm	P5	1	ND	0	ND	ND
11	Beech, hot plate	6 Sticks		P6	0	ND	82	338	256
24	Beech, hot plate	6 Sticks		P6	1	ND	474	376	156
32	Ethanol	1	30 x 30 cm	P6	1	6	9	20	18
17	Ethanol	1	30 x 30 cm	P6	0	5	10	8	6
41	Heptane	1	30 x 30 cm	P6	0	4	9	3	7
25	Heptane	1	30 x 30 cm	P6	1	6	9	4	26
40	Heptane	1	30 x 30 cm	P6	5	5	9	9	6

Table 6: Detection time of detectors (in seconds) during weather deck experiments in the first test series (ceiling height = 16 m, detectors' height = 5.5 m), sorted based on the ignition position. 'ND' indicates 'No Detection'. Empty fields indicate that the detector was not active during the test. The wind velocities were measured at the central wind sensor position shown in Figure 17.

Test nr	Fuel	Fuel amount	Pool size	Ignition position	Wind (m/s)	Flame wavelength detectors			Thermal imaging cameras		
						FD1	FD2	FD3	IR1	IR2a	IR2b
56	Ethanol	1 liter	30 x 30 cm	P1	0	ND	ND	ND	ND	ND	ND
45	Heptane	1 liter	30 x 30 cm	P1	0	ND	ND	ND	156	ND	ND
64	Heptane	1 liter	30 x 30 cm	P1	5	ND	ND	ND	ND	ND	ND
60	Ethanol	1 liter	30 x 30 cm	P4	0	ND	ND	ND	ND	ND	ND
43	Heptane	1 liter	30 x 30 cm	P4	0	ND	ND	ND	114	ND	ND
63	Heptane	1 liter	30 x 30 cm	P4	5	ND	ND	ND	ND	ND	ND
48	Ethanol	0.01 liter	∅ 10 cm	P5	0	ND	2	ND	19	ND	22
67	Ethanol	0.01 liter	∅ 10 cm	P5	5	ND	14	ND	19	ND	24
49	Heptane	0.01 liter	∅ 10 cm	P5	0	ND	4	ND	23	ND	60
66	Heptane	0.1 liter	∅ 10 cm	P5	5	69	46	134	57	ND	83
50	Beech, hot plate	0 Sticks	Hotplate	P6	0	ND	ND	ND	51	165	78
52	Beech, hot plate	0 Sticks	Hotplate	P6	0	ND	ND	ND	57	160	93
53	Beech, hot plate	6 Sticks	Hotplate	P6	0	ND	ND	ND	85	337	171
55	Ethanol	1 liter	30 x 30 cm	P6	0	4	0	8	2	6	5
57	Ethanol	0.01 liter	∅ 10 cm	P6	0	45	6	ND	23	59	25
58	Ethanol	0.01 liter	∅ 10 cm	P6	0	108	15	ND	ND	ND	ND
68	Ethanol	1 liter	30 x 30 cm	P6	5	7	4	9	5	26	16
70	Ethanol	0.01 liter	∅ 10 cm	P6	0	ND	77	249	178	ND	ND
44	Heptane	1 liter	30 x 30 cm	P6	0	5	0	8	9	4	8
59	Heptane	0.1 liter	∅ 10 cm	P6	0	72	57	135	105	ND	ND
61	Heptane	0.1 liter	∅ 10 cm	P6	0	39	4	298	12	42	14
65	Heptane	1 liter	30 x 30 cm	P6	5	5	0	6	0	5	8

Table 7: Detection time of detectors (in seconds) during ro-ro space experiments in the second test series with heptane pool fires and lithium-ion batteries (ceiling height = 5 m, detectors' height = 4 m), sorted based on the ignition position. 'ND' indicates 'No Detection', i.e., the detector did not detect the fire. 'Yes' indicates detection happened while the timing was not recordable. Empty fields indicate that the detector was not active during the test. VSD is video smoke detection and VFD is video flame detection. IR1 to IR3 are simply infrared thermal cameras 1 to 3, and there is no difference in their technology.

Test no	Fire size	Fuel amount (l)	Position	Beam	Burn time (s)	Average HRR (KW)	Flame detectors		Video detection		IR cameras		
							FD1	FD2	VDS	VDF	IR2	IR3	IR1
16	30 x 30 cm	1	F1	10% open	522	63	ND	ND	186	ND	ND	ND	ND
20	30 x 30 cm	1	F1	10% open	478	69	ND	ND		ND	ND		81
3	30 x 30 cm	1	F1	Closed	533	62	ND	ND		ND			
4	30 x 30 cm	1	F1	Closed	469	70	ND	ND	203	ND	ND		
9	30 x 30 cm	1	F1	Closed	530	62	ND	ND	199	ND	ND		ND
17	50 x 50 cm	3	F1	10% open	371	267	28	11	43	ND	yes	22	yes
18	50 x 50 cm	3	F1	10% open	378	262	25	20	60	ND	yes	19	
2	50 x 50 cm	1,5	F1	Closed	131	378	27	17		151		22	
5	50 x 50 cm	3	F1	Closed	304	326	33	19	64	ND	ND	21	
6	50 x 50 cm	3	F1	Closed	310	319	35	13	42	ND	yes	13	
10	50 x 50 cm	3	F1	Closed	378	262	20	17	43	ND	ND	11	yes
19	60 x 60 cm	4	F1	10% open	359	368	20	14	ND	ND	yes	16	12
7	60 x 60 cm	4	F1	Closed	367	360	17	12	154	ND	yes	11	
8	60 x 60 cm	4	F2	Closed	1098	120	ND	ND	78	ND	ND	ND	yes
11	30 x 30 cm	0,5	F3	Closed	402	41	ND	ND	ND	ND	ND	193	yes
13	30 x 30 cm	1,5	F3	Closed	722	69	ND	ND	ND	ND	ND	172	yes
12	50 x 50 cm	1,5	F3	Closed			ND	ND	ND	ND	yes	yes	
14	30 x 30 cm	1	F4	Closed	465	71		58	155	ND	ND	ND	ND
15	50 x 50 cm	3	F4	Closed	371	267	26	2	30	86	ND	9	157
27	Li-ion cells		F4	10% open			ND	ND	1516	ND	ND	ND	ND
28	Li-ion cells		F4	10% open			ND	ND	2912	ND	ND	ND	2132

Table 8: Detection time of detectors (in seconds) during weather deck experiments in the second test series with heptane pool fires (ceiling height = 16 m, detectors' height = 4 m). 'ND' indicates 'No Detection', i.e., the detector did not detect the fire. 'Yes' indicates detection happened while the timing was not recordable. Empty fields indicate that the detector was not active during the test. IR1 to IR3 are simply infrared thermal cameras 1 to 3, and there is no difference in their technology.

Test no	Pool size	Fuel amount (l)	Ignition position	Reflection distance (m)	Burn time (s)	Average HRR (kW)	Flame wavelength detectors		Video detection		IR thermal cameras		
							FD1	FD2	VSD	VFD	IR1	IR2	IR3
3	30 x 30 cm	1	F1		533	62	ND	ND	ND	ND			ND
4	30 x 30 cm	1	F1		469	70	ND	ND	192	ND		ND	ND
9	30 x 30 cm	1	F1		530	62	ND	ND	194	ND	ND	ND	ND
16	30 x 30 cm	1	F1		522	63	ND	ND	181	ND	ND	ND	ND
20	30 x 30 cm	1	F1		478	69	ND	ND	ND	ND	81	ND	ND
2	50 x 50 cm	1.5	F1		131	378	27	17	ND	ND			22
5	50 x 50 cm	3	F1		304	326	33	19	58	ND		ND	21
6	50 x 50 cm	3	F1		310	319	35	13	42	ND		yes	13
10	50 x 50 cm	3	F1		378	262	20	17	35	ND	yes	ND	11
17	50 x 50 cm	3	F1		371	267	28	11	35	ND	yes	yes	22
18	50 x 50 cm	3	F1		378	262	25	20	56	ND	ND	yes	19
7	60 x 60 cm	4	F1		367	360	17	12	146	ND		yes	11
19	60 x 60 cm	4	F1		359	368	20	14	39	ND	12	yes	16
11	30 x 30 cm	0.5	F3		402	41	ND	ND	ND	ND	yes	ND	193
12	50 x 50 cm	1.5	F3		not registered		ND	ND	ND	ND	yes	ND	yes
13	30 x 30 cm	1.5	F3		722	69	ND	ND	ND	ND	yes	ND	172
14	30 x 30 cm	1	F4		465	71	ND	58	151	ND	ND	ND	ND
15	50 x 50 cm	3	F4		371	267	26	2	26	86	157	ND	9
21	30 x 30 cm	0.2	F5	14.5	103	64	ND	ND	37	ND	ND	ND	ND
22	30 x 30 cm	0.2	F5	14.5	100	66	ND	21	67	ND	ND	ND	ND
23	50 x 50 cm	0.5	F5	14.5	83	199	ND	1			29	ND	ND
24	60 x 60 cm	0.7	F5	14.5	83	278	ND	3			17	ND	ND
25	60 x 60 cm	0.7	F5	9.5	77	300	10	2			5	27	ND
26	60 x 60 cm	0.7	F5	5	83	278	4	2			9	25	ND

8.1.3.1 Flame wavelength detectors

The flame wavelength detectors quickly detected those fires that were directly visible to the detectors, i.e., in ignition positions P5, P6, and F4, except for some cases of 10-cm-diameter pool fires which were too small at location P5. In test 66 with a wind velocity of 5 m/s, the 10-cm diameter heptane fire was also detected, perhaps because the wind helped the fire grow slightly bigger. Beechwood sticks on the hot plate did not produce flames so they were not detectable even at ignition positions P5, P6, and F4. For other ignition locations not directly visible to the detectors, no fire was detected by the flame wavelength detectors, except in tests with 50x50 and 60x60 cm² heptane fires which extended beyond the height of the containers (Table 7) as well as in the reflection tests 22 to 26 where a reflection path was made specifically toward the detectors (Table 8). Considering all the scenarios where the flame wavelength detectors did detect the fire, the detection times are well below 30 s in most cases. However, it is obvious that these detectors require a free line of sight to the flame or its reflection for detection. Therefore, the usage of these detectors below the deckhead of ro-ro decks is expected to be limited because of the tight arrangement of vehicles (see Figure 9), whereas the weather deck environment where they can have a better view of the area is expected to be more suitable for these detectors.

Of the three flame wavelength detectors evaluated during the first test series of weather deck experiments, FD2 was usually the fastest to trigger the alarm, followed by FD1 and finally FD3. This corresponds to the sensitivity tests that were conducted by moving a small 10-cm-diameter ethanol fire slowly towards the detectors, marking the maximum distance where each of the detectors triggered the alarm. These measurements of maximum detection distance are presented in Table 9 along with those of thermal imaging cameras IR1 and IR2. The differences in the detection distance are assumed to be mainly caused by software and alarm threshold settings, which can be adjusted for each detector to optimize the balance between early detection and the frequency of nuisance alarms.

Table 9: Maximum distance where the different detectors triggered the alarm based on a $\varnothing 10$ cm ethanol fire. IR1 and IR2 are thermal imaging cameras, and FD1 to FD3 are flame wavelength detectors.

Detector ID	Maximum distance of detection for a $\varnothing 10$ cm ethanol fire
IR1	31 m
FD2	23 m
FD1	13 m
IR2	13 m
FD3	11 m

Figure 24 shows an example image obtained using the built-in camera of a triple-IR flame wavelength detector during a LASH FIRE demonstration. The flame detector and its built-in video camera cover approximately the same field of view, so the operator looking at the video should be able to tell if the alarm is triggered by a real fire or a nuisance source. Triple-IR detectors cannot localise the fire on their own, but IR array flame wavelength detectors can, and thus IR array detectors are also able to highlight the fire location in their video output accordingly (see explanations for Figure 2).



Figure 24: Video image from the built-in camera of a triple-IR flame wavelength detector triggered by a flame during a LASH FIRE test. When the alarm is activated, the frame around the image turns red and the text "FIRE" is shown on the upper part.

8.1.3.2 Thermal imaging detectors

Figure 25 shows an example image obtained using a thermal imaging detection system during a demonstration test. The system software employs an infrared camera to detect hot areas, which are then highlighted in the captured thermal footage. Accordingly, operators looking at the footage will be able to see the location of the fire and respond appropriately.



Figure 25: Snapshot from the footage of a thermal imaging camera captured during a demonstration test. The high temperature area of the fire is marked with red, clearly drawing attention to the hot spot (see regular image in Figure 24).

The thermal imaging cameras were the only detectors that detected the beechwood sticks smouldering without flames on a hot plate, although detection was only possible for ignition position P6 which was directly visible to the cameras. Remarkably, the tests with the hot plate itself without wood sticks resulted in a shorter detection time than when wood sticks were used on the plate, suggesting that the visible portion of the hot plate surface has been more influential for detection using thermal imaging than the smouldering wood sticks (compare tests 50, 52, and 53 in Table 6).

Most of the $30 \times 30 \text{ cm}^2$ heptane pool fires were not detected as the flames from these fires did not reach the top of the containers (see Figure 22). Thermal imaging camera IR1 detected more of these fires than the other detectors. Thermal camera IR3 (here IR3 means third camera, not triple-IR technology) was the most sensitive to the heptane pool fires as it detected almost all the $50 \times 50 \text{ cm}^2$ and $60 \times 60 \text{ cm}^2$ fires. IR1 and IR2 detected some similar fires and some different fires. A slight difference appears for heptane pool fires in position F2, F3, and F4, where IR1 detects most of the fires while IR2 does not. These differences are expected to be due to the differences in the detection threshold sensitivity settings of the cameras.

In the tests with a 50×50 and $60 \times 60 \text{ cm}^2$ pool fires between two containers, the thermal imaging cameras were able to detect the heat reaching the top of the containers. Examples of this are shown through Figure 26 and Figure 27 from test 19 where the heat from the fire is clearly visible in the thermal image, which can be used for fire confirmation by the operators looking at the video. The tip of the flame was intermittently visible on top of the containers. The flickering temperatures of the flame tip can be seen in Figure 28 which shows the temperatures measured by the thermal imaging cameras. From the graph of the temperatures in the region of the flame tip, the flickering temperature is clearly visible from 0 to 300 seconds corresponding to the burn time of the fire. The recorded temperatures from IR2 and IR3 cameras also correspond well with each other up to the point where IR3 peaks at 200°C while IR2 continues to show the measured temperature values.



Figure 26: Screenshot from the software of thermal camera IR2 during test 19 (described in Table 8). Temperatures from selected hot areas are measured (see red rectangle) and recorded over time (see graph in Figure 28).

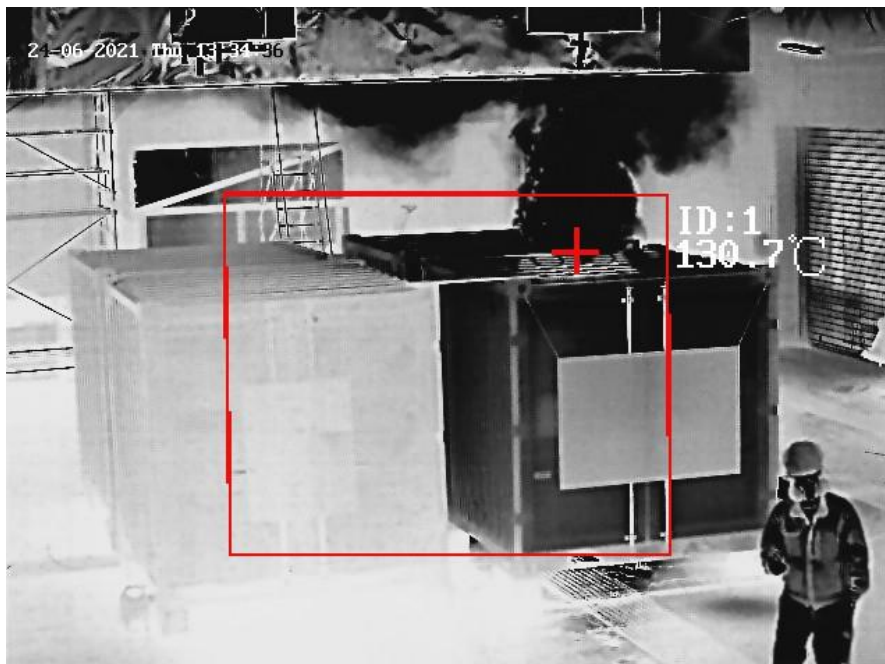


Figure 27: Image from the alarm of thermal imaging camera IR3 (here IR3 means third camera, not triple-IR technology) during test 19 (described in Table 8). The recorded maximum temperatures are presented in Figure 28.

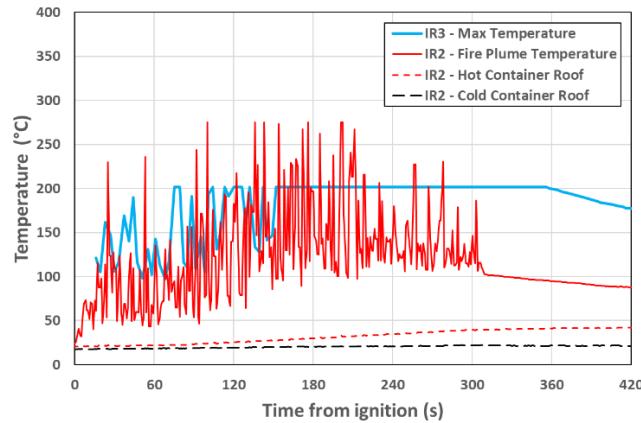


Figure 28: Flame and container roof temperatures measured using thermal imaging cameras IR1 and IR2 during test 19 (described in Table 8). Thermal images obtained using these cameras are shown in Figure 26 and Figure 27.

A clear advantage identified for thermal imaging cameras over the other tested detectors was the ability of thermal cameras to detect completely concealed fires without visible flames and smoke, e.g., a fire inside a closed cargo container as in tests 11, 12, and 13, where the hot container roof is detected by the thermal cameras and highlighted in their thermal image (see example in Figure 29). The thermal cameras recorded temperatures as high as 130-190 °C on top of the container in these tests, so the operator looking at the video should be able to perceive the fire risk and deal with the situation accordingly before it gets out of control. Moreover, a person walking in the area is clearly identifiable in the thermal image, which is valuable information to the operators in a fire situation. No other types of detectors could see flame/smoke in this test to trigger an alarm.



Figure 29: A fire inside a closed container detected by a thermal imaging detection system using an infrared camera (test 13 in Table 7). The hot roof of the container is marked with a red colour by the detection software to highlight the region of alarm.

The ignition positions P1 and P4 were not visible from the detector positions and only in two cases, namely in tests 43 and 45, one of the IR thermal cameras triggered an alarm from the heated surface or hot gases that were visible to the detector. This is expected to be due to the different nuances of the default threshold sensitivity settings of the three IR thermal cameras tested.

When the base of a 10-cm-diameter ethanol pool fire was shielded from the detectors (test 58 in Table 6), none of the thermal imaging cameras detected the fire. Similarly, when the base of a 10-cm-diameter heptane pool fire was shielded from the detectors (test 59 in Table 6), only one of the thermal cameras detected the fire. In contrast, the pool fires that had their base visible to the detectors (tests 57 and 61 in Table 6) were detected by all the thermal cameras. This suggests that an important part of the detection mechanism for the thermal camera was the hot surfaces at the base of the fire. This is while the flame wavelength detectors were much less influenced by the shielding of the fire base in their results, confirming that the visible flame tip is enough for these detectors to detect the fire.

All the flame reflection tests with 50 x 50 and 50 x 60 heptane pool fires were detected by some of the IR cameras. Moreover, as suggested by the measurements of the thermal camera IR2 shown in Figure 30, the properties of the reflecting surface determine the magnitude of the perceived temperatures. As Figure 30 indicates, the corrugated steel container located just 5 m away from the flame is perceived to have a temperature of 42.8°C, while the aluminium scaffolding located 25 m from the flame is perceived to have a temperature of 128.6°C. This illustrates that the reflectivity of the surface is more influential in determining its perceived temperature than the distance of the surface to the fire. Moreover, this indicates that the painted steel container walls are not very efficient in reflecting the relevant wavelengths of thermal radiation detected by the infrared cameras.

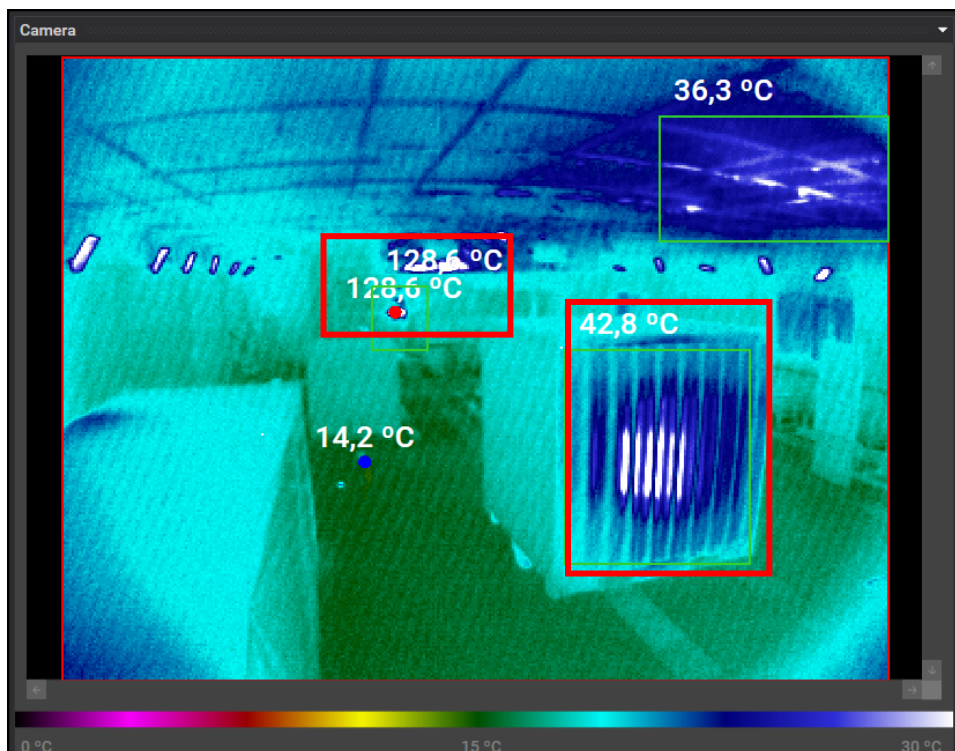


Figure 30: Image captured by a thermal camera during a flame reflection experiment (test 26 in Table 8). The maximum temperature in three different zones are shown in the image. The reflections from the corrugated steel container wall at 5 m from the fire show a maximum 42.8 °C, where the aluminium scaffolding approximately 25 m away from the fire shows 128.6 °C. The hot gases near the ceiling and the heated ceiling shows 36.3 °C. Minimum temperature is shown on the concrete floor at 14.2 °C.

In a nuisance alarm test where a forklift was driven into the test hall, an alarm was triggered by two of the three thermal imaging cameras due to hot surfaces on the exhaust muffler of the forklift. The software of thermal camera IR2 was set up with two independent alarm settings, namely, one which was the default settings (IR2b shown in Tables 5 and 6) and another which included a vehicle discrimination algorithm (IR2a shown in Tables 5 and 6). The algorithm disregarded moving hot surfaces of vehicles below a certain temperature if the hot surfaces started cooling after the vehicle had stopped. This feature prevented the forklift from triggering an alarm, while an alarm was triggered in the mode where this feature was disabled. The default mode in general detected the fires faster than the mode with the vehicle discrimination. Moreover, in the tests with fires in position P5 on top of the container, only the mode without the vehicle discrimination feature triggered an alarm. Thermal camera IR1 triggered alarms faster than IR2 in most tests, including the forklift nuisance alarm test, as it was set to activate the alarm at a lower temperature. This illustrates that selecting and setting the alarm threshold will be a trade-off between the detection time and the nuisance alarm frequency.

8.1.3.3 Video fire detection

An example image from a video detection software is shown in Figure 31, where the smoke and flame recognised by the detection software are marked as outlines and dots in the image. The same algorithms can also be used in real time on live video streams from CCTV cameras on board. Accordingly, the area of the image that is triggering the alarm is marked in real time on the screen, so the operator looking at the video should be able to confirm the fire or tell if the alarm is triggered by a nuisance source.



Figure 31: Image from a CCTV camera processed in real time by the video fire detection software during a demonstration test. The flame on the floor and the smoke along the ceiling are marked by the software with red and blue outlines, respectively.

Figure 32 shows an example of a nuisance alarm due to the moving reflective jacket of a person that is misinterpreted by the detection algorithm as a growing flame source. In this case, the operators looking at the highlighted area in the image can easily and quickly realize that the alarm has been caused by a nuisance source.

Figure 33 shows another example of a nuisance alarm due to the opening of a gate which has let in external light and thereby caused the detection algorithm to falsely identify it as a growing flame. Such

changing light conditions are difficult to distinguish from actual fire growth and flame flickering. For this reason, the outdoor use of most video fire detection algorithms is expected to be highly challenging due to nuisance alarms.



Figure 32: Example nuisance alarm from the video fire detection algorithm that has misinterpreted the moving reflective jacket of a person as a growing flame and has marked it with a red rectangle.



Figure 33: Example nuisance alarm from the detection algorithm due to the gate of the test hall rolling up to let light in, which has been recognised falsely as a growing flame (outlined using a red rectangle).

In some cases, the fire may be very difficult to identify by a human watching the video footage, e.g., the flame may be too small in the video image. In the same way, the manual distinction of smoke is often very challenging for visual confirmation. This is because smoke is usually grey and does not have a clear contrast against most background colours, whereas flames are usually very luminous with yellow and red colours which are more easily visible.

Figure 34 shows example snapshots from the lithium-ion battery overheating experiment before and after a video fire detection system has highlighted the smoke boundaries in the footage (25 min into the experiment). As the snapshots in Figure 34 illustrate, the smoke is very difficult to notice just seconds before it is detected by the video fire detection system.

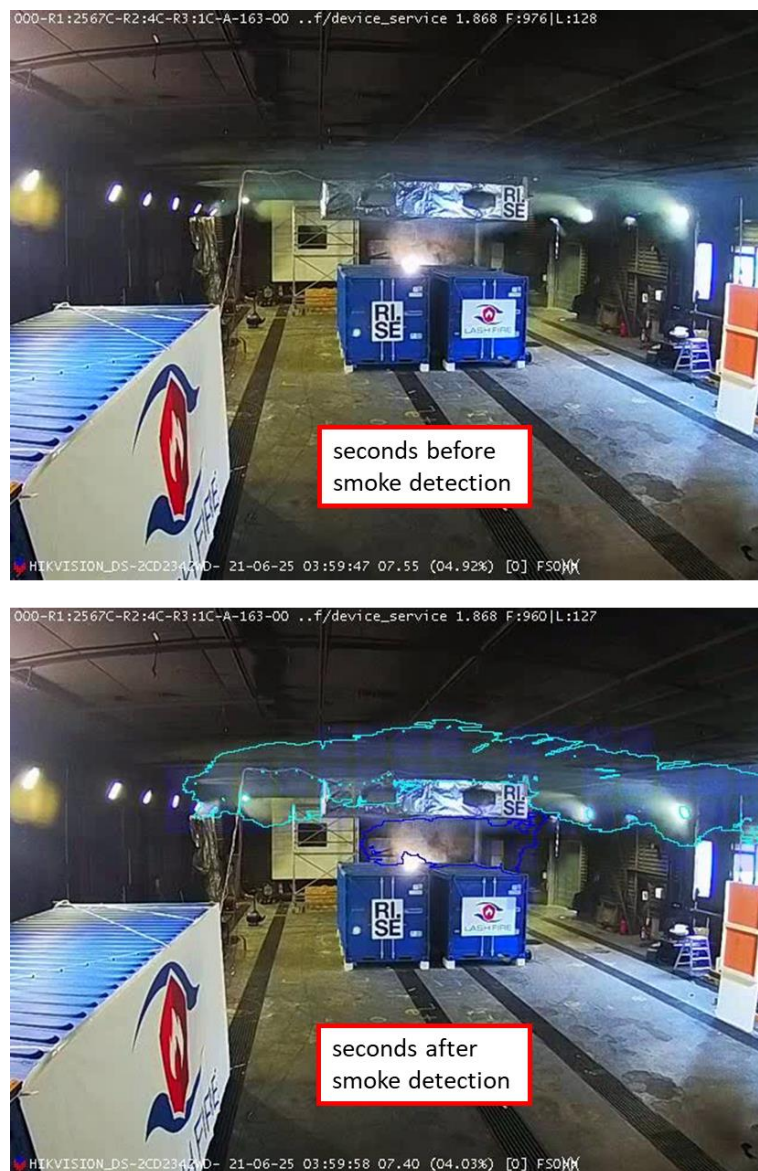


Figure 34: Example detection of smoke using video analytics when the smoke is barely visible just seconds before detection.

8.1.3.4 Lithium-ion battery tests

In the first test series, the short-circuit of the battery module broke within a second and did not produce much overheating or smoke, such that the temperature inside the battery module did not go above 60°C. However, the heat from the short-circuit device itself which produced steam and had

glowing hot parts was detected in the first experiment by the thermal cameras because the short-circuit device was outside the container (see Figure 35). Similarly, the overheating of the single pouch cell on the hot plate did not produce much flame or smoke to be detected by any of the detectors.

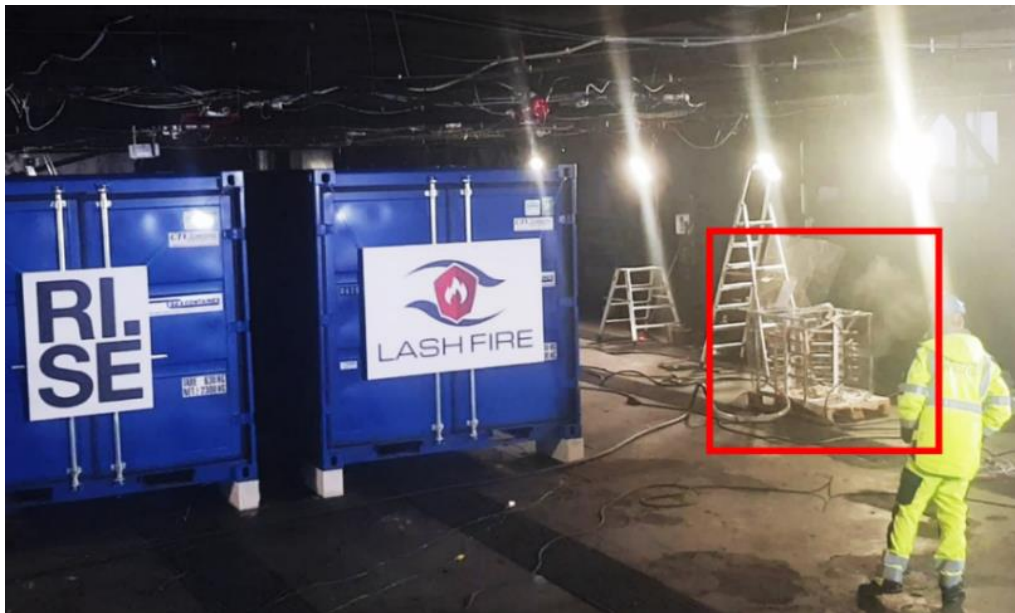


Figure 35: The short-circuit device used in the two first lithium-ion battery tests (highlighted with a red rectangle). The unit produced steam and had hot glowing parts which triggered the IR detectors.

In the second test series, the overheating of three pouch cells in a steel box produced heavy smoke which was visible from the battery cells 20 min after the heating was initiated ($t = 0$ s). In test 27, the video smoke detection algorithm triggered the alarm at ~ 25 min, i.e., nearly 2 minutes after the battery cells had caught fire ($t = 1376$ s), while flames were visible until ~ 45 min ($t = 2713$ s). In test 28, thermal camera IR1 triggered the alarm at ~ 35.5 min, i.e., nearly 7.5 min after the battery cells caught fire ($t = 1690$ s), followed by an alarm from the smoke detection algorithm at ~ 48.5 min, while flames were visible until ~ 44 minutes ($t = 2631$ s).

8.2 Propane burner calibrations for wind tests and onboard evaluations

According to EN 54-10 [11], a heptane pool fire can be used for the testing of optical detectors such as flame wavelength detectors. However, an equivalent gas burner had to be produced during the LASH FIRE project as the standard testing method using a heptane pool fire was not practical for tests on the DFDS ship for onboard evaluations. The designed gas burner measures $30 \times 30 \times 30$ cm³ operated using a small propane bottle (see Figure 36). The inside of the gas burner was filled with lightweight clay aggregates that disperse the propane uniformly, creating a flame that looks very much like that of the heptane pool fire source described in EN 54-10 [11].

The gas burner was calibrated such that its heat release rate (~ 120 kW), flame height (~ 0.9 - 1.1 m), and heat fluxes (~ 5 kW/m²) were comparable to those of the standard heptane pool fire (see data shown in Figure 37).

The heptane burner used for the calibrations was almost identical in construction, except the inside of it contained water at the bottom and heptane at the top during the test. This was to make sure that the heptane pool surface had the same free height from the top edge of the tray as mentioned in EN 54-10 [11], i.e., 45 mm after adding 500 ml heptane with 3% toluene.



Figure 36: Tray for the heptane pool fire (left) and the equivalent gas burner (middle) used with a propane bottle (right).

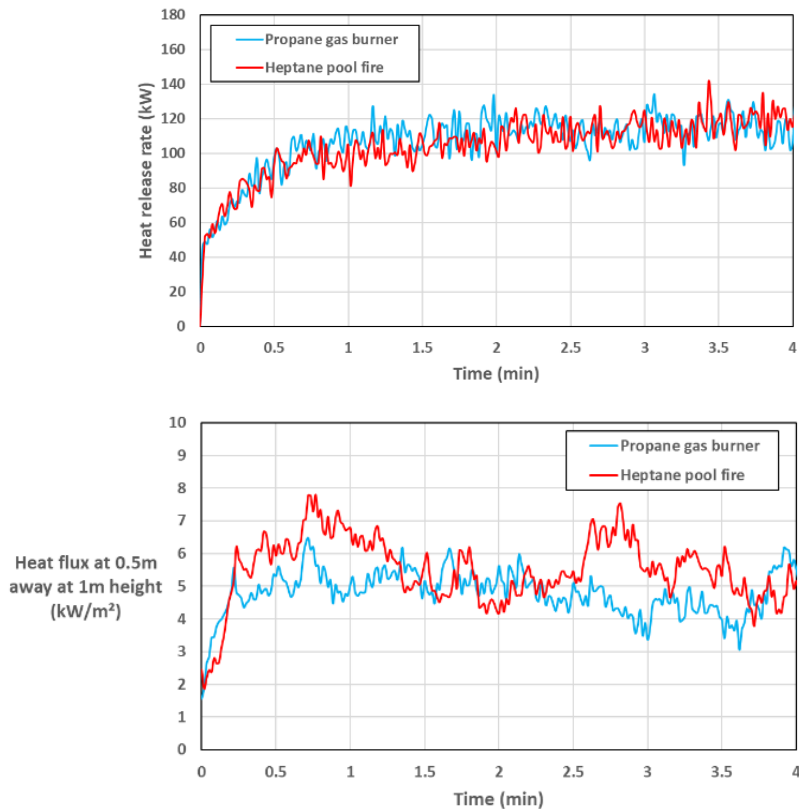


Figure 37: Snapshots of standard heptane fire versus the propane fire (top), heat release rate of each fire (middle), and heat fluxes (bottom) measured at 0.5 m horizontal distance from the edge of each burner at the height of 1 m.

Figure 38 shows the heat release rate of the burner when operated at the maximum possible power using the propane bottle shown in Figure 36. Using the maximum power of the burner (140-kW peak), the maximum flame height was slightly higher than 1.5 m which is enough to be visible above the height of most passenger cars. Therefore, optical detectors such as video fire detection systems and flame wavelength detectors are expected to detect this flame within seconds if the camera/detector sees the fire area or the flame reflections. However, the flame height is not high enough to be visible above the height of trucks. Therefore, optical detectors are not expected to see this fire behind trucks unless the fire gets bigger or reflected toward the detector.

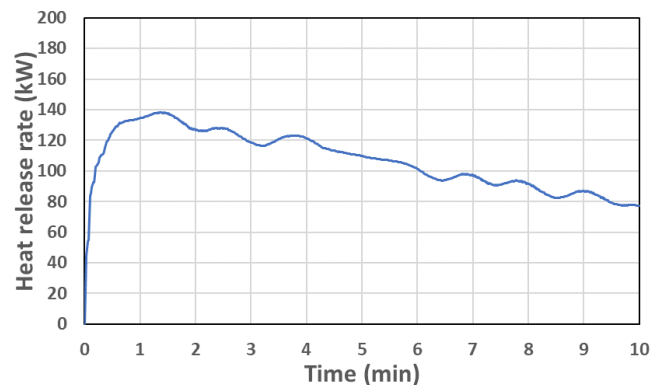


Figure 38: Heat release rate of the burner operated at the maximum possible power using the bottle shown in Figure 36.

8.3 Wind experiments

High wind speeds can affect fire dynamics and thereby the ability of detection systems to detect the fire. Several tests were conducted to investigate this effect, complementing the lower wind speed tests discussed in 8.1.3. These tests are relevant both for detectors in open ro-ro spaces and for detectors on the weather deck, which can have windy conditions.

8.3.1 Experimental set-up

The wind experiments were conducted using the propane gas burner discussed in the previous section and the heat release rate shown in Figure 38. Fans were placed at 3.45 m distance from the burner, and a wind speed sensor was placed in between at 1.5 m from the burner and 1.95 m from the fans at the height of 0.5 m as shown in Figure 39. A CCTV camera and a thermal camera were used to monitor the flame. These were installed on a tripod placed on a scaffolding at 10 m height as shown in Figure 40. The horizontal distance between the burner and the cameras was 27.1 m. Nine experiments were conducted in total with wind speeds ranging from 4.5 to 11 m/s.

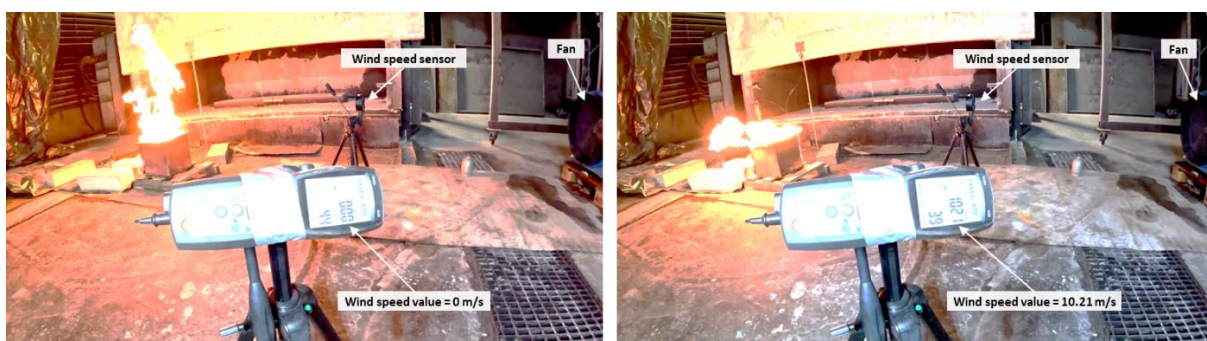


Figure 39: Snapshots showing a wind test with the propane burner before and after fan activation.



Figure 40: Thermal imaging (IR) camera and regular CCTV camera installed at 10 m height and 27.1 m horizontal distance from the burner shown in Figure 39.

8.3.2 Results

As the snapshots in Figures 41 and 42 illustrate, the flame shape recorded in the footage of thermal imaging and regular video cameras is highly affected by high wind speeds. The wind usually makes the flame occupy fewer pixels in images from both regular video and thermal imaging cameras, but the reflections of the flame on nearby surfaces could sometimes make the fire appear much larger in images captured by regular video cameras. This effect is quantified in Table 10, which presents the average number of footage pixels occupied by the flame obtained based on the data of 20 random footage frames for each camera type.

Table 10 shows quantitative results from the flame size in the footage in terms of image pixels. As the pixel numbers suggest, lower wind speeds in the order of 4.5 m/s cause the biggest amount of change in the recorded size of the flame, whereas the highest wind speeds in the order of 11 m/s cause the smallest amount of change in the recorded size of the flame. This is because the higher speeds cause the flame to pulsate back and forth more chaotically, such that the overall recorded size of the flame on average is still considerable compared to the original flame size recorded without wind. This is while lower wind speeds cause more regular flame tilting that keeps the size of the flame smaller than that with no wind. As a result, it is expected that lower wind speeds cause more challenge for fire confirmation than high wind speeds, although a threshold of high wind speed can be expected beyond which the flame is not identifiable or simply blown out.



Figure 41: Wind effects visible in footage snapshots of a flame captured by a camera at 27.1 m horizontal distance and 10 m height: the wind causes the fire to appear smaller sometimes (middle photo) and bigger at some other times (right photo) due to the image saturation and flame reflections from nearby surfaces.

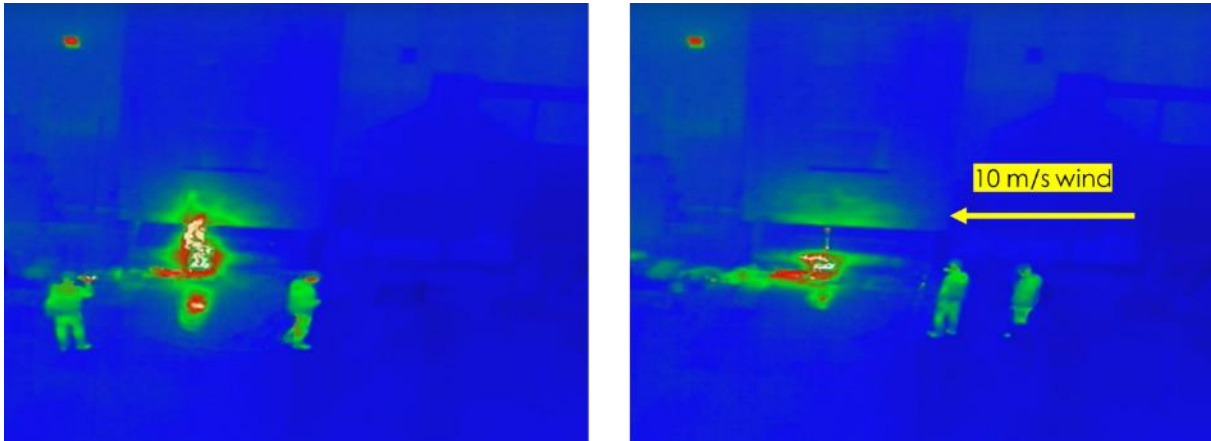


Figure 42: Wind effects visible in footage snapshots of a flame captured by a thermal imaging camera at 27.1 m horizontal distance and 10 m height: the wind causes the flame to occupy fewer pixels, which makes it more difficult to detect.

Table 10: Average number of image pixels occupied by the flame in thermal imaging and regular video footage from the wind tests.

Wind source	Regular video footage		Thermal imaging footage		% of change with wind for regular video camera	% of change with wind for thermal imaging camera
	Flame pixels without wind	Flame pixels with wind	Flame pixels without wind	Flame pixels with wind		
Small fan (~4.5 m/s)	24054	6840	5921	1758	-72%	-70%
Big fan (~10 m/s)	27288	12797	4692	1518	-53%	-68%
Both fans (~11 m/s)	23322	18719	3066	1941	-20%	-37%

The quantitative results of flame pixels in the images also suggest that the change in flame size due to wind is bigger in thermal images than in regular video images for all cases with wind, except the case with the small fan where both image types have the same level of change. The smaller change in more cases with regular video is because their images tend to get saturated by highly luminous sources such as flames, making it appear bigger and thus offsetting the reduced flame size due to wind. Reflections over shiny surfaces are also perceived more strongly in regular video images. In contrast, thermal images tend to be more precise in their localization of the actual flame boundaries, with minimal image saturation. This precision quality of thermal images is usually beneficial for surveillance of hot areas, but it may make manual confirmation of fires more difficult in occasions with windy conditions, especially with lower wind speeds which reduce the flame size the most (note that overwhelming image saturation and high-speed changes due to strong wind can also confuse some video analytics algorithms). However, systematic fire detection based on temperature thresholds in the thermal image is still highly reliable. To the contrary, video detection systems that rely on flame flicker patterns across a certain number of pixels and in the vertical direction may have more difficulty detecting a tilted flame under windy conditions in a systematic way.

8.4 Large-scale fire detection combined with fire suppression

Several large-scale fire extinguishment tests were performed outdoors at the test facility of RISE Fire Research in Trondheim, Norway, which are discussed in detail in deliverable D10.3 [12]. In the present document, the evaluations of thermal imaging and regular video cameras are discussed for visual fire confirmation and localisation during the tested large-scale suppression scenarios.

8.4.1 Experimental set-up

The tests were conducted in an area measuring 40 m by 30 m, representing a section of a weather deck. The goal of the tests was to simulate a freight truck trailer fire with cargo containers on both sides and consisted of a main array of stacked idle wood and plastic pallets, which was partly covered by a steel roof as shown in Figure 43. Parallel with and 0.5 m to the sides of the main array, 20-foot cargo containers were positioned to mimic the compactness of vehicles, trailers, and other cargo on a weather deck.

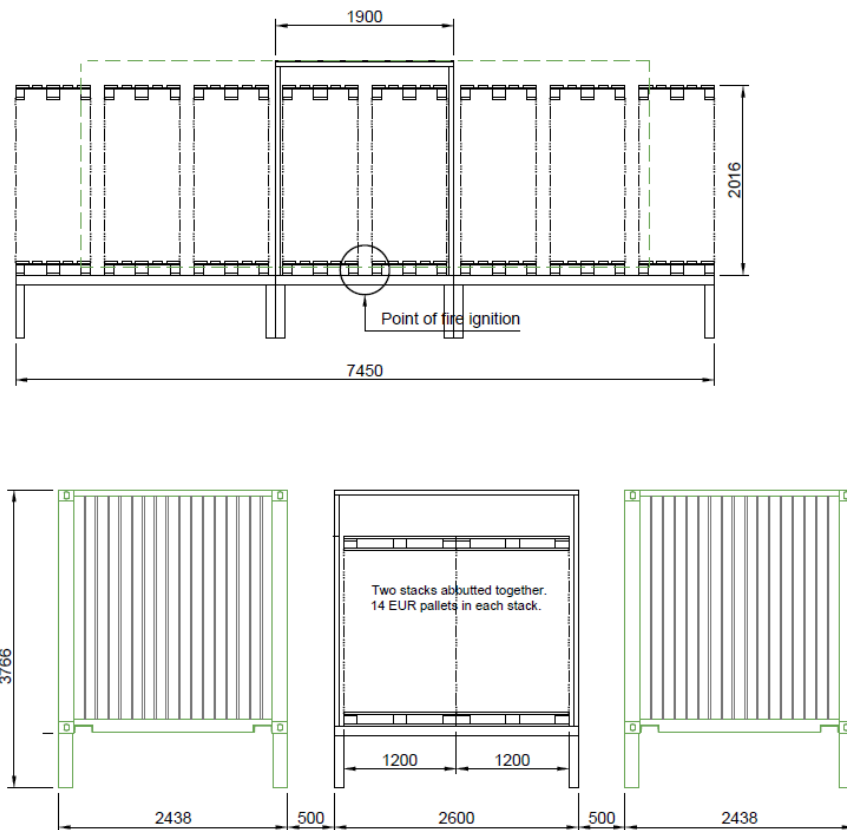


Figure 43: Photo showing the arrangement of pallets used as a fire source for the large-scale fire suppression experiments with fire monitors for a weather deck environment. The fire source was a heptane tray located at the centre of the setup as shown (see text for the specifications of the fire source).

As shown in Figure 43, the fire source consisted of 224 pallets (192 wood and 32 plastic pallets), arranged in 16 stacks, i.e., 8 stacks along the length and 2 stacks along the width, with each stack containing 14 pallets along the height (12 wood pallets with 2 plastic pallets on top). Three, 2-inch remote controlled fire monitors were positioned at a height of 7.2 m above the ground, and tests were conducted with one monitor and two monitors from various angles. Moreover, tests with both short and long pre-burn times were conducted in order to evaluate early or late fire suppression initiation scenarios.



Figure 44: Photo showing the activation of a fire monitor during a late-suppression scenario (300-s waiting time)

The fuel stacks were covered by a roof sized 2,6 m wide by 1, 9 m long made of steel sheets. The intent of the roof was to prevent suppression or extinguishment of the initial fire, especially when using a short delay time from fire ignition to the application of the suppression agent. The vertical and horizontal supports of the roof were cooled by water circulating through the square iron structure. The vertical distance measured from the ground to the top of the roof and the tops of the surrounding cargo containers was about 3,15 m. The length of the cargo containers was less (nominally 6,1 m) than the overall array.

The fire was initiated using a heptane tray sized 1200 mm (L) by 150 mm (W) by 150 mm (H) filled with a depth of 20 mm (3,6 l) of heptane on a 20-mm layer of water (3,6 l). The heptane fuel on the tray was ignited by a torch. The fire tray was on the platform used to stack the pallets and was placed symmetrically between the centremost flue space of the array of pallets as shown in Figure 43.

The fires were allowed to develop until flames were visually observed above the top of the array. Thereafter, either a 30 s or 300 s delay time was applied before the application of water using fire monitors was initiated. The shorter delay time was designed to simulate rapid activation by an autonomous system, while the longer delay time simulated manual activation and remote-controlled operation by the ship's crew (a photo from this latter scenario is shown in Figure 44).

The fire monitors were programmed to direct the water stream with a predefined pattern around the fire area to quantify the optimal suppression effect possible using one or two fire monitors from different angles, while the autonomous functionality of the fire monitors with guidance using an optical detection system was already evaluated in a separate study as explained in section 6.2 (setup shown in Figure 5). Nevertheless, thermal imaging cameras and regular video cameras were installed beside the fire monitors (see Figure 45), with the purpose to evaluate their usefulness for visual fire confirmation and localisation during large-scale suppression scenarios.



Figure 45: Detection sensors installed at the height of 7 m beside one of the fire monitors during the large-scale fire suppression tests. The sensors include thermal imaging and regular video cameras, as well as a triple-IR flame wavelength detector.



Figure 46: A snapshot from a regular video camera (top) and a snapshot from a thermal imaging camera (bottom) during a fire suppression experiment with two fire monitors in the late fire suppression scenario (300-s waiting time). The persons in the background have been highlighted manually to illustrate the usefulness of this information from the thermal camera.

8.4.2 Results

Figure 46 shows a snapshot from a regular video camera (top) and a snapshot from a thermal imaging camera (bottom) during a fire suppression experiment with two fire monitors in the late fire suppression scenario (300-s waiting time after flames were visible). As Figure 46 illustrates, the application of water on the fire caused the field of view of the regular camera to be filled with a cloud

of smoke and water vapor which made it difficult to see what is happening behind the smoke. At certain intervals, the amount of smoke was so much that almost the entire setup was covered in the field of view of the regular camera, while the thermal camera was still able to highlight the hot regions of the containers and the fire area through the smoke very effectively. For this reason, during large-scale fires, it is expected that the fire confirmation and localisation capability of regular video cameras is more limited to the early stages, whereas they become much less useful for continued monitoring of fire development later, especially during fire suppression when a large amount of smoke is produced. In contrast, the thermal cameras are expected to be very useful for continued monitoring of fire development owing to their ability to see through thin smoke, even during fire suppression. Thermal cameras can also help identify people in the area better than regular video cameras as highlighted in Figure 46, which is valuable information to the operators in a fire situation.

As opposed to thin smoke which does not pose a significant problem for thermal camera surveillance of fire localisation, the water stream from the fire monitor does block the field of view of both thermal imaging and regular video cameras. This water stream blockage of the field of view can be seen in Figure 47, and it is due to the attenuating effect of water on the transfer of thermal radiation [23]. This observation highlights how the placement of the camera may cause the water stream to compromise the surveillance coverage (partially or completely, depending on the inappropriateness of camera placement). Moreover, this highlights the importance of having several thermal cameras at different positions to be able to view the fire area from different angles with less compromise in the surveillance.

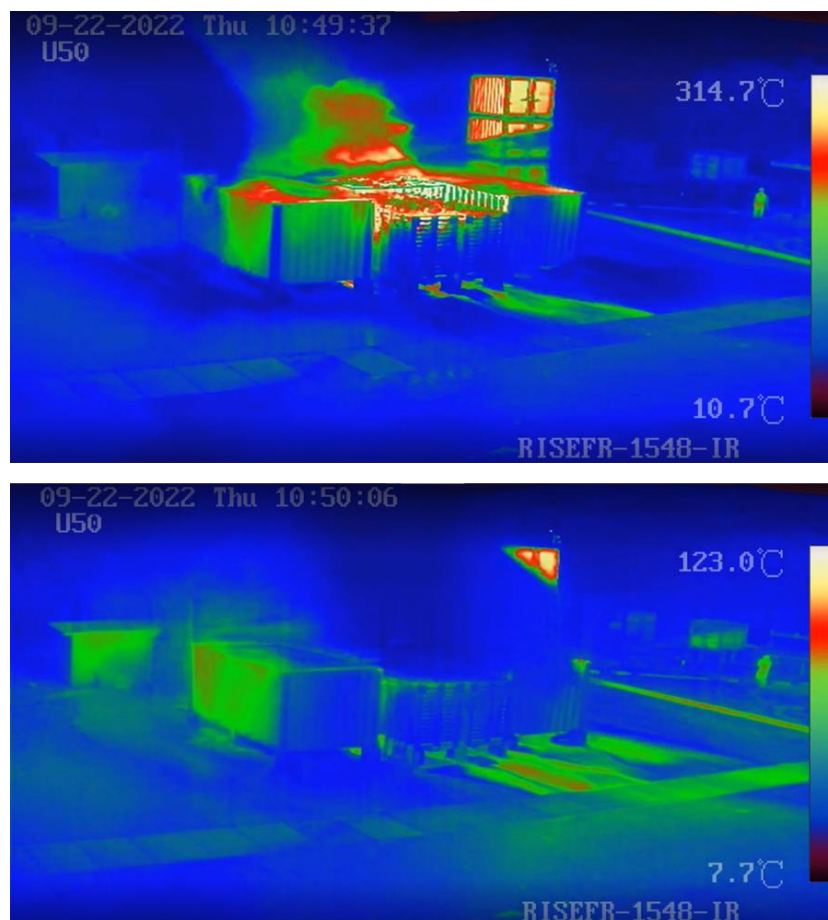


Figure 47. The blockage of the field of view of the thermal camera as a water stream is applied using a fire monitor (placed to the left of the thermal camera that has captured the images). The top image shows the first moment where the water stream starts to come into the frame from the left side of the field of view, while the bottom image shows the full blockage of the field of view as the water stream has reached the centre of the view.

As Figure 48 indicates, it is remarkable that the reflections of the fire on the wet floor or other shiny metallic surfaces are visible to the thermal camera (and IR array flame wavelength detectors), which could be misinterpreted as secondary sources of fire. Not only can this misinterpretation distract the resources of the autonomous fire extinguishment system guided by the detector, but it might also confuse the humans watching the footage. As Figure 48 shows, regular video cameras are easier to interpret despite the reflections, at least as long as the field of view is not filled with smoke.

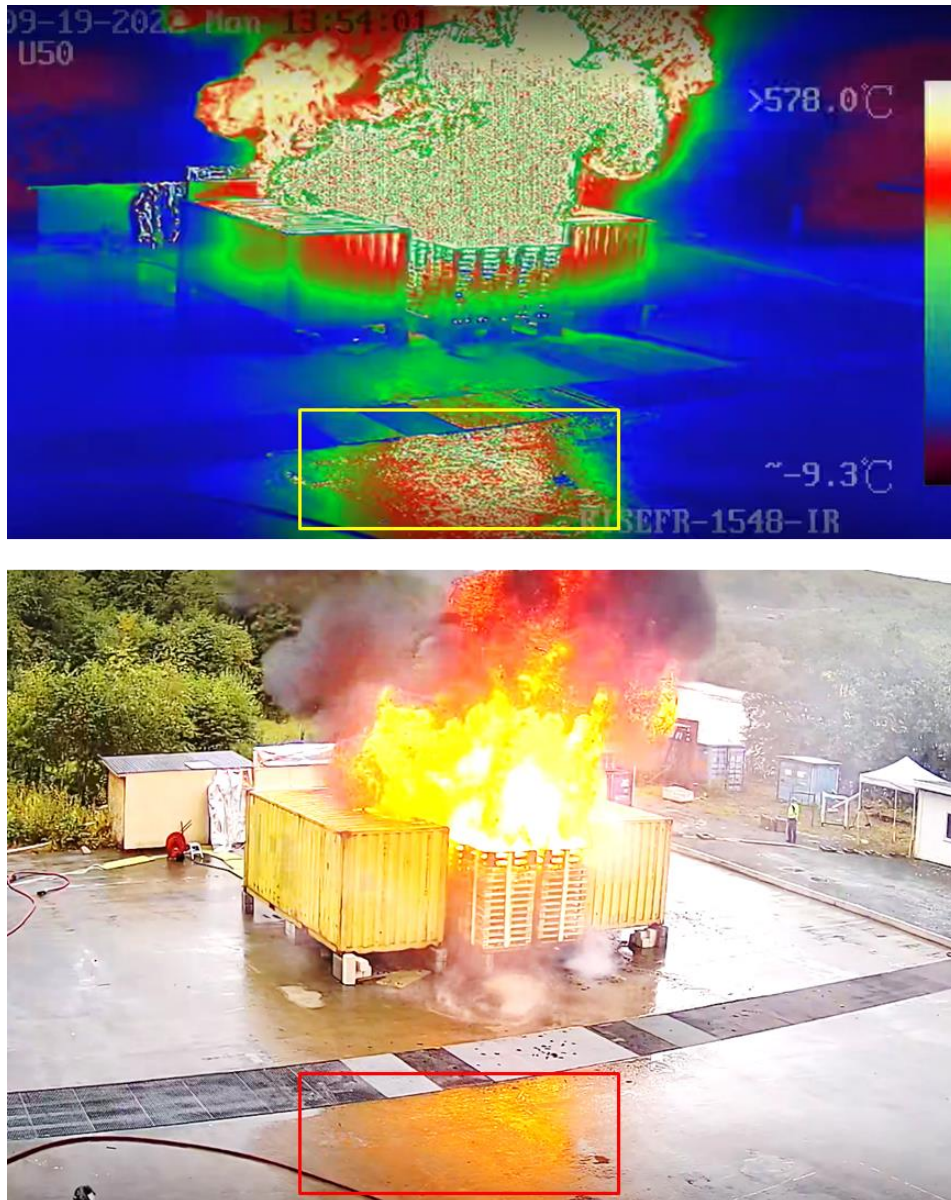


Figure 48. Reflection of the fire on the wet floor as perceived by a thermal imaging camera (left, highlighted with a yellow rectangle) and that perceived by a video regular video camera (right, highlighted with a red rectangle).

The triple-IR flame wavelength detector was able to detect the flames within seconds in the beginning the experiments, such that looking at the footage of the detector's built-in video camera made it possible to confirm and locate the flame very easily in the beginning (see Figure 49).



Figure 49. Video images from the built-in camera of the triple-IR flame wavelength detector during a fire suppression test scenario with a 300-s waiting time after flames were visible. Top figure shows the first fire alarm. Middle figure shows moments before fire suppression. Bottom figure shows another fire alarm immediately after fire suppression.

The continuous presence of big flames in the field of view of the flame wavelength detector caused it to become saturated and less sensitive, such that it did not trigger subsequent alarms until fire suppression started and made the flames much smaller (see Figure 49). This relates to a well-known flame detection problem which often arises due to the presence of a strong non-flame source of thermal radiation in the background of a flame, making the flame difficult to detect via its radiation signature [24]. Due to this effect, triple-IR flame wavelength detectors are known to be saturated by strong sources of thermal radiation in their field of view. In the LASH FIRE experiments, it was the continuous presence of the flame itself that saturated the detector and made the flame difficult to detect in a continuous way. In terms of systematic fire localisation for the guidance of autonomous fire extinguishment monitors, such lack of continuous information from the detector is expected to prevent quick adjustments of the water aiming system according to the instantaneous developments of the fire area. Therefore, the best course of action for the autonomous fire monitor is to primarily rely on the first fire detection information for guiding the water nozzle, while later the nozzle must continue to focus on the initial spot until new fire location information becomes available from the detector.

8.5 Main findings from laboratory tests

The laboratory experiments showed that optical detectors such as thermal imaging cameras can significantly improve the confirmation and localisation of fires. Specifically, flame wavelength detectors accompanied by a built-in video camera could quickly detect small flames and draw attention to the fire for manual investigation using the footage. For a more systematic approach, IR array flame wavelength detectors can be used to find and highlight the precise location of the fire area in the footage, the X/Y coordinates of which could be used for guiding autonomous fire suppression systems. Moreover, thermal imaging and video fire detection systems could visualise the fire area for a quick confirmation of the fire and ruling out nuisance alarms. An advantage of thermal imaging cameras over other detectors in this case was that thermal imaging could detect hidden fires by identifying the heated surfaces affected by the fire. Moreover, thermal images could help locate any persons in the area surrounding the fire which is valuable information during a fire situation. The laboratory experiments also showed that the beam compartments along the ceiling had limited influence on the flame and general fire detection using the optical detectors, although the smoke initially accumulated in one area and was very difficult to see visually in the footage of thermal and regular video cameras. In such scenarios, the video smoke detection algorithm proved to be highly effective for detecting and outlining the boundaries of smoke for fire localisation.

Thermal imaging cameras were the only optical detectors which triggered an alarm during the experiments with beechwood sticks smouldering on a hot plate without flames, namely by sensing the high temperatures on the hot plate, which can be compared to a hot spot on a vehicle.

Ethanol and heptane pool fires were detected by some of the optical detectors when the flame was visible to the detectors. In cases when the fire was not visible, video analytics was able to detect the smoke in several cases, while thermal imaging cameras were able to detect the heated regions. Most remarkably, in the experiments where the fire was concealed inside a container, the heated roof was detected by thermal imaging, while no other detector triggered an alarm as there were no flames or smoke visible to the detectors.

In tests with lithium-ion batteries, video smoke analytics and thermal imaging cameras triggered an alarm in several cases. In one experiment, video analytics identified the smoke at ~25 min, i.e., nearly 2 minutes after the battery cells caught fire, but the detection in other cases took up to 16 minutes after the battery cells were on fire. The measurements show that the CO concentrations at the floor level exceeded 40 ppm, but the concentrations just 25 cm above the floor were much lower. The smoke

initially dropped to the floor level before rising and triggering the video smoke detection algorithm and thermal imaging detectors. This suggests that installing optical detectors with a view of the lower heights along the floor where lithium-ion batteries are placed (e.g., below EVs) may reduce the detection time significantly. However, such installations with a view to the lower heights are not expected to be practical in ro-ro spaces.

Based on the fire tests conducted with wind speeds from 0 to 5 m/s opposite the ISO 8ft containers surrounding the fire, it seems that the performance of optical detectors is not significantly sensitive to such low wind speeds, as no clear trend of effects from wind can be seen in the detection time results, whereas point detectors were more significantly sensitive to wind as discussed in deliverable D09.2 [5]. Therefore, it is expected that the optical detection systems tested can improve fire detection and confirmation to a greater extent in open ro-ro spaces where there are wind effects.

Based on the fire tests conducted with wind speeds from ~5 m/s to 11 m/s blowing against a propane burner fire, it is found that the flame size in the footage of thermal and regular video cameras changes more dramatically for lower wind speeds than for high wind speeds. Moreover, the change in flame size was more dramatic for thermal imaging cameras than for regular video cameras. As a result, manual observations of the flame in the footage are expected to be more challenging in windy conditions. As for systematic fire detection, it is expected that thermal imaging systems based on temperature thresholds can detect the fire more reliably than video fire detection systems, although it is noteworthy that thermal imaging systems can be prone to frequent nuisance alarms if the detection criteria of maximum temperatures or rate of rise of temperatures are not fixed with the right sensitivity thresholds.

Several nuisance alarm sources were also found as part of the laboratory experiments. Firstly, the tested video fire detection system produced nuisance alarms during the tests where the ambient light conditions were changed, such as when the gate to the test hall was opened. Secondly, the video fire detection system produced nuisance alarms due to the moving reflective jacket of a person walking in the field of view. Due to this, it is expected that some areas must be masked out by the detection software. For example, the smoke detection zone must be along the ceiling, and the flame detection zone must be just above the height of trucks. Moreover, the use of the tested video fire detection system must be limited to closed ro-ro spaces where the ambient lighting conditions can be controlled, while it cannot be recommended for weather decks or open ro-ro spaces. Some video fire detection systems based on other working principles may be suited to environments with changing ambient light conditions, but no such video fire detectors were available for testing during the laboratory experiments.

In addition to the nuisance alarms of the video fire detection system, several nuisance alarms were observed for the thermal imaging detection system due to the exhaust muffler of the forklift used to adjust the configuration of the experimental setup. In this regard, one camera had an option to detect the nuisance alarm source on moving vehicles, but the detection with this feature was slower. Therefore, it is expected that either the detection temperature threshold must be increased to avoid nuisance alarms from the vehicle exhaust mufflers, or a vehicle discrimination algorithm must be used. Either way, the result would be a trade-off between detection speed and frequency of nuisance alarms.

During the large-scale fire extinguishment tests, it was found that thermal imaging cameras can see through smoke better than regular video cameras, such that thermal cameras are more useful for continued monitoring of fire development during fire suppression when a large amount of smoke was produced. This is while regular video cameras are generally easier to interpret intuitively and more suitable for the early stages of the fire before major smoke spread. The reflections of the fire on the

wet floor or other shiny metallic surfaces were also visible to the thermal camera, which could be misinterpreted as secondary sources of fire. This reflection could distract the resources of the autonomous fire extinguishment system and might also confuse the humans watching the footage. Regular video cameras, on the other hand, were found to be easier to interpret despite the reflections, at least as long as the field of view is not blocked by smoke. Moreover, it was found during the larger fire experiments that the continuous presence of big flames in the field of view can saturate the flame wavelength detector, preventing it from producing continuous updates on the presence of the flame. Therefore, it is expected that for larger fires, the initial fire detection information can be used to aim the water nozzle of an autonomous fire monitor system at the fire, while later the nozzle must continue to focus on the initial spot until new fire location information becomes available from the detector.

9 Onboard evaluations

Main author of the chapter: Davood Zeinali, FRN

Following the laboratory experiments discussed in chapter 8, several candidate detectors were selected and tested on board Hollandia Seaways (DFDS ro-ro cargo ship) between February 2022 and July 2023. The present chapter discusses the operational evaluations as well as the fire experiments performed on board to test the sensitivity of the sensors in the beginning and after one year on board.

9.1 Objective and selection of detectors

The main objective of the evaluations on board Hollandia Seaways was to provide a realistic validation for the operational performance of optical detection systems for visual fire confirmation and localisation. Another important objective was to evaluate how the alarm threshold settings can be optimized for the different systems to balance early detection with a low number of nuisance alarms during normal operations.

For open ro-ro spaces, a triple-IR flame wavelength detector with a built-in camera was selected for onboard evaluations based on the conducted laboratory experiments that showed the system reacted quickly to flames and was suitably small and robust for outdoor installations. The installation in the open ro-ro space allowed investigating how the flame detector performs with the limited field of view available in the open deck and whether there are any nuisance alarms.

For closed ro-ro spaces, video fire detection was selected for onboard evaluations, as it was found cost-effective and suitable for average-sized closed decks where the light conditions are stable. Accordingly, a system was installed on the main deck of Hollandia Seaways, employing the video fire analytics algorithm tested during the laboratory experiments.

For weather deck evaluations, a hybrid detector (video fire detector + thermopile heat detector), two thermal imaging detectors, three flame wavelength detectors (two IR3 and one IR array), and a video flame detector (different from that on the closed deck) were installed on the weather deck of Hollandia Seaways to investigate their performance during real operational conditions and to evaluate how the alarm threshold settings could be optimized.

9.2 Installations and initial testing

A list of the LASH FIRE detector installations and their locations on Hollandia Seaways is provided in Table 11. The first detection system installed on board was a triple-IR flame wavelength detector configured using its default medium sensitivity settings and a pre-defined 5-s delay for detection. This detector overlooked the aft part of the uppermost open ro-ro space (deck 7) of Hollandia Seaways as shown in Figures 50 and 51. After installation, the detector was tested using a flare with flames which was detected within a few seconds (see footage snapshot in Figure 52).

The second onboard installation was for the aft weather deck, including two thermal imaging detectors, a video flame detector, three flame wavelength detectors (two IR3 and one IR array), and a hybrid detector which combined video fire analytics with thermopile heat detection (note: a thermopile is a set of thermocouples connected in a series on a circuit to detect heat based on the thermoelectric effect [25], and as such, a thermopile sensor is less sensitive compared to microbolometers used in thermal imaging cameras for infrared radiometry). All the detectors were configured using their default medium sensitivity settings and overlooked the aft weather deck as shown in Figures 50 and 51. After installation, the detectors were tested using a flare with flames which was detected within a few seconds (see example footage snapshot in Figure 53).

The third system installed on board Hollandia Seaways was the video fire detection system tested during the laboratory experiments. This system was installed on the main deck, i.e., in the closed ro-ro space in deck 3, as shown in Figure 54. The video fire detection system was configured with default low sensitivity settings and a pre-defined 5-s delay for detection. Moreover, two detection zones were defined, namely, one for smoke and one for flames, as shown in Figure 54. This was to avoid nuisance alarm sources at lower heights, such as moving vehicle lights, which could be misinterpreted as fire sources. It is noteworthy, however, that the system does monitor the lower heights for the purpose of its analyses, while alarms are only triggered when the detected smoke/flame reaches the pre-defined detection zones. More precisely, the system monitors the light levels across all the footage pixels, and when a group of pixels has a certain light level change and moves in an organized pattern consistent with learned smoke/flame examples, the system triggers an alarm. In this regard, it is noteworthy that there may still be additional nuisances to each proprietary software used for video analytics.

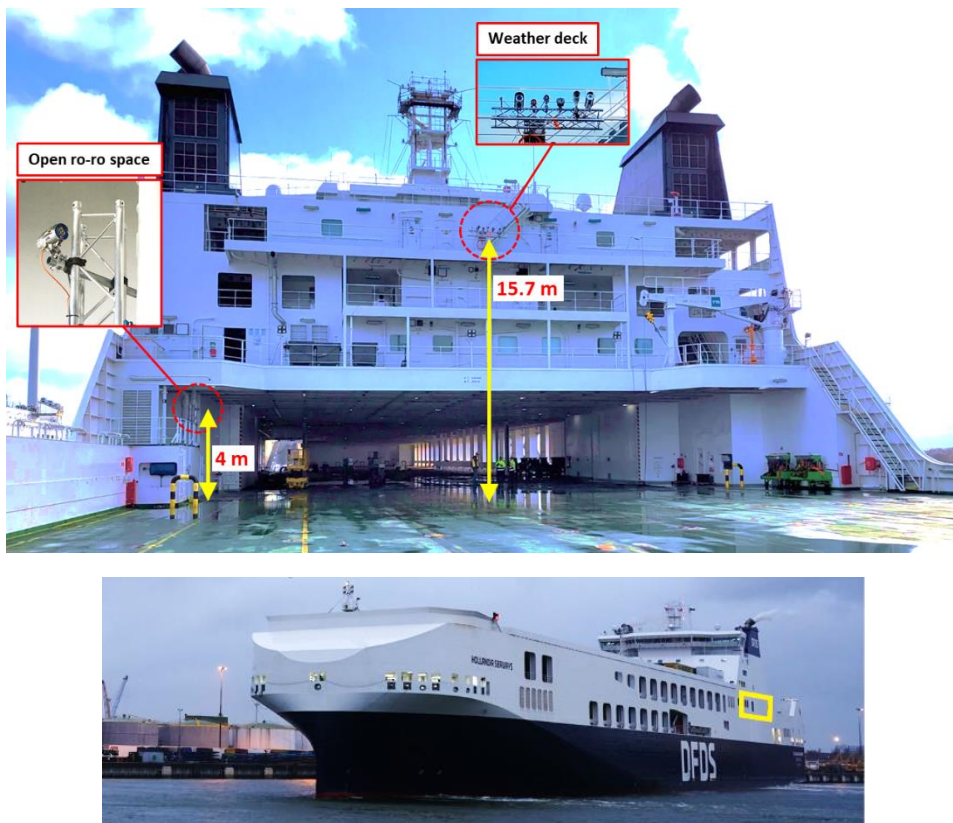


Figure 50: Detector installations on deck 7 of Hollandia Seaways for the LASH FIRE trials. For the open ro-ro space, a triple-IR flame wavelength detector was installed. For the aft weather deck, a hybrid detector (video + thermopile), two thermal imaging detectors, three flame wavelength detectors (two IR3 and one IR array), and a video flame detector were installed.

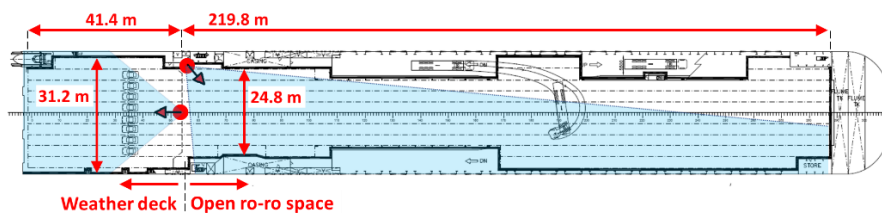


Figure 51: Locations of detector installations on deck 7 of Hollandia Seaways for the LASH FIRE trials. The blue shade indicates the area of coverage offered by the detectors. The open ro-ro space is monitored by a triple-IR flame wavelength detector, while the weather deck is monitored by a hybrid detector (video + thermopile), two different thermal imaging detectors, a video flame detector, and two flame wavelength detectors (one IR3 and one IR array).

Table 11: Optical detectors evaluated through the operational trials on board Hollandia Seaways.

ID	Detector type	Detection area
FD1	Triple-IR flame wavelength detector 1	Aft weather deck (deck 7)
FD2	Triple-IR flame wavelength detector 2	Aft weather deck (deck 7)
FD3	IR array flame wavelength detector (16x16 IR sensors)	Aft weather deck (deck 7)
VFD1*	Video flame detector	Aft weather deck (deck 7)
IR1	IR thermal imaging camera 1	Aft weather deck (deck 7)
IR2	IR thermal imaging camera 2	Aft weather deck (deck 7)
H1	hybrid detector (video fire analytics with thermopile heat detection)	Aft weather deck (deck 7)
FD4	Triple-IR flame wavelength detector 3	Open ro-ro space (deck 7)
VFSD2**	Video flame and smoke detection analytics using a regular camera**	Closed ro-ro space (deck 3)

* VFD1 was a detector unit with video analytics for flame detection, which was different from the video analytics software tested on the closed deck using a regular CCTV camera.
 ** The camera was HIKVISION DS-2CD2342WD-I, 2.8mm Lens, 4 MP.

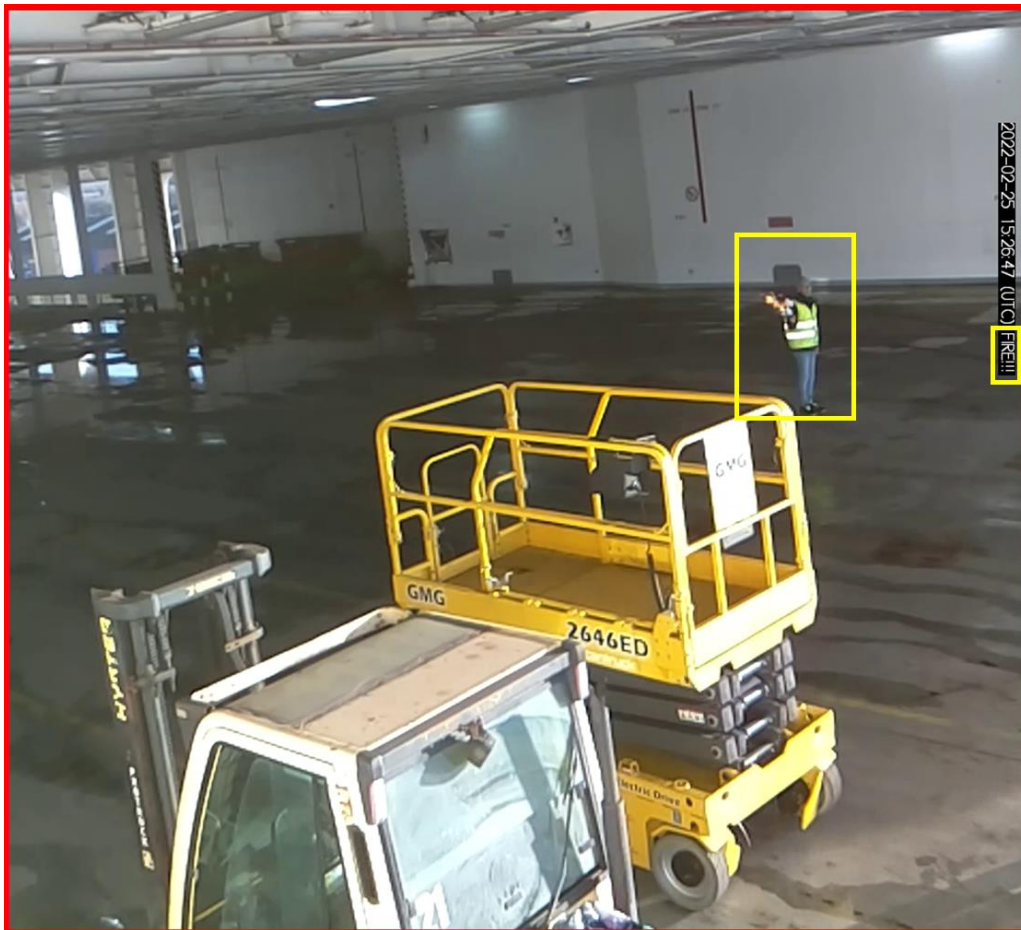


Figure 52: Snapshot from footage recorded by the built-in camera of the triple-IR flame wavelength detector in the open ro-ro space as the flame is detected during the initial testing within seconds. The person holding the flare and the “fire” message have been highlighted manually for clarification. The original footage was recorded sideways (rotated 90 degrees) due to the wrong orientation of the installation, but the rotation of the image has been corrected here to improve the demonstration.

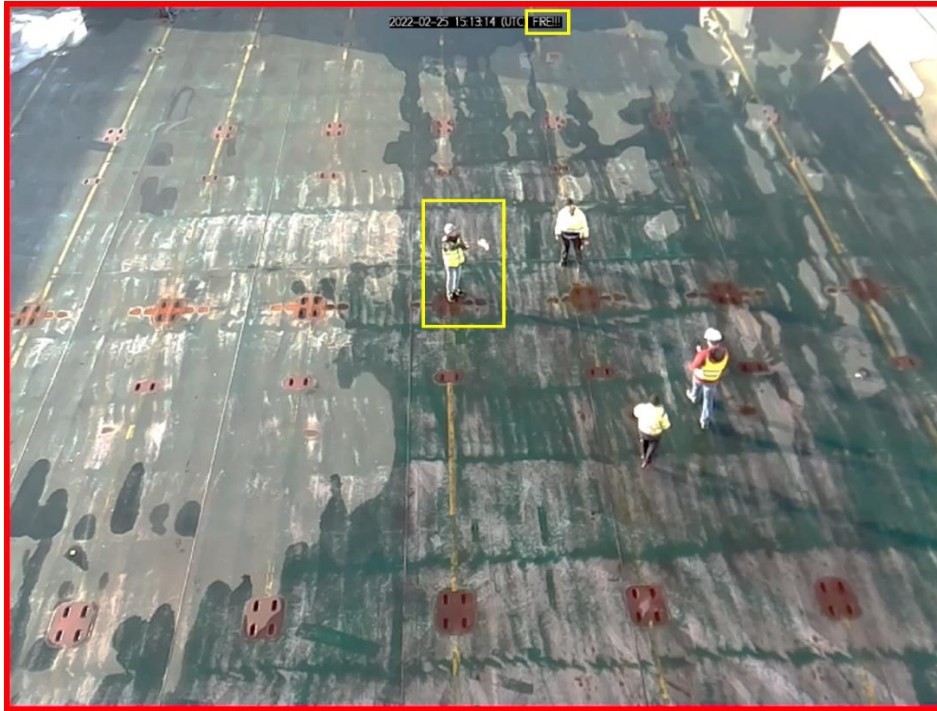


Figure 53: Snapshot from footage recorded by the built-in camera of the triple-IR flame wavelength detector on the aft weather deck as the flame is detected during the initial testing within seconds. The person holding the flare and the “fire” message have been highlighted manually for clarification.

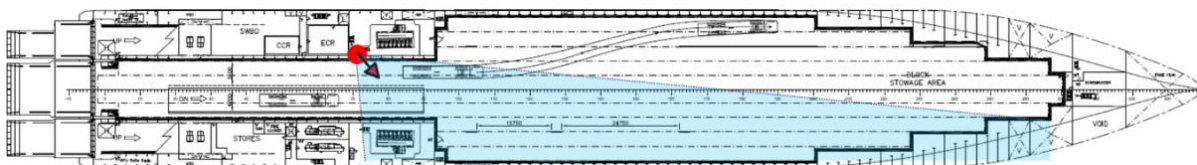
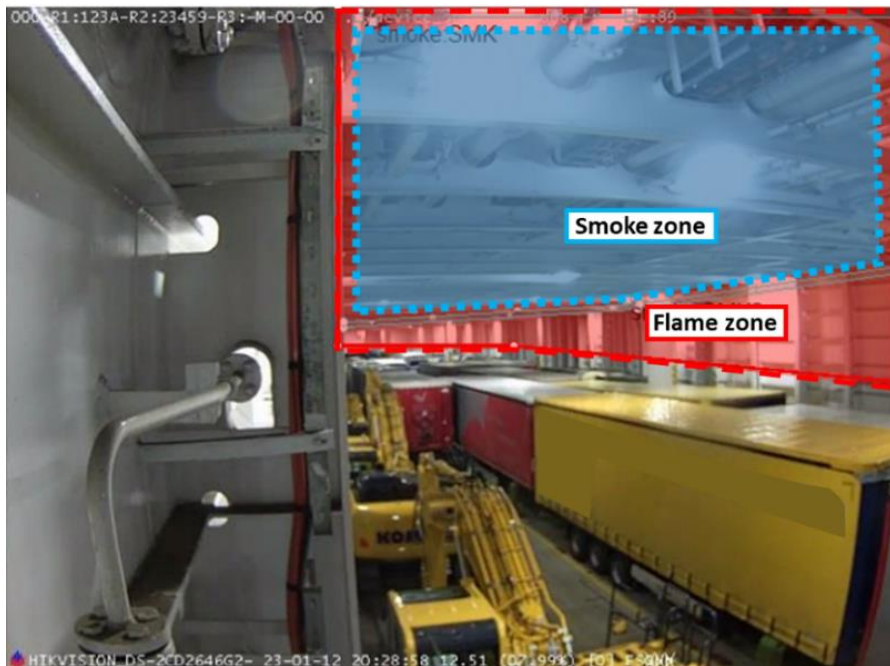


Figure 54: Location of video fire detection camera installed in the closed ro-ro space of deck 3 on Hollandia Seaways and a snapshot from the footage recorded by the camera showing the defined detection zones (outlined in the top figure). The ship itself has conventional point detectors of smoke/heat on this deck.

9.3 Alarms during normal operations on board

The history of nuisance fire alarms from the new systems installed on Hollandia Seaways is shown in Table 12 for the period from February 2022 to July 2023 while the ship operated as usual. Note that although a low number of nuisance alarms is considered beneficial, the performance of the systems cannot be judged solely based on these results, because a low number of nuisance alarms might be linked to a low sensitivity and thus less ability to detect a real fire.

Table 12: History of nuisance fire alarms from the new systems installed on Hollandia Seaways as part of LASH FIRE.

	Weather deck							Open deck	Closed deck
	Thermal cameras		Hybrid (video + thermopile)	Video flame detector	Flame wavelength detectors				Video analytics
	IR1	IR2 ¹	H1 ²	VFD1 ²	FD1	FD2	FD3	FD4	VFSD1 ³
Feb 2022	0	3	0	-	0	0	0	0	-
March	4	4	2	-	0	0	0	0	-
April	3	5	3	-	0	0	0	0	-
May	9	22	0	-	0	0	0	0	-
June	0	2	1	-	0	0	0	0	-
July	5	0	0	-	0	0	0	0	-
Aug	1	0	0	-	0	0	0	0	-
Sept	0	0	0	-	0	0	0	0	-
Oct	0	4	0	-	0	0	0	0	-
Nov	0	1	0	-	0	0	0	0	-
Dec	0	1	0	-	0	0	0	0	-
Jan 2023	0	3	0	-	0	0	0	0	-
Feb	0	2	0	-	0	0	0	0	-
March	0	2	0	-	0	0	0	0	4
April	0	1	1	-	0	0	0	0	1
May	0	6	0	-	0	0	0	0	1
June	0	6	0	-	0	0	0	0	1
July 2023	0	2	0	-	0	0	0	0	4

1 Camera IR2 first had a detection temperature threshold of 90°C. On May 31, 2022, this was raised to 160°C, and a 20-s delay was added.
 2 The video flame detector on the weather deck produced no record of alarms in the control panel.
 3 The alarms of the video flame and smoke detection system in the closed deck were overwritten every 6 months.

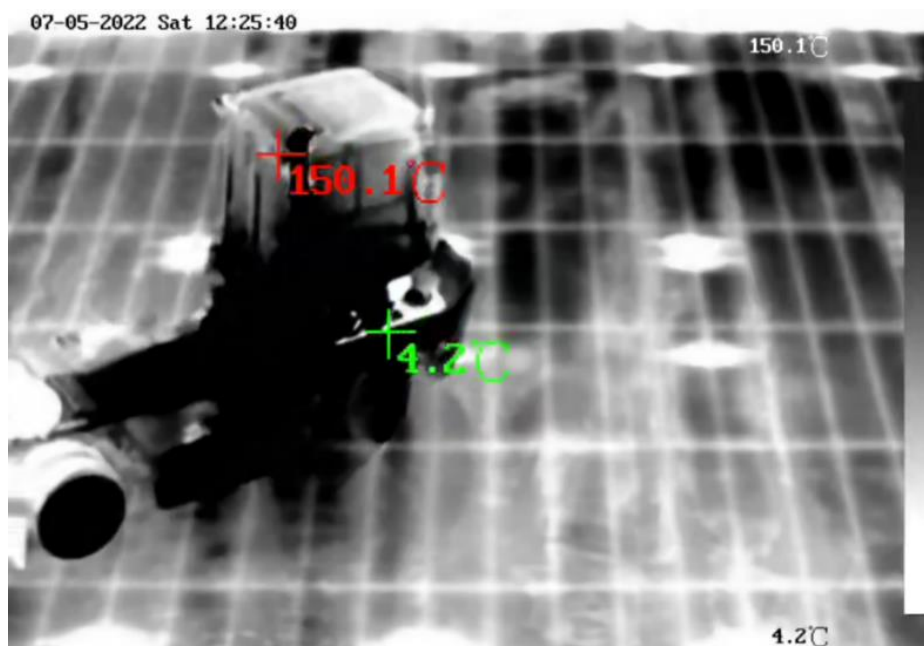


Figure 55: Example nuisance alarm source identified by the thermal imaging detection system on the weather deck: the exhaust pipe of a truck with a temperature of ~150°C has been detected as a potential fire source.

There were no real fires during the trials, and the flame wavelength detectors had no nuisance alarms during the normal operations, but the other detection systems did have some nuisance alarms (see Table 12). In the case of the video flame detector on the weather deck, the history of alarms was not recorded in the control panel other than the alarms generated during the initial flare testing. This was due to an error in the installation of the system which was discovered during the final fire tests where the detector was observed to detect the fire (based on LED on the device) while no record of the alarms was available in the control panel. The hybrid detector produced a few nuisance alarms. No photos were available from the related alarm incidents, but they are usually expected to be due to the light conditions in the open environment as well as camera flare or saturation caused by sun reflections.



Figure 56: Nuisance alarm example from the video fire detection system in the closed deck during washdowns: the droplets landing and moving on the lens of the camera are misinterpreted as smoke (boundaries highlighted using grey and blue contours in mid-top and top right of the two pictures, respectively).

There were frequent nuisance alarms from the thermal imaging cameras due to the exhaust pipes of vehicles (example shown in Figure 55). This includes the muffler and the tailpipe of the vehicles' exhaust system, which have operational temperatures ranging from 150°C to 310°C [26], [27], while performance vehicles may have exhaust pipes at average temperatures ranging from 430°C to 540°C [28]. This makes the hot exhaust pipes very hard to avoid using thermal imaging detectors as they rely on the detection of heat based on much lower thresholds of temperature, in some case as low as 70°C. For thermal imaging camera IR2, the threshold was raised from 90°C to 160°C several months into the trial (May 31, 2023), with the addition of a 20-s delay for detection. However, there were still frequent alarms from this camera subsequently. As opposed to thermal camera IR2 which had regular nuisance alarms throughout the trial despite changing its settings, thermal camera IR1 had 22 alarms within the first 7 months and no alarms during the next 11 months, while no changes were made to its default detection settings (which considered alarms for hotspots beyond 90°C with a short delay, excluding vehicle surfaces identified by the algorithm described in section 8.1.3.2). As a result, it is likely that some nuisance alarms will be generated from the hot exhaust pipes of vehicles despite the settings. This reduces the reliability of thermal imaging detectors for *systematic* fire detection. However, the *manual* use of these systems is still expected to be highly beneficial and effective for fire confirmation and localisation, i.e., operators can use these detection systems for the surveillance of hotspots without connecting the camera(s) to the control panel for fire alarms.

The video analytics algorithm tested for the closed ro-ro deck generated nuisance alarms only during the routine washdowns of the deck. This is because the water droplets landing and moving on the lens of the camera were interpreted as smoke movements, as shown in Figure 56. This type of nuisance alarm can be avoided either by switching off the detection system during the washdowns or by proactively muting the alarms during the washdown operation around the cameras used for video analytics. Another isolated incident of a nuisance alarm generated by the video fire detection system was from a crewmember on a scissors lift appearing in front of the camera. However, this was not a regular problem during the onboard evaluations because of the defined detection zones (see Figure 54), such that people and vehicles normally visible in the footage at lower heights could not trigger nuisance alarms.



Figure 57: Camera tilting observed due to the connections getting loose over time.

9.4 Other operational observations

As shown in Figure 57, some camera mounts on the weather deck got loose just after two months into the operational trial, such that they had to be adjusted upright by tightening the bolts in the mount.

This happened once again for one of the said cameras after nearly a year. It is expected that weather elements and ship vibrations contributed to the natural loosening of the connections, which highlights one of the operational challenges involved with the use of detectors for weather deck environments as well as the need for a robust design of their connection against tilting.



Figure 58: LASH FIRE box on board Hollandia Seaways containing a fire alarm panel, draw-out monitor and keyboard, several computer cases, some data acquisition systems, and associated accessories.

The nuisance alarms from the LASH FIRE detectors on Hollandia Seaways did not sound the fire alarm on board because the detectors were not connected to the ship's main fire control panel. Instead, a separate fire control panel was installed and used for the operational trial (see Figure 58). The used control panel allowed for only one active alarm for each detection system, i.e., if an alarm was triggered by detection system 'A', a new alarm could not be triggered from system 'A' until its previous alarm was manually dismissed. Due to this limitation, the active alarms had to be muted as soon as they appeared so that the involved systems could produce new alarms, while if the alarms were not deactivated for a long period, it was not possible to know whether those systems with an active alarm had triggered multiple alarms during that period or just one. Moreover, one of the detection systems had a non-latching relay that produced a non-stop alarm signal, i.e., an alarm from this system could not be dismissed manually on the fire control panel. Dismissing the persisting alarm from this detection system was only possible through its dedicated software installed on a separate computer connected to the detector. This made it difficult to centralise the control over the fire alarms from different systems. Nevertheless, it is expected that the deactivation of the alarms would have been easier if the systems had been integrated into the ship's fire alarm panel monitored regularly by the ship's operators, such that the limitation regarding the active alarms may not be a big issue.

9.5 Fire experiments in open ro-ro space with side walls simulating trucks

9.5.1 Setup

Several fire experiments were conducted on the uppermost open deck of Hollandia Seaways at the end of the operational trial with the setup and scenarios described in detail in deliverable D09.2 [5]. The experiments were done using the propane gas burner shown in Figure 36 with the heat output shown in Figure 38 by placing it at several different locations as shown in Figure 59. This simulated a fire beside either one or two trucks, where the fire was expected to be difficult to detect due to its distance from the deckhead and because the flames were not directly visible to the flame wavelength detector installed in the open ro-ro space.

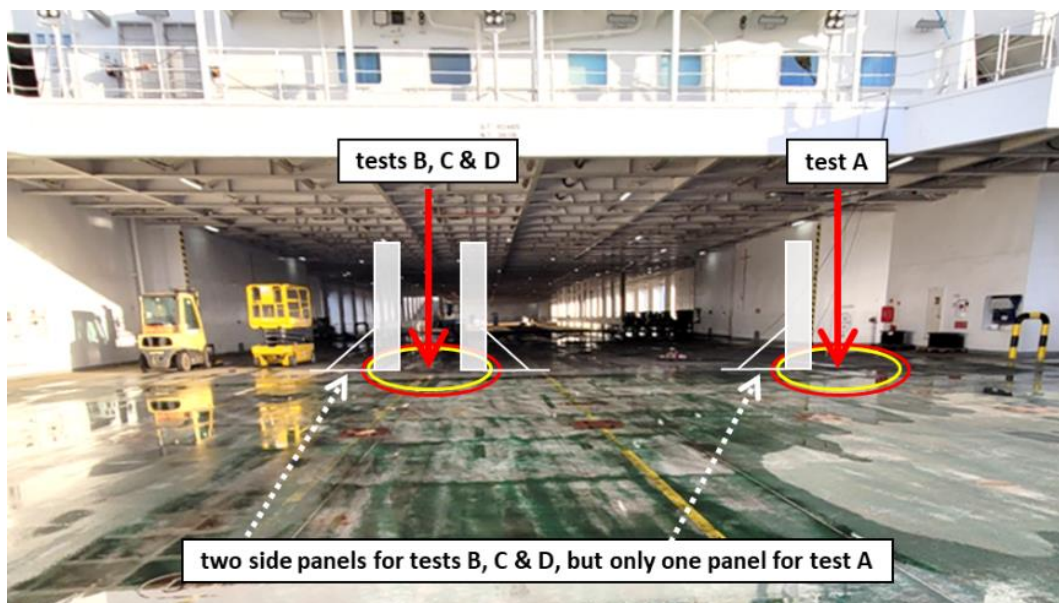


Figure 59: Setup of fire experiments on the uppermost open ro-ro deck of Hollandia Seaways (details described in D09.2 [5]).

9.5.2 Results

During the experiments in the open ro-ro space, the triple-IR flame wavelength detector installed in the open ro-ro space detected the reflection of the flame within seconds in test scenarios B, C and D, but the flame in scenario A was not detected, perhaps due to the absence of a reflection. In these cases, the surface reflecting the flame was outside the field of view of the detector's built-in video camera, so it was not possible to confirm the fire source using the live video. However, the reflection surface is expected to have been either the surface of small puddles on the floor or the surfaces of two cars parked on the side of the deck (visible in Figure 60).

The detection of flame reflections in the open deck experiments happened quickly owing to the deck being empty at the time of the experiments. With a deck full of cargo, the reflections of flames are not expected to be so easily visible along the side of the deck where the LASH FIRE detector was installed. The only way to provide a reflection of flames toward the sides of the deck where detectors may be installed is to install small convex mirrors along the centre of the deckhead at regular intervals. This facilitates flame detection based on its reflection. However, confirming and localising the fire from the video footage in this way will be difficult, as the flame reflection from a convex mirror is smaller than the flame itself (the level of size difference depends on the mirror's angle of convexness and its distance to the flame). The installation should also be such that no sun reflections are directed toward

the detectors in the open deck, as strong non-flame sources of thermal radiation are known to saturate most optical detectors relying on radiation for flame detection. This is especially problematic when there is a sizable source of black-body radiation in the background of the flame (see also explanations for Figure 49).

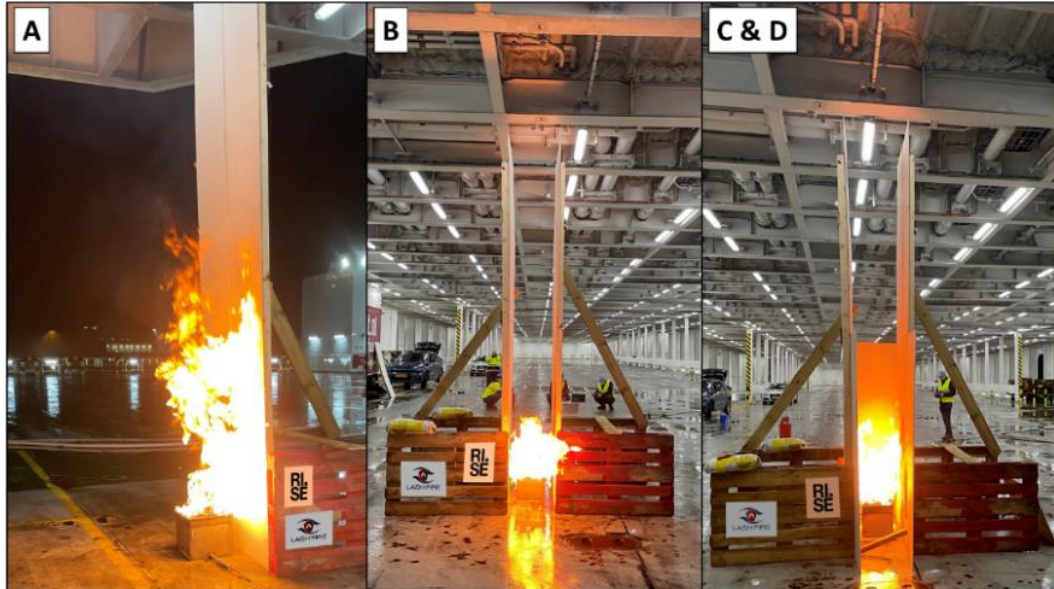


Figure 60: Different fire experiments on the uppermost open ro-ro deck of Hollandia Seaways (details described in D09.2 [5]).

9.6 Fire experiments on the weather deck

9.6.1 Setup

Several fire experiments were conducted on the aft weather deck of Hollandia Seaways at the end of the operational trial with the setup and scenarios described in detail in deliverable D09.1 [29]. The experiments were done using the propane burner shown in Figure 36 with the heat output shown in Figure 38 by placing it at several different locations as shown in Figure 61. This was done to challenge the weather deck detectors (installed at the height of 15.7 m with respect to the covered deck area) in terms of both on-axis and off-axis detection performance at different distances.

The ship was available for experiments at nighttime, while the ambient temperature was 10°C and the relative humidity level was between 75 and 100%. According to the ship's control room, there was crosswind blowing against the ship at the time of the experiments with a velocity in the order of 13 m/s. This is while the local wind velocities in the test area on the weather deck were in the order of 2-4 m/s on average according to the measurements made using a portable probe (wind data shown in Figure 62 along with the direction of flame tilt).

According to the European standard EN 54-10 [11], the fire performance of optical flame detectors is examined through the detection of a fire tray (including firstly heptane and then a methylated spirit) which must be achieved within 30 s for eight identical detectors arranged on a line at a height of 1.5 m and a horizontal distance of 25 m from the fire for a rating class 1, a horizontal distance of 17 m for a rating class 2, and a horizontal distance of 12 m for a rating class 3. For the LASH FIRE experiments on board Hollandia Seaways, the propane burner served as the fire tray (see equivalency discussed in section 8.2), and the horizontal distances ranged from 12 m to 40 m (i.e., farthest distance on the deck), while the height of the detectors was 15.7 m (fixed on deck 11). The off-axis angle (i.e., angle

with respect to the optical axis of each detector) ranged from 0 to 46 degrees along the horizontal plane during the onboard experiments, while EN 54-10 considers a maximum off-axis angle of 5 degrees [11]. As a result, it is expected that the detectors were more significantly challenged during the onboard experiments than they usually are according to standard tests based on EN 54-10.

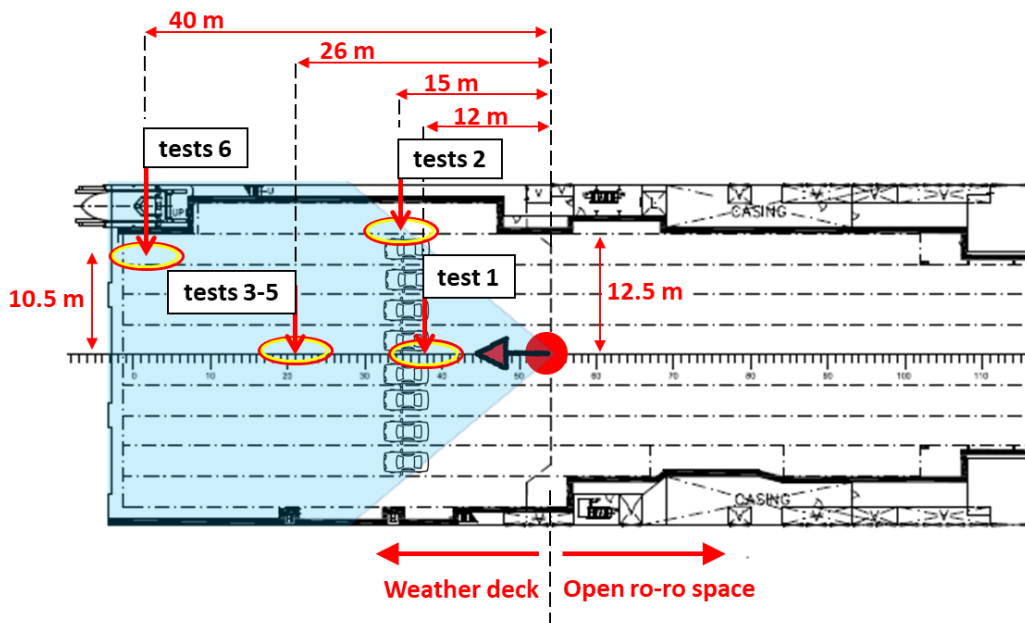
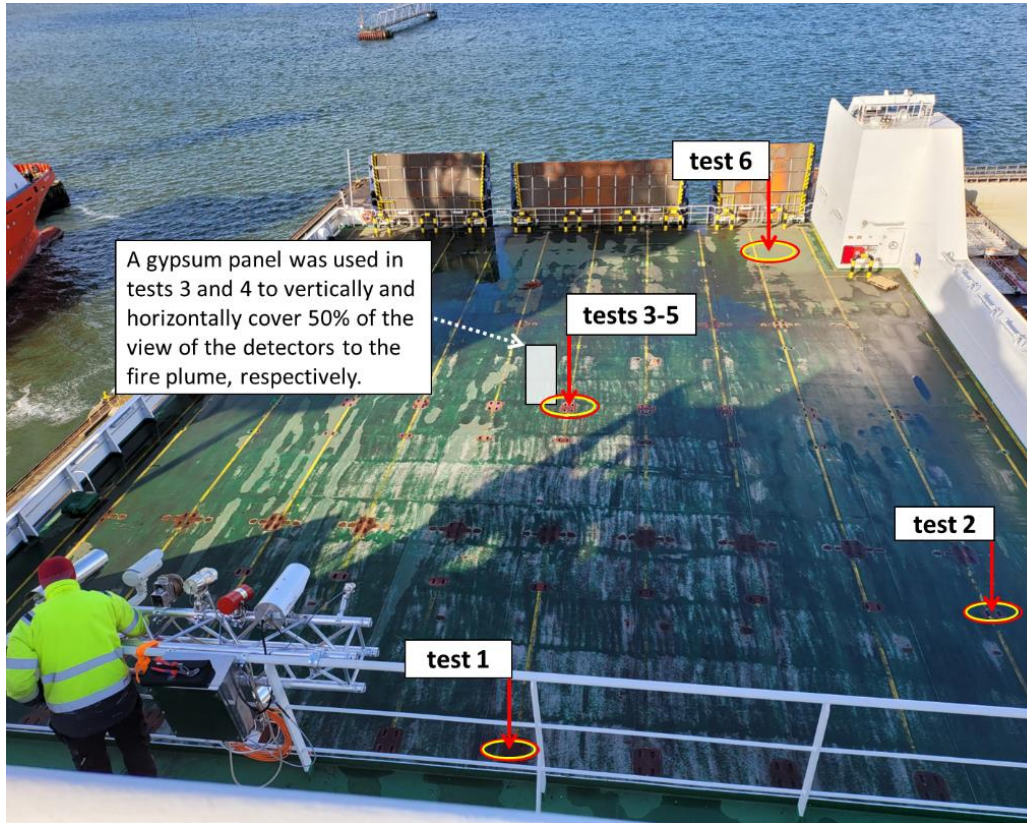


Figure 61: Setup and scenarios of fire experiments on the aft weather deck of Hollandia Seaways.

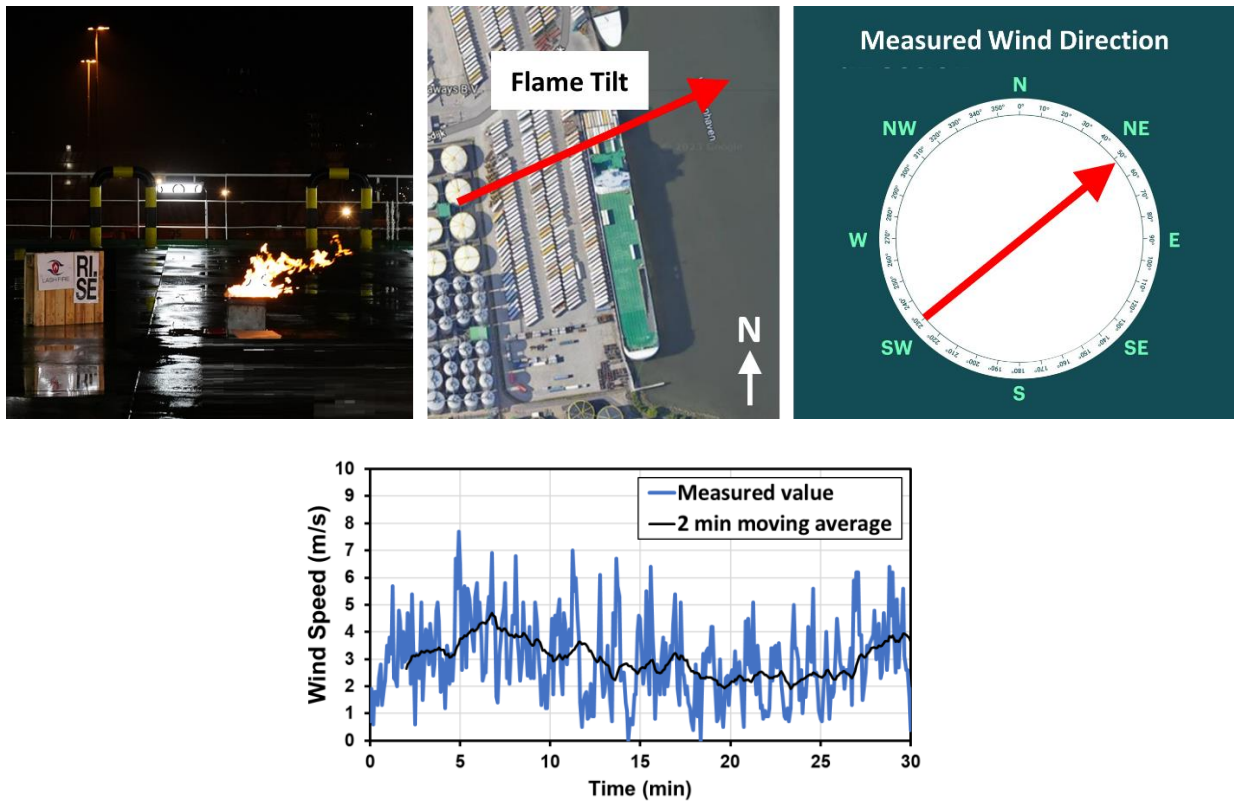


Figure 62: Flame tilt observations versus wind measurements made using a portable probe in the middle of the weather deck in the aft part of Hollandia Seaways during onboard fire experiments.

Table 13: Detection time of detectors (in seconds) during weather deck experiments on board Hollandia Seaways. The detector IDs are explained in Table 11. ‘ND’ indicates ‘No Detection’, i.e., the detector did not detect the fire after several minutes. ‘Yes’ indicates detection happened while the timing was not recordable. ‘Fault’ means the detector unit’s LED was indicating a fault in the system. IR1 and IR2 are simply infrared thermal cameras 1 and 2, and there is no difference in their technology.

Test no	Ignition position	Horizontal distance to fire (m)	Off-axis angle (degrees)	Obstruction of view to flame	Flame wavelength detectors			Video flame detection	IR thermal cameras		Hybrid (video + thermopile)
					FD1	FD2	FD3	VFD1	IR1	IR2	H1
1	Center 1	12	46	None	7	Yes	Yes	Yes	2	ND	8
2	Off-axis 1	15	40	None	5	Yes	Yes	Yes	128	201	15
3	Center 2	26	0	None	7	46	Yes/Fault	Yes	2	22	11
4	Center 2	26	0	Left 50%	7	Yes	Yes/Fault	Yes	3	23	14
5	Center 2	26	0	Top 50%	7	Yes	Yes/Fault	ND	2	46	10
6	Off-axis 2	40	17	None	8	Yes	Yes/Fault	Yes	7	ND	ND

9.6.2 Results

The results of the weather deck experiments in terms of detection time for the different detectors are summarised in Table 13. These results indicate that the systems managed to detect the fire like they did in the laboratory experiments, with only four cases of no detection, namely, one associated with thermal camera IR2 for a fire position which was at the very bottom of its field of view, two associated with hybrid camera H1 for the farthest off-axis fire position, and lastly, one associated with the video flame detector VFD1 when the top half of the flame was obstructed. Given that a single detector is usually not expected to cover the entire deck, it is considered acceptable to see such limitations and detection failures at the borders of field of view of detectors IR2 and H1, such that their results can be considered highly promising. The lack of detection for the obstructed flame by VFD1, however, is a

discouraging weakness of video analytics relying on flame flicker patterns which are not easily identifiable for obstructed flames.

Based on the detection time results in Table 13, flame wavelength detector FD1 offered the most reliable results, as it detected all the fires consistently within 5 to 8 s, while it did not have any nuisance alarms during the operational trial (see FD1 results in Table 12). This is while the most sensitive detection system during the fire experiments was the thermal imaging detection system employing thermal camera IR1, although this system took a long time to detect the off-axis fire during test 2 and generated nuisance alarms for several months during the operational trial (see IR1 results in Table 12).

One challenge faced during the fire experiments was that flame wavelength detector FD3 maintained a fire alarm status in the control panel while it did not allow recording alarms for FD3 or FD2 into the history of fire alarms in the control panel. It is expected that this was due to an error in the combined installation of these detectors, as FD3's LED was lit with a yellow colour, which indicated a fault mode according to the instruction manual of this detector. When not in a fault mode, FD3's LED was lit with a red colour during the fire experiments, which indicated that the detector was detecting a fire.

It is found that the abovementioned visual information provided by the LED that is physically located on the detector unit itself is considered vital information for the crew and fire patrols walking by, especially in situations where there is a fault in the connection between the detector and the fire alarm panel. Firstly, if the detector's LED is indicating a fire, it could help the crew confirm and localise the fire within the area covered by the detector. Secondly, in situations where there is a fault in the system, the crew can investigate the problem and respond accordingly, despite the general expectation that such connection faults must also be visible in the fire alarm panel for the ship operators to see and fix.

9.7 Video fire detection experiments in closed ro-ro space

9.7.1 Setup

To test the video fire detection system installed in the closed ro-ro space, a fog machine was used to conduct smoke tests. The fog machine essentially heated up a mixture of water and glycol to create artificial smoke, and it was operated as shown in Figure 64. The tests were performed at the locations shown in Figure 64, i.e., at 27 m and 72 m horizontal distance from the camera used for video analytics.

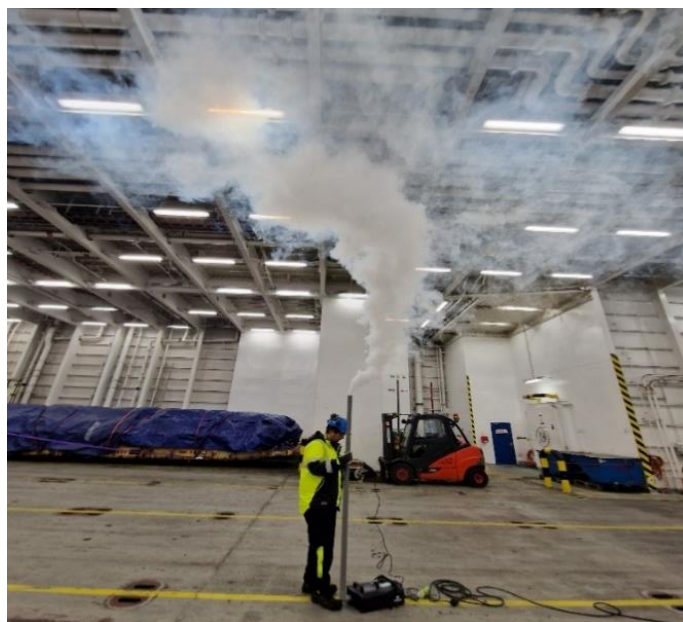


Figure 63: Smoke test setup in the closed deck using a fog machine connected to a duct (2 m long, and 50 mm diameter).

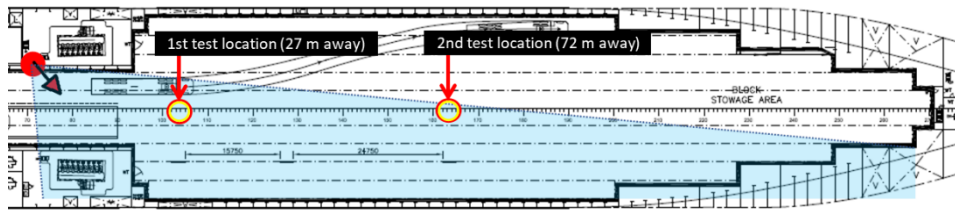


Figure 64: Locations of smoke tests in the closed deck using the fog machine setup shown in Figure 63.

The video analytics settings were set to low sensitivity and a time delay of 5 s. The alarm was set to trigger when the smoke reached the ceiling. Given that the detection zone for flames was defined at high heights (shown in Figure 54), flame experiments could not be performed in the closed deck on board due to safety concerns, so the flame detection capability of the video analytics system was not tested during the onboard experiments. However, it is expected that the results of the laboratory experiments discussed in section 8.1.3.3 are representative of the performance expected on board.

9.7.2 Results

The video detection system detected the smoke in both the smoke tests. When the smoke source was placed 27 m from the camera, the detection time was 30 s, while when the smoke source was placed 72 m from the camera, the detection time was 114 s (see Figure 65).

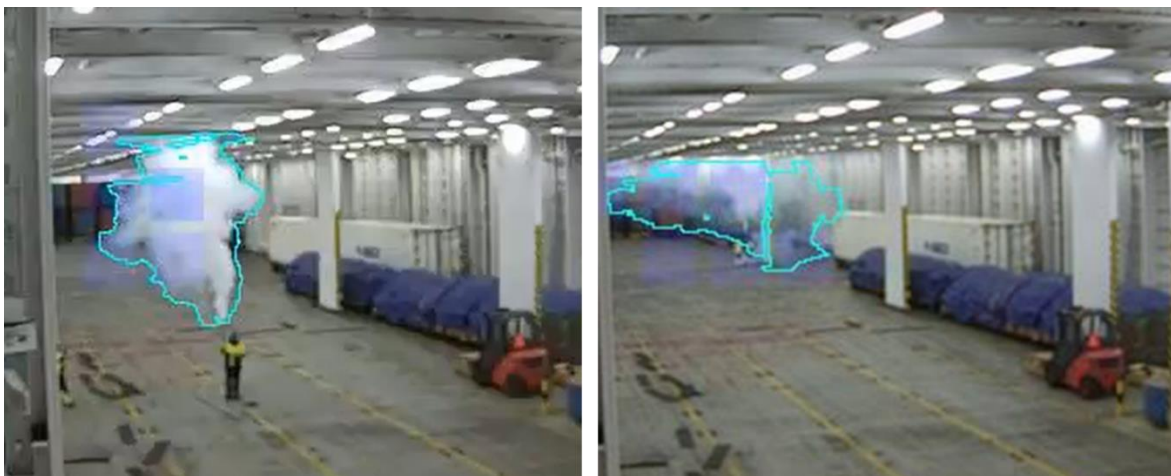


Figure 65: Smoke detected in the closed ro-ro space using video fire detection in 30 s when the smoke source was placed 27 m from the camera (left) and in 114 s when the smoke source was placed 72 m from the camera (right).

The ventilation system was off during the smoke tests, so the detection times may be somewhat longer in reality as the ventilation system is expected to delay the accumulation of smoke, namely by means of extraction through output vents placed at higher heights (exhaust flow in the order of 52000 m³/hour). Nevertheless, if the smoke source is further away from the output vents, it is expected that the effect of the ventilation system on video smoke detection is not very significant. This is especially likely because the vents are normally placed at the two ends of the deck, whereas the possible fire area could be anywhere along the length of the deck, albeit the fire must generate visible smoke to be detected using the video fire detection system. During the conducted tests, the artificial smoke produced by the fog machine was highly visible and took approximately 5 minutes to fill up the area visible in the camera footage. By switching the fans on, the smoke was cleared within several minutes. It is also noteworthy that the deck was empty during the tests. This caused the smoke to expand and

scatter more easily than in a real fire situation in which the deck is expected to be fully loaded such that the presence of vehicles in the deck would help accumulate more substantial and thicker smoke, resulting potentially in a shorter detection time in a real situation than in the tests.

The video fire detection system outlined the smoke very clearly in its footage which made it easy to confirm and localise the smoke (see Figure 65). This visualisation of the smoke boundary was found to be very useful in the ship's closed environment, because the manual identification and detection of smoke via regular CCTV is expected to be very difficult (if not impossible), especially when the deck is full of cargo such that the smoke occupies only the narrow free space above the cargo (see explanations for Figure 34 from laboratory experiments).

9.8 Main findings from onboard evaluations

Considering the operational trial of the detection systems installed on the weather deck, it was found that the flame wavelength detectors offered the most reliable results, as they did not have any nuisance alarms while they detected all the fire experiments consistently within seconds, both at the onset of the operational trial and at the end of the trial period. Moreover, these detectors did not experience the gradual tilting observed for other detectors, as the flame wavelength detectors had the smallest size (diameter ranging from 50 mm to 130 mm) and smallest weight (ranging from 650 g to 4.4 kg), as opposed to IR cameras which were the largest and heaviest (3 to 20 kg depending on the housing material). In the case of thermal imaging detection systems (i.e., systems using IR cameras), frequent nuisance alarms were observed due to the hot exhaust pipes of vehicles which regularly exceeded the infrared radiation thresholds used by the thermal cameras for fire detection. As a result, it is expected that despite the adjustment of detection threshold settings within reasonable bounds, some nuisance alarms for thermal cameras will persist from the hot exhaust pipes of vehicles. This reduces the reliability of thermal imaging cameras for *systematic* fire detection. However, the *manual* use of these detection systems is still expected to be highly beneficial and effective for fire confirmation and localisation, i.e., operators can use thermal imaging camera installations for the surveillance of hotspots without connecting the cameras to the control panel for fire alarms. The hybrid detector (video + thermopile) produced only a few alarms, but no footage/photos were available from its related alarm incidents. The alarms from the video flame detector were not recorded on the control panel due to an installation problem, but the detector was able to detect flames during the fire experiments both at the onset of the operational trial and at the end of the trial period, except for one flame when its top half was obstructed from the view. Nevertheless, it was not possible to draw any firm conclusions regarding the operational performance of this detector due to its missing fire alarm history. Lastly, the operational trials suggest that the detectors to be used on board ro-ro ships must be tested for progressive tilting based on regular shakes and vibrations, using the detector's own dedicated mount and fixing accessories.

The triple-IR flame wavelength detector installed on the open deck did not produce any nuisance alarms, while it responded to flames during fire experiments both at the onset of the operational trial and at the end of the trial period. In the final fire experiments, the fire was detected by virtue of its reflection in the empty deck, but such reflections are expected to be difficult to achieve in a deck fully loaded with cargo. To facilitate such detection of flame reflections from the narrow spaces between cargo items, it is considered possible to use small convex mirrors installed along the centre of the deckhead at regular intervals, although confirming and localising the fire using the footage will not be easy in this way, as the reflections on convex mirrors will be small. Moreover, sun reflections toward the detectors must be avoided.

The video fire detection system in the closed deck only produced nuisance alarms when the crew did a routine washdown of the deck. This type of nuisance alarm can be avoided either by switching off

the detection system during the washdowns or by proactively muting the alarms during the washdown operation around the cameras used for video analytics. However, the video fire detection system can remain operational during cargo operations, which is considered a great advantage over the point detectors that are normally deactivated using a timer during cargo operations to avoid nuisance alarms. For the closed ro-ro deck where light conditions were stable, the video analytics performed as expected and was able to visualise the smoke boundaries in the footage during the experiments with a fog machine such that the smoke was easy to confirm and localise. It is expected that the confirmation and localisation of the smoke will be otherwise very difficult using regular CCTV without the help of video fire analytics. Therefore, video fire detection seems to be very useful for closed decks where the light conditions are stable and just a few cameras can be used to cover a large distance for fire detection.

The weather deck fire experiments conducted on board at the end of the operational trial were found to be more challenging for the systems than standard tests performed according to EN 54-10 [11]. This was due to the long distances involved, the extensive height of the detectors on the weather deck, and the large off-axis angles faced by the detectors in the ship's geometry. First and foremost, this highlights the importance of placing enough detectors on the weather deck to cover the entire area with some overlaps. Moreover, this draws attention to the detector limitations in terms of field of view and distance ratings which are not covered by class 1 to 3 defined in EN 54-10 [11].

The weather deck experiments also showed that the visual information provided by the LED of the detector units can provide useful information to the crew and fire patrols walking by, as it could help the crew confirm and localise the fire within the area covered by the detector, and the crew can investigate the problem in situations where there is a fault in the connection between the detector and the fire alarm panel.

10 Recommendations

As part of Risk Control Option 12 (RCO12) of LASH FIRE, the following Risk Control Measures (RCMs) are considered for visual systems of fire confirmation and localization relevant to ro-ro ships:

- (1) Video fire detection: this RCM mainly includes the analysis of video footage for the recognition of flames and smoke using a systematic algorithm, namely, for Video Flame Detection (VFD) and Video Smoke Detection (VSD). Nevertheless, the manual use of video footage for visual fire confirmation and localisation is also considered relevant.
- (2) Thermal imaging fire detection: this RCM mainly includes systematic fire detection using a thermal imaging detection system that relies on infrared cameras. Nevertheless, the manual use of thermal imaging footage for visual fire confirmation and localisation is also considered relevant.

This chapter includes a summary of recommendations for the respective RCMs which are found appropriate for weather decks as well as open and closed ro-ro decks.

10.1 Video fire detection

For video fire analytics systems, the only currently existing standard that is relevant to this technology is FM 3232 [30]. According to the SOLAS Fire Safety Systems (FSS) Code [31], point detectors of flame shall be tested as per EN 54-10 [11, pp. 54–10], but the standard does not mention specific testing configurations which will challenge video flame detectors with respect to real fire detection expectations. A detailed set of recommendations to be considered based on the LASH FIRE evaluations for ro-ro ships have been provided in deliverable D09.2 [5], including both VFD and VSD systems from the viewpoint of systematic fire detection.

From the specific viewpoint of fire confirmation and localisation using video systems, the following items are recommended to be considered in the design and implementation of the systems for ro-ro ships:

- Closed ro-ro decks where light conditions are stable are recommended for video analytics.
- Based on the nuisance alarm sources observed during the laboratory experiments, it is recommended that the lower heights of the deck are masked out by video fire analytics software to avoid frequent nuisance sources which erode trust in the system (see explanations for the zones defined in Figure 54).
- Smoke is expected to accumulate along the deckhead of closed ro-ro decks either regularly from the vehicles or during a fire situation, and thus cameras must be installed on the side plating and approximately 1 to 2 m below the deckhead, but higher than the maximum height expected for the cargo items.
- The confirmation and localisation of fires using video analytics can be facilitated when the smoke and flame boundaries are highlighted using adaptive colours which contrast according to the changing background colours. To improve information accessibility, the used colours must avoid simultaneous combinations of green and red as well as blue and yellow [32]. Moreover, colour must not be the only means of distinction, so text and patterns must be used to maximise alternative means of accessibility to the information.
- Video fire detectors must incorporate an LED light on the detector unit that can alert the crew and fire patrols walking by regarding the detection of fires as well as faults in the system based on the colour of the LED light. This can help the crew to confirm and localise the fire within the area covered by the detector, and the crew can investigate the problem in situations where there is a fault in the connection between the detector and the fire alarm panel.

- Video fire detectors that rely on flicker pattern recognition are most likely reliant on the correct orientation of the device for their optimal operation, so the installer must make sure that the detector is oriented correctly, such that the video footage is upright.
- Flame wavelength detectors that come with a built-in video camera do not rely on a correct orientation for their detection functionality. However, for the live footage to be useful for visual fire confirmation and localisation, the detector must be oriented correctly such that its video footage is upright. This is also important for the combination of the system with video analytics software for fire localisation.
- Many ships switch off their lights in the closed cargo decks when at sea. This is expected to make it easier to identify flames in the video. However, the detection of smoke becomes almost impossible using video in such scenarios because of the lack of contrast between the smoke and its background in the footage. As a result, it is recommended to always keep the lights on if a video fire detection system is used.
- The operational trials suggest that the cameras to be used on board ro-ro ships must be tested with their dedicated mounts and fixing accessories for their immunity to progressive tilting due to shaking, vibrations, and thermomechanical stresses which contribute to the natural loosening of bolts. This is to make sure that the camera can remain pointed at the desired location.
- The design of camera mounts and fixing accessories must mitigate spontaneous camera tilting. In this regard, the part of the camera mount that allows tilting the angle of the camera is best to be placed along the centre of gravity of the unit such that the distribution of weight is equal on both sides of the pivot point. Moreover, the tilting mechanism must not rely on a single bolt, as this causes progressive wear and premature failure.
- Heavier camera units are much more prone to tilting and requiring maintenance, so smaller and lighter units are more recommendable.
- To facilitate the detection of flame reflections from the narrow spaces between cargo items, it is possible to install small convex mirrors along the centre of the deckhead at regular intervals in the closed deck. If such a solution is to be used in open ro-ro decks, the installations should make sure that sun reflections toward the cameras are avoided.
- VFD and VSD may use existing CCTV cameras, but it must be made sure that the area coverage of the cameras is adequate and that their picture quality is reasonable.
- Systematic video fire localisation is generally not recommended to be used for the guidance of autonomous fire extinguishment monitors used outdoors (section 6.2). IR array detectors are considered much more reliable due to their immunity to nuisance alarms, although the continued presence of big flames in the field of view is expected to desensitise the detector over time. Therefore, the first fire detection information must be used to aim the water nozzle of the autonomous fire monitor at the fire, while later the nozzle must continue to focus on the initial spot until new fire location information becomes available from the detector.

10.2 Thermal imaging fire detection

Based on the results of laboratory and operational evaluations, the following recommendations can be made regarding the design and implementation of thermal imaging fire detection systems for visual fire confirmation and localisation on ro-ro ships:

- Due to the excellent ability of thermal imaging systems to see through thin smoke (example shown in Figure 46) and their ability to identify various heat sources, developing fires, and concealed fires which are otherwise undetectable using other means (example shown in Figure

29), the *manual* use of thermal imaging fire detection systems is recommended for fire confirmation and localisation, i.e., the ship operators are recommended to use thermal imaging camera installations for surveillance without connecting the cameras to the fire control panel (to avoid frequent nuisance alarms due to the hot exhaust pipes of vehicles).

- An option to detect moving vehicles was found to be useful in reducing the number of nuisance alarms due to the hot exhaust pipes of vehicles, but the fire detection sensitivity was worse with this vehicle discrimination option. Therefore, it is recommended to further develop and improve the vehicle discrimination algorithm using big data [33] and deep learning [34].
- Unlike video fire analytics, thermal imaging can employ (IR) cameras on open decks and weather decks, but this means that the cameras must be protected well from weather elements and the harsher environmental conditions outdoors.
- An important factor to consider for the outdoor use of IR cameras is their accessibility for maintenance, as they need to be checked periodically for their functionality and to adjust their tilt so that the camera is pointed at the intended area. This is especially important for IR cameras as they are relatively heavy and can easily weigh between 3 and 10 kg.
- Some thermal imaging fire detection software allow the user to choose the colour scaling of the thermal images based on arbitrary maximum and minimum values and using default colour bars. In such cases, the user must make sure to set the limits of maximum and minimum values such that the image can make sense and be interpreted properly. Figure 66 illustrates how the selection of wrong limits can render the image less useful for fire confirmation.

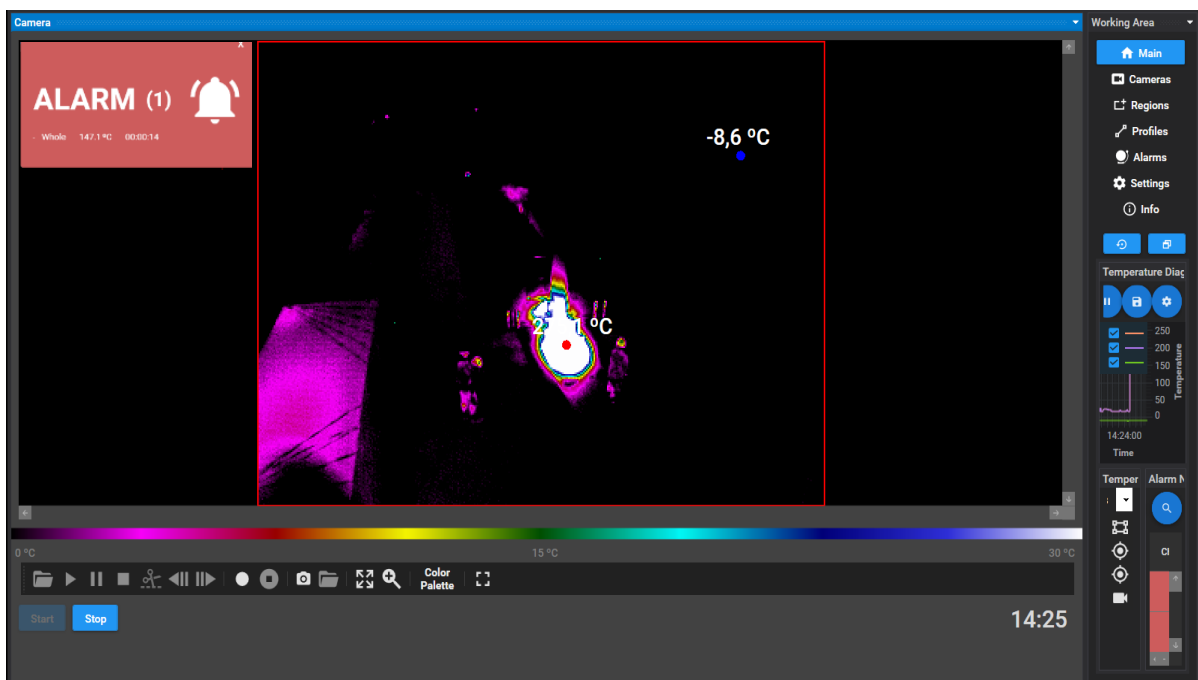


Figure 66: Snapshot from the footage of a thermal imaging detection system during a LASH FIRE demonstration test. An extended temperature range fixed in the display software has caused the image to have much less contrast in the cold regions, making it difficult to interpret intuitively. The regular image of the test has been presented in Figure 24.

- Certain areas of the field of view of IR cameras may be masked in the thermal imaging fire detection software in case they are known to cause nuisance alarms (such as the smokestack).

- IR camera detectors must incorporate an LED light on the detector unit that can alert the crew and fire patrols walking by regarding the detection of fires as well as faults in the system based on the colour of the LED light. This can help the crew to confirm and localise the fire within the area covered by the detector, and the crew can investigate the problem in situations where there is a fault in the connection between the detector and the fire alarm panel.
- The operational trials suggest that the cameras to be used on board ro-ro ships, especially on weather decks and open ro-ro decks, must be tested with their dedicated mounts and fixing accessories for their immunity to progressive tilting due to recurring weather elements, shaking, vibrations, and thermomechanical stresses which contribute to the natural loosening of bolts. This is to make sure that the camera can remain pointed at the desired location.
- The design of camera mounts and fixing accessories must mitigate spontaneous camera tilting. In this regard, the part of the camera mount that allows tilting the angle of the camera is best to be placed along the centre of gravity of the unit such that the distribution of weight is equal on both sides of the pivot point. Moreover, the tilting mechanism must not rely on a single bolt, as this causes progressive wear and premature failure.
- Heavier camera units are much more prone to tilting and requiring maintenance, so smaller and lighter units are more recommendable.
- To facilitate the detection of flame reflections from the narrow spaces between cargo items, it is possible to install small convex mirrors along the centre of the deckhead at regular intervals in the closed deck. If such a solution is to be used in open ro-ro decks, the installations should make sure that sun reflections toward the cameras are avoided.
- Systematic thermal imaging fire localisation is generally not recommended to be used for the guidance of autonomous fire extinguishment monitors (section 6.2). IR array detectors are considered much more reliable due to their immunity to nuisance alarms, although the continued presence of big flames in the field of view is expected to desensitise the detector over time. Therefore, the first fire detection information must be used to aim the water nozzle of the autonomous fire monitor at the fire, while later the nozzle must continue to focus on the initial spot until new fire location information becomes available from the detector.

11 Conclusion

Main author of the chapter: Davood Zeinali, FRN

Efficient collection and analysis of information is vital when it comes to fire alarms and potential fires on board ro-ro ships. It is especially important for the bridge to visually confirm the fire and its location as early as possible to respond swiftly, e.g., to activate the fire suppression system in the affected area. However, manual fire confirmation by runners is not always possible safely and efficiently. A strategic alternative is the use of visual fire detection systems, i.e., systems that enable assessing the area causing a fire alarm remotely using live video (regular or thermal footage). This was the focus of the present document to enable good assessments and decision-making for the mitigation of fire incidents and their respective consequences on board ro-ro ships. Other types of sensor data, such as smoke alarms from point detectors as well as heat maps from linear heat detection systems, can also provide information on the conditions in the fire zone, and this may be used in combination with cameras to localise and assess the fire development, but such data cannot visualise the fire like video images from a camera can for a direct confirmation of the fire which is crucial to the bridge operators.

Despite the many advantages of manual observations, there are some limitations to what a human can do, and that is where visual systems can be of assistance. For instance, IR thermal cameras can see through thin smoke more easily, and this allows for locating the fire source when regular cameras or manual observations are not possible. In this regard, the collected information needs to be processed and presented to the operators in an efficient and understandable interface, highlighting the most relevant information for decision-making.

The laboratory experiments and the operational evaluations show that cameras (both regular and thermal types) provide a lot of useful information regarding the fire situation if they are not obstructed by objects or smoke. Live video can give the operators on the bridge a visual image of the fire area before and after the activation of the alarm, providing a better understanding of the cause of the alarm and how the fire may be developing. Moreover, thermal infrared cameras provide visual data of temperatures in different areas, unlike ordinary video cameras or manual observations.

Thermal infrared imaging cameras have various advantages over other systems due to their excellent ability to see through thin smoke and to identify various heat sources, developing fires, and concealed fires which are otherwise undetectable using other means without direct line of sight to flames or smoke. Moreover, IR cameras do not require the presence of stable ambient light conditions. However, the hot exhaust pipes of vehicles cause frequent nuisance alarms which are difficult to avoid. Overall, the ship operators are recommended to use thermal imaging camera installations for the surveillance of hotspots, but only without connecting the cameras to the fire alarm panel (to avoid frequent nuisance alarms).

Video fire analytics algorithms have ample potential for closed decks where light conditions are stable, as they can reliably highlight the location of the fire by outlining the boundaries of smoke and flames when they are otherwise difficult to identify manually in CCTV footage. This is especially useful as CCTV systems used on ro-ro cargo decks are in principle compatible with video fire detection.

Other types of fire detection systems that come with video cameras are similarly useful for the confirmation and localisation of fires when they provide live video. In this regard, flame wavelength detectors offered the most reliable operational results on the weather deck, as they did not have any nuisance alarms while they detected all the fire experiments within seconds, providing video from the tested fires. Such video outputs are further useful if they highlight the location of the fire in the images.

12 References

- [1] S. Bram, U. Millgård, and H. Degerman, *Systemperspektiv på brandsäkerhet till sjöss- en studie av organisering och användbarhet i brandskyddet på RoPax-fartyg*. 2019. Accessed: Feb. 21, 2023. [Online]. Available: <http://urn.kb.se/resolve?urn=urn:nbn:se:ri:diva-38935>
- [2] IMO, *SOLAS, International Convention for the Safety of Life at Sea, consolidated edition 2014*, Sixth edition, 2014. in IMO publication. London: International Maritime Organization, 2014. Accessed: Mar. 17, 2023. [Online]. Available: http://books.google.com/books?id=Ycp31_i-tzsC
- [3] EMSA, 'Guidance on the carriage of AFVs in RO-RO spaces', European Maritime Safety Agency. Accessed: Mar. 13, 2023. [Online]. Available: <https://www.emsa.europa.eu/publications/reports/item/4729-guidance-on-the-carriage-of-afvs-in-ro-ro-spaces.html>
- [4] J. Wikman *et al.*, *Study investigating cost effective measures for reducing the risk from fires on ro-ro passenger ships (FIRESAFE)*. European Maritime Safety Agency, 2017. Accessed: Mar. 03, 2023. [Online]. Available: <http://urn.kb.se/resolve?urn=urn:nbn:se:ri:diva-29418>
- [5] D. Zeinali, R. Stølen, and E. S. Skilbred, 'LASH FIRE D09.2 – Developed ro-ro spaces fire detection solutions and recommendations', LASH FIRE deliverable report D09.2, Aug. 2023. [Online]. Available: <https://lashfire.eu/deliverables/>
- [6] K. Ukaj and E. D. Carvalho, 'LASH FIRE D04.1 – Review of accident causes and hazard identification report', LASH FIRE deliverable report D04.1, May 2020. [Online]. Available: <https://lashfire.eu/deliverables/>
- [7] DNV GL, 'Fires on ro-ro decks', DNV GL. Accessed: Mar. 09, 2023. [Online]. Available: <https://www.dnv.com/news/enhancing-fire-safety-on-ro-ro-decks-69059>
- [8] The North of England P&I Association, 'Ro-Ro Fires', *Loss prevention briefing*, 2017.
- [9] A. Verzoni, 'Felicity Ace Fire', NFPA Journal. Accessed: Mar. 24, 2023. [Online]. Available: <https://www.nfpa.org/News-and-Research/Publications-and-media/NFPA-Journal/2022/Spring-2022/News-and-Analysis/Dispatches/EV-Ship-Fire>
- [10] J. Leroux *et al.*, *FIRESAFE II Containment and Evacuation*. 2018. Accessed: Mar. 01, 2023. [Online]. Available: <http://urn.kb.se/resolve?urn=urn:nbn:se:ri:diva-39903>
- [11] EN 54-10, 'Fire detection and fire alarm systems – Part 10: Flame detectors – Point detectors'. European Committee for Standardization, CEN-CENELEC, Brussels, Feb. 08, 2002.
- [12] M. Arvidson, 'LASH FIRE D10.3 – Description of the development of weather deck fire-extinguishing systems and selected solutions', LASH FIRE deliverable report D10.3, Feb. 2023. Accessed: Aug. 08, 2023. [Online]. Available: https://lashfire.eu/media/2023/03/D10.3_Description-of-the-development-of-weather-deck-fire-extinguishing-systems-and-selected-solutions.pdf
- [13] R. James, M. Eggert, and M. Arvidson, 'LASH FIRE D10.2 – Onboard demonstration of weather deck fire-extinguishing solutions', LASH FIRE deliverable report D10.2, Jun. 2023. [Online]. Available: <https://lashfire.eu/deliverables/>
- [14] M. Arvidson, 'LASH FIRE D10.1 – Description of the development of automatic first response fire protection systems for ro-ro spaces on vehicle carriers', LASH FIRE deliverable report D10.1, Jan. 2022. Accessed: Aug. 08, 2023. [Online]. Available: https://lashfire.eu/media/2022/06/LASH-FIRE_D10.1_Description-of-the-development-of-local_application-system-solutions.pdf
- [15] M. Arvidson, 'LASH FIRE D10.4 – Large-scale validation of the new fire test standard for alternative fixed fire-fighting systems', LASH FIRE deliverable report D10.4, Feb. 2023. Accessed: Aug. 08, 2023. [Online]. Available: https://lashfire.eu/media/2023/03/LASH-FIRE_D10.4_Large-scale-validation-of-the-new-fire-test-standard-for-alternative-fixed-fire-fighting-systems-1.pdf
- [16] V. Radolovic, 'LASH FIRE D05.6 – Ship integration requirements', LASH FIRE deliverable report D05.6, Aug. 2022. Accessed: Jul. 06, 2023. [Online]. Available: https://lashfire.eu/media/2022/10/LASH-FIRE_D05.6_Ship-integration-requirements-V02.pdf

- [17] V. Radolovic and O. Kuzmanovic, 'LASH FIRE D05.7 – Ship integration evaluation', LASH FIRE deliverable report D05.7, Feb. 2023. Accessed: Jul. 06, 2023. [Online]. Available: https://lashfire.eu/media/2023/03/LASH-FIRE_D05.7_Ship-integration-evaluation-Version2.pdf
- [18] V. Radolovic, O. Kuzmanovic, and I. Vidic, 'LASH FIRE D05.8 – Ship integration cost and environmental assessment', LASH FIRE deliverable report D05.8, Feb. 2023. Accessed: Jul. 06, 2023. [Online]. Available: https://lashfire.eu/media/2023/04/LASH-FIRE_D05.8_Ship-integration-cost-and-environmental-assessment-V3.pdf
- [19] V. Radolovic and O. Kuzmanovic, 'LASH FIRE D05.9 – Performance, feasibility and integration assessment', LASH FIRE deliverable report D05.8, Jun. 2023. Accessed: Jul. 06, 2023. [Online]. Available: <https://lashfire.eu/deliverables/>
- [20] EN 54-22, 'Fire detection and fire alarm systems – Part 22: Resettable line-type heat detectors'. CEN, European Committee for Standardization, 2020.
- [21] V. Radolovic and O. Kuzmanovic, 'LASH Fire D5.7 - Ship integration evaluation', Feb. 2023.
- [22] EN 54-29, 'Fire detection and fire alarm systems - Part 29: Multi-sensor fire detectors - Point detectors using a combination of smoke and heat sensors'. CEN, European Committee for Standardization, Apr. 2015.
- [23] D. Zeinali, F. Ingold, Z. Acem, R. Mehaddi, G. Parent, and P. Boulet, 'Experimental study of radiation attenuation using water curtains in a reduced-scale deck of a ro-ro ship', presented at the STAB&S 2021, Online, 2021, p. 8. [Online]. Available: <http://www.stability-and-safety-2021.org/>
- [24] Tyco User Manual, 'FlameVision FV300 IR Array Flame Detector Series'. Accessed: Aug. 20, 2023. [Online]. Available: https://tycosafetyproducts-anz.com/public/Manuals/120-415-886_UM35_FV300_User_iss4_full_manual.pdf
- [25] T. M. Tritt, 'Thermoelectric Materials: Principles, Structure, Properties, and Applications', in *Encyclopedia of Materials: Science and Technology*, K. H. J. Buschow, R. W. Cahn, M. C. Flemings, B. Ilschner, E. J. Kramer, S. Mahajan, and P. Veyssi re, Eds., Oxford: Elsevier, 2002, pp. 1–11. doi: 10.1016/B0-08-043152-6/01822-2.
- [26] X. Yang *et al.*, 'Improvement of flow field uniformity and temperature field in gasoline engine catalytic converter', *Applied Thermal Engineering*, vol. 230, p. 120792, Jul. 2023, doi: 10.1016/j.applthermaleng.2023.120792.
- [27] D. Johnston, 'How Hot Does a Muffler Get?' Accessed: Sep. 04, 2023. [Online]. Available: <https://mycarmakesnoise.com/emissions/how-hot-does-a-muffler-get/>
- [28] D. Hawley, 'How Hot Does A Car Exhaust Pipe Get?' Accessed: Sep. 04, 2023. [Online]. Available: <https://www.jdpower.com/cars/shopping-guides/how-hot-does-a-car-exhaust-pipe-get#:~:text=Typically%2C%20the%20car%20exhaust%20pipes,Engine%20and%20exhaust%20pipe%20condition.>
- [29] D. Zeinali, R. St len, and L. Jiang, 'LASH FIRE D09.1 – Developed weather deck fire detection solutions and recommendations', LASH FIRE deliverable report D09.1, Aug. 2023. [Online]. Available: <https://lashfire.eu/deliverables/>
- [30] FM 3232, 'Video image fire detectors for automatic fire alarm signalling'. 2023. Accessed: Jun. 14, 2023. [Online]. Available: https://www.techstreet.com/standards/fm-approvals-3232?product_id=2562667#jumps
- [31] 'IMO Res. MSC.98(73) International Code for Fire Safety Systems (FSS Code)'. International Maritime Organization, 2016.
- [32] {Colorado State University}, 'What is Color Contrast?' Accessed: Sep. 11, 2023. [Online]. Available: <https://www.chhs.colostate.edu/accessibility/best-practices-how-tos/color-contrast/>
- [33] K. Cukier and V. Mayer-Schoenberger, 'The Rise of Big Data: How It's Changing the Way We Think About the World', *Foreign Affairs*, vol. 92, no. 3, pp. 28–40, 2013, Accessed: Sep. 10, 2023. [Online]. Available: <http://www.jstor.org/stable/23526834>
- [34] Y. LeCun, Y. Bengio, and G. Hinton, 'Deep learning', *Nature*, vol. 521, no. 7553, pp. 436–444, May 2015, doi: 10.1038/nature14539.

13 Indexes

13.1 Index of tables

Table 1. Classification/location of fires on vehicle decks, from the North of England P&I Association [8].	10
Table 2. Estimated costs for the proposed thermal imaging detection system shown in Figure 11 for Magnolia Seaways.	23
Table 3. Estimated costs for the proposed video detection system shown in Figure 12 for closed ro-ro spaces on Magnolia Seaways, consisting of 11 cameras for the main deck (top figure) and 4 cameras for the tank top (bottom figure).	24
Table 4: List of the tested detectors in the two series of laboratory experiments for open and closed ro-ro spaces.	26
Table 5: Detection time of detectors (in seconds) during ro-ro space experiments in the first test series (ceiling height = 3 m, detectors' height = 2 m), sorted based on the ignition position. 'ND' means 'No Detection'. Empty fields mean that the detector was not active during the test. The wind velocities were measured at the central wind sensor position shown in Figure 17.	33
Table 6: Detection time of detectors (in seconds) during weather deck experiments in the first test series (ceiling height = 16 m, detectors' height = 5.5 m), sorted based on the ignition position. 'ND' indicates 'No Detection'. Empty fields indicate that the detector was not active during the test. The wind velocities were measured at the central wind sensor position shown in Figure 17.	34
Table 7: Detection time of detectors (in seconds) during ro-ro space experiments in the second test series with heptane pool fires and lithium-ion batteries (ceiling height = 5 m, detectors' height = 4 m), sorted based on the ignition position. 'ND' indicates 'No Detection', i.e., the detector did not detect the fire. 'Yes' indicates detection happened while the timing was not recordable. Empty fields indicate that the detector was not active during the test. VSD is video smoke detection and VFD is video flame detection. IR1 to IR3 are simply infrared thermal cameras 1 to 3, and there is no difference in their technology.	34
Table 8: Detection time of detectors (in seconds) during weather deck experiments in the second test series with heptane pool fires (ceiling height = 16 m, detectors' height = 4 m). 'ND' indicates 'No Detection', i.e., the detector did not detect the fire. 'Yes' indicates detection happened while the timing was not recordable. Empty fields indicate that the detector was not active during the test. IR1 to IR3 are simply infrared thermal cameras 1 to 3, and there is no difference in their technology.	35
Table 9: Maximum distance where the different detectors triggered the alarm based on a Ø10 cm ethanol fire. IR1 and IR2 are thermal imaging cameras and FD1 to FD3 are flame wavelength detectors. The	36
Table 10: Average number of image pixels occupied by the flame in thermal imaging and regular video footage from the wind tests.	48
Table 11: Optical detectors evaluated through the operational trials on board Hollandia Seaways.	60
Table 12: History of nuisance fire alarms from the new systems installed on Hollandia Seaways as part of LASH FIRE.	62
Table 13: Detection time of detectors (in seconds) during weather deck experiments on board Hollandia Seaways. The detector IDs are explained in Table 11. 'ND' indicates 'No Detection', i.e., the detector did not detect the fire after several minutes. 'Yes' indicates detection happened while the timing was not recordable. 'Fault' means the detector unit's LED was indicating a fault in the system. IR1 and IR2 are simply infrared thermal cameras 1 and 2, and there is no difference in their technology.	69

13.2 Index of figures

Figure 1. Timeline of actions when a fire is detected.	11
--	----

Figure 2: Concept of flame localisation with an IR array flame wavelength detector using a 16x16 array of infrared sensors.....	13
Figure 3: Fire detection panel on Pearl Seaways.	16
Figure 4: CCTV panel from Pearl Seaways (left) and imagined presentation of the alarm information via highlighting the CCTV from fire area. The flame and smoke boundaries may also be highlighted by the detection system as shown in Figure 31.	17
Figure 5: Setup of LASH FIRE experiments with autonomous fire monitors (suppression system for weather decks) [12]. The photo shows an experiment where one fire monitor is projecting water towards a fire identified using two IR array flame wavelength detectors. The test area is 50 m by 30 m and has been marked on the ground with squares measuring 5 m by 5 m.....	18
Figure 6: Coordinates identified for three flames using Fike video fire analytics. The numbers written beside each flame are X and Y coordinates based on the number of horizontal and vertical pixels from the top left side of the image, respectively.....	19
Figure 7: Example thermal imaging (infrared) camera installed on board Hollandia Seaways for LASH FIRE evaluations.	21
Figure 8: Square law between distance and area of detection (applicable when $D2 \gg D1$): if an object that has an area of $A1$ is detectable at the distance of $D2$, detection at a distance of $2 \times D2$ requires nearly an area of $4 \times A1$	21
Figure 9: Typical free space above cargo items (height shown with yellow arrows) which limit the field of view of cameras installed on the deckhead of ro-ro spaces. The tallest items in the field of view will define the extent of free height available.....	22
Figure 10: Integrated example of a thermal imaging fire detection system for the closed ro-ro spaces on Magnolia Seaways consisting of 4 cameras for the main deck (top figure) and 2 cameras for the tank top (bottom figure).	22
Figure 11: Concept of a detection system based on thermal imaging (infrared) cameras for closed ro-ro spaces on Magnolia Seaways, i.e., on the main deck and the tank top as shown in Figure 10.....	23
Figure 12: Integrated example of a video fire detection system for the closed ro-ro spaces on Magnolia Seaways consisting of 11 cameras for the main deck (top figure) and 4 cameras for the tank top (bottom figure).	24
Figure 13: The large fire test hall at RISE Fire Research in Trondheim, Norway. The purple arrows indicate the wind direction across the test hall when using an open western gate measuring 4.5 m wide and 4.3 m high (marked with a red rectangle) and ventilation fans at the top of the hall (numbered 1 to 7 with red digits). The adjustable ceiling measuring 25 m long and 16 m wide was fixed at heights of 3 m and 5 m for ro-ro space tests, and at 16 m for weather deck tests as illustrated.	27
Figure 14. The experimental setup with 5 m ceiling height. The detectors relevant for visual fire confirmation and localisation can be seen to the left, marked with a yellow rectangle (location specified more accurately in Figure 17).....	27
Figure 15: Positions of the ignition sources relative to the steel containers. Positions used in test series 1 are marked with P1, P4, P5 and P6, and positions used in test series 2 are marked with F1 to F4...	28
Figure 16: Side view sketch of the experiment configuration in the second test series with a ceiling height of 5 m. The camera height was different for other ceiling heights tested (see explanations for Figure 17).....	28
Figure 17: Top view of setup used in the two series of LASH FIRE tests. The numbers indicate the X and Y positions of items in the test hall. The four green squares indicate the outlines of the ISO 8ft containers. During the first test series, the detector cameras were mounted at the height of 2 m for ro-ro space tests with a ceiling height of 3 m, while they were mounted at the height of 5.5 m during weather deck tests with a ceiling height of 16 m. During the second test series, the detector cameras were mounted at the height of 4 m for ro-ro space tests with a ceiling height of 5 m and weather deck	

tests with a ceiling height of 16 m. The wind sensor was used only during the first test series and its central location was at the height of 1.5 m. Other wind measurements were made across the transversal plane which is marked with a dotted line in the diagram (wind data shown in Figure 18).

..... 29

Figure 18: Wind velocities (m/s) along the wind measurement plane shown in Figure 17 with active fans shown in Figure 13: (top) ro-ro space test with fans 1 & 2; (middle) ro-ro space test with fan 2; (bottom) weather deck test with fans 1, 2, 6 & 7. 30

Figure 19: Sketch of deck 3 in Stena Flavia with ceiling beams drawn with blue lines and smoke detectors marked with red dots. The star indicates a worst-case fire position where smoke needs to pass the most beams to reach smoke detectors..... 30

Figure 20: Top view sketch of the test configuration used in the reflection tests in the second test series. The fire was placed in a container with open doors outside the field of view of the detectors and a steel container was used as a reflective surface with distances of 5 m, 9.5 m, and 14.5 from the detectors. 31

Figure 21: Beechwood sticks on a hot plate generating light grey smoke without flames. 31

Figure 22: Maximum extension of the flame lengths for the three heptane pan fires of 30 x 30 cm (left), 50 x 50 cm (middle) and 60 x 60 cm (right)..... 32

Figure 23: Overheating three lithium-ion battery cells in a steel enclosure with electric heating elements. The steel box was open in the front. Insulation was placed on top of the box during tests to get a more uniform heating of all three cells..... 32

Figure 24: Video image from the built-in camera of a triple-IR flame wavelength detector triggered by a flame during a LASH FIRE test. When the alarm is activated, the frame around the image turns red and the text “FIRE” is shown on the upper part. 36

Figure 25: Snapshot from the footage of a thermal imaging camera captured during a demonstration test. The high temperature area of the fire is marked with red, clearly drawing attention to the hot spot (see regular image in Figure 24)..... 37

Figure 26: Screenshot from the software of thermal camera IR2 during test 19 (described in Table 8). Temperatures from selected hot areas are measured (see red rectangle) and recorded over time (see graph in Figure 28). 38

Figure 27: Image from the alarm of thermal imaging camera IR3 (here IR3 means third camera, not triple-IR technology) during test 19 (described in Table 8). The recorded maximum temperatures are presented in Figure 28..... 38

Figure 28: Flame and container roof temperatures measured using thermal imaging cameras IR1 and IR2 during test 19 (described in Table 8). Thermal images obtained using these cameras are shown in Figure 26 and Figure 27..... 39

Figure 29: A fire inside a closed container detected by a thermal imaging detection system using an infrared camera (test 13 in Table 7). The hot roof of the container is marked with a red colour by the detection software to highlight the region of alarm..... 39

Figure 30: Image captured by a thermal camera during a flame reflection experiment (test 26 in Table 8). The maximum temperature in three different zones are shown in the image. The reflections from the corrugated steel container wall at 5 m from the fire show a maximum 42.8 °C, where the aluminium scaffolding approximately 25 m away from the fire shows 128.6 °C. The hot gases near the ceiling and the heated ceiling shows 36.3 °C. Minimum temperature is shown on the concrete floor at 14.2 °C. 40

Figure 31: Image from a CCTV camera processed in real time by the video fire detection software during a demonstration test. The flame on the floor and the smoke along the ceiling are marked by the software with red and blue outlines, respectively..... 41

Figure 32: Example nuisance alarm from the video fire detection algorithm that has misinterpreted the moving reflective jacket of a person as a growing flame and has marked it with a red rectangle. 42

Figure 33: Example nuisance alarm from the detection algorithm due to the gate of the test hall rolling up to let light in, which has been recognised falsely as a growing flame (outlined using a red rectangle). 42

Figure 34: Example detection of smoke using video analytics when the smoke is barely visible just seconds before detection..... 43

Figure 35: The short-circuit device used in the two first lithium-ion battery tests (highlighted with a red rectangle). The unit produced steam and had hot glowing parts which triggered the IR detectors.... 44

Figure 36: Tray for the heptane pool fire (left) and the equivalent gas burner (middle) used with a propane bottle (right)..... 45

Figure 37: Snapshots of standard heptane fire versus the propane fire (top), heat release rate of each fire (middle), and heat fluxes (bottom) measured at 0.5 m horizontal distance from the edge of each burner at the height of 1 m. 45

Figure 38: Heat release rate of the burner operated at the maximum possible power using the bottle shown in Figure 36. 46

Figure 39: Snapshots showing a wind test with the propane burner before and after fan activation. 46

Figure 40: Thermal imaging (IR) camera and regular CCTV camera installed at 10 m height and 27.1 m horizontal distance from the burner shown in Figure 39. 47

Figure 41: Wind effects visible in footage snapshots of a flame captured by a camera at 27.1 m horizontal distance and 10 m height: the wind causes the fire to appear smaller sometimes (middle photo) and bigger at some other times (right photo) due to the image saturation and flame reflections from nearby surfaces. 47

Figure 42: Wind effects visible in footage snapshots of a flame captured by a thermal imaging camera at 27.1 m horizontal distance and 10 m height: the wind causes the flame to occupy fewer pixels, which makes it more difficult to detect..... 48

Figure 43: Photo showing the arrangement of pallets used as a fire source for the large-scale fire suppression experiments with fire monitors for a weather deck environment. The fire source was a heptane tray located at the centre of the setup as shown (see text for the specifications of the fire source)..... 49

Figure 44: Photo showing the activation of a fire monitor during a late-suppression scenario (300-s waiting time) 50

Figure 45: Detection sensors installed at the height of 7 m beside one of the fire monitors during the large-scale fire suppression tests. The sensors include thermal imaging and regular video cameras, as well as a triple-IR flame wavelength detector. 51

Figure 46: A snapshot from a regular video camera (top) and a snapshot from a thermal imaging camera (bottom) during a fire suppression experiment with two fire monitors in the late fire suppression scenario (300-s waiting time). The persons in the background have been highlighted manually to illustrate the usefulness of this information from the thermal camera. 51

Figure 47: The blockage of the field of view of the thermal camera as a water stream is applied using a fire monitor (placed to the left of the thermal camera that has captured the images). The top image shows the first moment where the water stream starts to come into the frame from the left side of the field of view, while the bottom image shows the full blockage of the field of view as the water stream has reached the centre of the view. 52

Figure 48: Reflection of the fire on the wet floor as perceived by a thermal imaging camera (left, highlighted with a yellow rectangle) and that perceived by a video regular video camera (right, highlighted with a red rectangle). 53

Figure 49: Video images from the built-in camera of the triple-IR flame wavelength detector during a fire suppression test scenario with a 300-s waiting time after flames were visible. Top figure shows the

first fire alarm. Middle figure shows moments before fire suppression. Bottom figure shows another fire alarm immediately after fire suppression..... 54

Figure 50: Detector installations on deck 7 of Hollandia Seaways for the LASH FIRE trials. For the open ro-ro space, a triple-IR flame wavelength detector was installed. For the aft weather deck, a hybrid detector (video + thermopile), two thermal imaging detectors, three flame wavelength detectors (two IR3 and one IR array), and a video flame detector were installed..... 59

Figure 51: Locations of detector installations on deck 7 of Hollandia Seaways for the LASH FIRE trials. The blue shade indicates the area of coverage offered by the detectors. The open ro-ro space is monitored by a triple-IR flame wavelength detector, while the weather deck is monitored by a hybrid detector (video + thermopile), two different thermal imaging detectors, a video flame detector, and two flame wavelength detectors (one IR3 and one IR array). 59

Figure 52: Snapshot from footage recorded by the built-in camera of the triple-IR flame wavelength detector in the open ro-ro space as the flame is detected during the initial testing within seconds. The person holding the flare and the “fire” message have been highlighted manually for clarification. The original footage was recorded sideways (rotated 90 degrees) due to the wrong orientation of the installation, but the rotation of the image has been corrected here to improve the demonstration. 60

Figure 53: Snapshot from footage recorded by the built-in camera of the triple-IR flame wavelength detector on the aft weather deck as the flame is detected during the initial testing within seconds. The person holding the flare and the “fire” message have been highlighted manually for clarification. ... 61

Figure 54: Location of video fire detection camera installed in the closed ro-ro space of deck 3 on Hollandia Seaways and a snapshot from the footage recorded by the camera showing the defined detection zones (outlined in the top figure). The ship itself has conventional point detectors of smoke/heat on this deck. 61

Figure 55: Example nuisance alarm source identified by the thermal imaging detection system on the weather deck: the exhaust pipe of a truck with a temperature of ~150°C has been detected as a potential fire source. 62

Figure 56: Nuisance alarm example from the video fire detection system in the closed deck during washdowns: the droplets landing and moving on the lens of the camera are misinterpreted as smoke (boundaries highlighted using grey and blue contours in mid-top and top right of the two pictures, respectively). 63

Figure 57: Camera tilting observed due to the connections getting loose over time..... 64

Figure 58: LASH FIRE box on board Hollandia Seaways containing a fire alarm panel, draw-out monitor and keyboard, several computer cases, some data acquisition systems, and associated accessories. 65

Figure 59: Setup of fire experiments on the uppermost open ro-ro deck of Hollandia Seaways (details described in D09.2 [5]). 66

Figure 60: Different fire experiments on the uppermost open ro-ro deck of Hollandia Seaways (details described in D09.2 [5]). 67

Figure 61: Setup and scenarios of fire experiments on the aft weather deck of Hollandia Seaways... 68

Figure 62: Flame tilt observations versus wind measurements made using a portable probe in the middle of the weather deck in the aft part of Hollandia Seaways during onboard fire experiments. . 69

Figure 63: Smoke test setup in the closed deck using a fog machine connected to a duct (2 m long, and 50 mm diameter)..... 70

Figure 64: Locations of smoke tests in the closed deck using the fog machine setup shown in Figure 63. 71

Figure 65: Smoke detected in the closed ro-ro space using video fire detection in 30 s when the smoke source was placed 27 m from the camera (left) and in 114 s when the smoke source was placed 72 m from the camera (right)..... 71

Figure 66: Snapshot from the footage of a thermal imaging detection system during a LASH FIRE demonstration test. An extended temperature range fixed in the display software has caused the image to have much less contrast in the cold regions, making it difficult to interpret intuitively. The regular image of the test has been presented in Figure 24. 76